# A LABORATORY STUDY OF ANISOTROPY IN ENGINEERING PROPERTIES OF ANKARA CLAY

A THESIS SUBMITTED TO
THE GRADUATE SCHOOL OF NATURAL AND APPLIED SCIENCES
OF
MIDDLE EAST TECHNICAL UNIVERSITY

BY

MUSTAFA ERDEM İSPİR

IN PARTIAL FULFILLMENT OF THE REQUIREMENTS
FOR
THE DEGREE OF MASTER OF SCIENCE
IN
CIVIL ENGINEERING

SEPTEMBER 2011

Approval of the thesis:

**A LABORATORY STUDY OF ANISOTROPY IN ENGINEERING PROPERTIES OF ANKARA CLAY**

submitted by **MUSTAFA ERDEM İSPİR** in partial fulfillment of the requirements for the degree of **Master of Science in Civil Engineering Department, Middle East Technical University** by,

Prof. Dr. Canan Özgen _____
Dean, Graduate School of **Natural and Applied Sciences**

Prof. Dr. Güney Özcebe _____
Head of Department, **Civil Engineering**

Prof. Dr. Mehmet Ufuk Ergun _____
Supervisor, **Civil Engineering Dept., METU**

**Examining Committee Members:**

Prof. Dr. Orhan A. Erol _____
Civil Engineering Dept., METU

Prof. Dr. M. Ufuk Ergun _____
Civil Engineering Dept., METU

Prof. Dr. Erdal Çokça _____
Civil Engineering Dept., METU

Prof. Dr. Sadık Bakır _____
Civil Engineering Dept., METU

Dr. Mutlu Akdoğan _____
Geoteknik Çözüm ve Proje Ltd. Şti.

**Date:** September 16, 2011

**I hereby declare that all information in this document has been obtained and presented in accordance with academic rules and ethical conduct. I also declare that, as required by these rules and conduct, I have fully cited and referenced all material and results that are not original to this work.**

Name, Last Name : Mustafa Erdem İSPİR

Signature :

# ABSTRACT


## A LABORATORY STUDY OF ANISOTROPY IN ENGINEERING PROPERTIES OF ANKARA CLAY

İspir, Mustafa Erdem

M.Sc., Department of Civil Engineering

Supervisor: Prof. Dr. Mehmet Ufuk Ergun

September 2011, 94 Pages

Anisotropy in engineering properties of soils occurs due to the depositional process forming the soil fabric and/or different directional stresses in soil history. This study investigates the anisotropy in undrained shear strength and drained compressibility of preconsolidated, stiff and fissured Ankara Clay. The compressibility behavior is determined using standard oedometer testing while the shear strength anisotropy is investigated through large diameter unconsolidated-undrained triaxial testing on undisturbed samples taken in vertical and horizontal directions from several deep excavation sites along the Konya Road in Çukurambar-Balgat Area, Ankara. According to the results achieved, Ankara Clay is slightly anisotropic in compressibility, with an anisotropy ratio between 0.72 and 1.17 in terms of coefficient of volume compressibility for several pressure ranges between 50 kPa and 1600 kPa. On the other hand, while a slight anisotropy in undrained shear strength at a ratio ranging between 0.87 and 1.19 in terms of deviator stress can be observed in Ankara Clay, considering the great variation in the test results of samples in same direction which mostly overlaps with the range of results obtained in the other direction, it has been concluded that the Ankara Clay located in this area can be regarded as isotropic in terms of shear strength for practical purposes.

**Keywords:** Anisotropy, Stiff Clay, Undrained Shear Strength, Compressibility, Ankara Clay

# ÖZ

## ANKARA KİLİNİN MÜHENDİSLİK ÖZELLİKLERİNİN LABORATUVARDA ANİZOTROPİ YÖNÜNDEN İNCELENMESİ

İspir, Mustafa Erdem

Yüksek Lisans, İnşaat Mühendisliği Bölümü

Tez Yöneticisi: Prof. Dr. Mehmet Ufuk Ergun

Eylül 2011, 94 Sayfa

Zeminlerin mühendislik özelliklerinde görülen anizotropi, zeminin yapısal dokusunu oluşturan çökelme sürecine ve/veya zeminin geçmişte maruz kaldığı farklı yönlerdeki gerilmelere bağlı olarak gelişir. Bu çalışmada, ön konsolidasyona uğramış, katı ve fisürlü Ankara Kili'nin drenajsız kayma mukavemeti ve drenajlı sıkıştırılabilirlik özellikleri anizotropi yönünden incelenmiştir. Çukurambar-Balgat bölgesinde Konya Yolu boyunca çeşitli derin kazılardan alınan dikey ve yatay yöndeki örselenmemiş numuneler üzerinde, yapılan standart ödometre deneyleri ile sıkıştırılabilirlik özellikleri; büyük çaplı konsolidasyonsuz-drenajsız üç eksenli basınç deneyleri ile drenajsız kayma mukavemeti özellikleri belirlenmiştir. Alınan sonuçlara göre, Ankara Kili, 50 kPa ile 1600 kPa arasında değişen çeşitli basınç aralıklarında hacimsel sıkışma katsayısı yönünden 0.72-1.17 arasında değişen oranlarda, sıkıştırılabilirlik yönünden anizotropiktir. Öte yandan, Ankara Kili'nin drenajsız kayma mukavemetinin 0.87-1.19 arasında değişen oranlarda bir miktar anizotropik olduğu gözlenmesine karşın, aynı yöndeki numunelerde geniş bir dağılım gösteren sonuçlar elde edilmesi ve bunların diğer yöndeki sonuç aralıkları ile büyük oranda çakışması nedeni ile bu bölgede yer alan Ankara Kili'nin kayma mukavemeti yönünden pratik amaçlar için izotropik kabul edilebileceği sonucuna varılmıştır.

**Anahtar Kelimeler:** Anizotropi, Katı Kil, Drenajsız Kayma Mukavemeti, Sıkıştırılabilirlik, Ankara Kili.

*To My Grandparents...*

# ACKNOWLEDGEMENTS

I would like to express my sincere appreciation to my supervisor Prof. Dr. M. Ufuk Ergun, without whom I would not be able to complete my thesis, for his valuable supervision, guidance, criticism, patience and encouragement throughout this study.

I offer my sincere acknowledgement to Mr. Muzaffer Çevik for his understanding, encouragement and the facilities provided for the completion of this study.

The solutions of some of the problems at critical stages wouldn't be possible without the fine workmanship of personnel of SONAR's Workshop. I am grateful for their efforts and help.

The assistance and help provided by the laboratory staff, Ulaş Nacar and Kamber Bölgen in Soil Mechanics Laboratory of METU deserves my sincere appreciation. I would like to thank Ali Bal for his assistance during sampling works.

The permissions granted and assistance provided by the companies and site engineers during sampling works also deserves my sincere appreciation. In this manner, I would also like to thank my friend Mehmet As whose contribution for finding suitable sampling sites is invaluable.

I would like express my sincere thanks to my friends and colleagues for their support and encouragement throughout the thesis works, especially Hüseyin Karancı for his assistance during my study in METU.

Most of all, I would like to express my gratitude to my family, who provided endless support not only for this thesis but throughout my life. I would like to thank them for everything.

# TABLE OF CONTENTS

# LIST OF TABLES

## TABLES

# LIST OF FIGURES

## FIGURES

# LIST OF ABBREVIATIONS AND SYMBOLS

| | |
|---|---|
| A | : Cross-sectional area of the specimen |
| $A_0$ | : Initial cross-sectional area of the specimen |
| $A_c$ | : Corrected cross-sectional area of the specimen |
| c | : Cohesion intercept in terms of total stresses |
| c’ | : Cohesion intercept in terms of effective stresses |
| d | : Point of intersection of modified failure envelope and y-axis |
| CH | : High plasticity clay |
| CL | : Low plasticity clay |
| e | : Overall void ratio of soil |
| $G_s$ | : Specific gravity of solid particles |
| $H_0$ | : Initial height of specimen at the beginning of the loading phase |
| $H_1$ | : Final height of specimen at the end of the loading phase |
| H/V | : Anisotropy ratio, horizontal over vertical |
| HCA | : Hollow cylinder apparatus |
| $I_p$ | : Plasticity Index |
| K | : Anisotropy ratio, horizontal over vertical |
| $K_0$ | : Lateral earth pressure at rest. |
| LL | : Liquid limit |

LVDT : Linear variable differential transformer

MH : High plasticity Silt

ML : Low plasticity Silt

MSL : Median Sea Level

$m_v$ : Coefficient of Volume Compressibility

OCR : Overconsolidation ratio

p : x-coordinate of Mohr Circle

$P_a$ : Axial load applied in triaxial test

PL : Plastic limit

q : y-coordinate of Mohr Circle

$w_n$ : Moisture Content of Soil

USCS : Unified Soil Classification System

UU : Unconsolidated-Undrained

$\alpha$ : Angle of modified failure envelop

$\varepsilon$, $\varepsilon_a$ : Axial strain

$\varepsilon_v$ : Volumetric strain

$\phi$ : Angle of internal friction in terms of total stresses

$\phi'$ : Angle of internal friction in terms of effective stresses

$\sigma'_0$ : Initial effective stress at the beginning of the loading phase

$\sigma'_1$ : Final effective stress at the end of the loading phase

$\sigma_1$ : Major principal stress

$\sigma_3$ : Minor principal stress, confining/cell pressure

$\sigma_d$ : Deviator stress

$\Delta\sigma$ : Deviator stress

# CHAPTER 1

# INTRODUCTION

A major portion of Ankara, the capital city of Turkey, settles on a sedimentary clayey formation which is called Ankara Clay. This clayey formation is predominant in Southwestern parts of the city which is the major development axis with lots of high-rise building developments with multi-story basements. For the design of the retaining structures or slopes required for these deep excavations, the mechanical properties of Ankara Clay need to be known.

Most of the clayey soils, especially overconsolidated clays tend to behave anisotropic in terms of mechanical strength. The term anisotropy defines the difference between the properties of a soil structure in different directions. Anisotropy in engineering properties of soils occurs due to the depositional process forming the soil fabric and/or different directional stresses in soil history.

In this study, the anisotropy in undrained shear strength and drained compressibility of preconsolidated, stiff and fissured Ankara Clay has been investigated. For this purpose a comprehensive sampling work has been executed at four areas in three different deep excavation sites along the Konya Road, in Çukurambar/Balgat Area which is one of the most active development axes of the city.

A total number of 56 large diameter unconsolidated-undrained triaxial testing has been performed on undisturbed samples taken in vertical and horizontal directions in order to investigate the undrained shear strength behavior. Additionally, the compressibility behavior of the clay in both vertical and horizontal directions is

determined by oedometer testing on 22 specimens. All of these results are presented in graphical form and evaluated in order to understand the presence of anisotropy which may exist in Ankara Clay.

# CHAPTER 2

# LITERATURE REVIEW

## 2.1. The Term of Anisotropy in Soils

Anisotropy is a term defining non-homogenous properties of a material in different directions.

*Structural / Inherent anisotropy* is defined as a physical characteristic inherent in the material due to history of loading and environmental conditions and entirely independent of the applied stresses and strain (Casagrande and Carrilo, 1944).

In addition to the particle orientation due to deposition, directional distribution of particles can be modified during shearing into a different anisotropic micro-structure which is called the *induced anisotropy* (Casagrande and Carrilo, 1944).

Due to differences in stress in different directions, all soils including isotropic soils, respond anisotropic in terms of micro-structure to stress change under undrained condition. This phenomenon is called *stress induced anisotropy* (Hansen & Gibson, 1949; Duncan and Seed, 1966a; Otha and Nishihara, 1985 as cited by Kurukulasuriya et al, 1999).

In the sense of micro-structure, soil particles, especially platy clay minerals, are likely to align their faces perpendicular to the direction of $K_0$-Consolidation, resulting micro-structure of soil skeleton to become inherently anisotropic (Mitchell, 1956; Martin, 1962).

Anisotropy occurs in clayey soils when they are overconsolidated for a long period and are exposed to different depositional progressions (Mitachi and Fujiwara, 1987). Therefore many overconsolidated cohesive soils exhibit anisotropic properties and mechanical behavior up to a limited extent, such as shear strength, compressibility, permeability and swelling (Clough & Hansen, 1981; Lo, Leonards & Yuen, 1977). On the other hand, some sedimentary, especially soft, normally consolidated clays may also have an anisotropic structure, which will show different shear strength characteristics at varying inclinations (Wesley, 2010).

## 2.2. Anisotropy in Engineering Properties of Clays

Undrained shear strength anisotropy of clays was first reported by Hansen and Gibson (1949) and studied further by Bishop (1966), Duncan & Seed (1966a & 1966b), Aas (1967), Berrre & Bjerrum (1973), Vaid & Campanella (1974), Ladd et al (1977) in order to develop the understanding of the anisotropic behavior of the clays.

Notable early studies conducted for the determination of anisotropic behavior of clayey soils were by Jacobson (1955), and Ward et al (1959), which were followed by other researchers' laboratory and field studies for different clay deposits.

Jacobson (1955), who studied anisotropy in compressibility of normally consolidated clayey soils of Stockholm, concluded that the clayey soil of Stockholm is isotropic regarding the oedometer and unconfined compression test results conducted on specimens taken in vertical, diagonal (45 degrees) and horizontal directions.

Ward et al (1959) studied overconsolidated "London Clay" and concluded that it is anisotropic in terms of compressibility and shear strength, as there was significant difference between the compressibility properties of horizontal and vertical specimens and the unconfined compression test results of horizontal

specimens were higher than the vertical specimens. Bishop (1966) reported in his state-of-art report that, while the ratio of horizontal to vertical shear strength of London Clay varies between 1.23 to 1.63, there is a great reduction in the shear strength of inclined samples such that the shear strength of an inclined sample with 45 degrees angle to the horizontal, is only 0.77 of the vertical shear strength, probably due to the lower shear strength parameters of the bedding planes.

Lo (1965) performed high number of unconfined compression tests on lightly overconsolidated (OCR ≅ 2) clay specimens of Welland (Ontario), taken in several inclined directions. The shear strengths of horizontal specimens were lower than the vertical specimens about a ratio of $c_h/c_v \cong 0.64 \sim 0.80$. Most of the further studies on different lightly overconsolidated clays also revealed similar results with anisotropy ratios lower than one (Nishimura et al., 2007).

Wesley (1975) worked on undisturbed samples gathered from a normally consolidated sedimentary soft clay, namely "Mucking Clay" which was a recent marine deposit found in Mucking, UK. The undrained shear strength of the sample decreased as the inclination of the sample became closer to the horizontal as shown in the Figure 2.1.

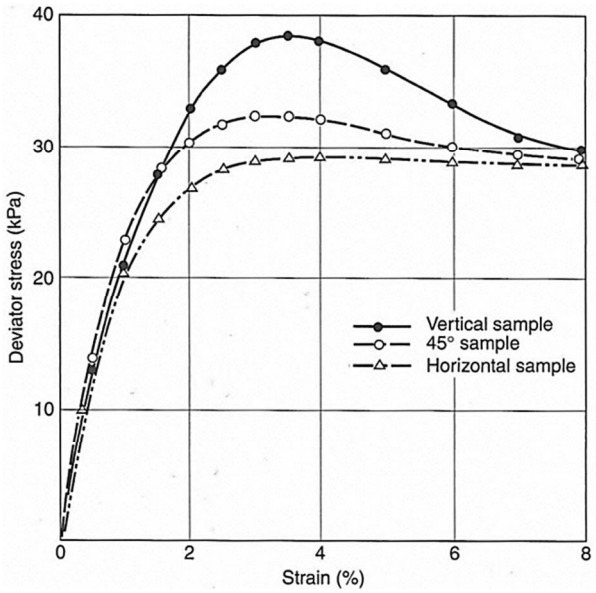


**Figure 2.1.** Undrained Triaxial Compression Test Results of Sedimentary Mucking Clay at Different Inclinations (Wesley, 2010)

In addition to the studies regarding the anisotropic behavior of certain clays, many early studies were concerned on understanding the relationship of anisotropy with the soil properties. Most of them concluded that anisotropy becomes more pronounced as the plasticity index of cohesive soil decreases (Bjerrum, 1973; Ladd et al., 1977; Nakase and Kamei, 1983).

Nakase and Kamei (1983) studied the influence of index properties, mainly the soil plasticity, on the undrained shear strength anisotropy through a series of consolidated undrained triaxial tests. Stating that testing of natural soils may have several limitations for the purpose of investigating the influence of index properties; authors have constituted several sets of artificial specimens with controlled index properties. As samples, remolded "Kawasaki Clay" and three artificially mixed soil samples, with different values of plasticity index $I_p$ were used. They classified their artificial soil samples with low plasticity as intermediate soil, which carry intermediate properties between both cohesionless and cohesive soils. After the pre-consolidation, fully saturated artificial samples were trimmed into triaxial samples of 50 mm diameter with 120 mm height. Four types of consolidated undrained triaxial tests were carried out depending on the combination of consolidation type ($K_0$ or isotropic) and whether it is compression or extension test. Their results also have agreed that the undrained shear strength anisotropy increases with decrease in plasticity index, $I_p$. Additionally, they concluded that undrained shear strength anisotropy becomes more dependent on stress condition in consolidation process, as the plasticity index of the soil increases.

Kamei and Nakase (1989) further investigated the effect of overconsolidation history on undrained shear strength anisotropy of $K_0$-consolidated cohesive soils, performing undrained triaxial compression and extension tests with $K_0$-consolidated and $K_0$-rebound on artificially reconstituted soils from Kawasaki and marine clays. Their results have shown that undrained shear strength anisotropy being approximately constant within the range of OCR's of 1 to 10, although it depends on the plasticity index and amount of clay fractions.

Kurukulasuriya et al (1999) stated that anisotropic shear strength behavior of overconsolidated Kaolin Clay is caused by the direction-dependent shear strength parameters (c' and $\phi$') in terms of effective stresses, instead of the anisotropic excess pore-pressure developed during shearing. Authors also concluded that the changes in over consolidation ratio up to 32, does not affect the anisotropic behavior significantly. For such samples, it was also observed that changing boundary conditions (such as using plane shear testing or triaxial testing) do not affect the anisotropic behavior of Kaolin Clay.

It must be noted that, the findings of Kurukulasuriya et al (1999) regarding boundary conditions contradicts with the statements of Vaid and Campanella, (1974) and Ladd et al. (1977), which reported that undrained strength anisotropy is more pronounced in triaxial test compared to the plane strain test.

Nishimura et al. (2007) investigated the shear strength of anisotropy of the highly overconsolidated, fissured, stiff London Clay at different depths using hollow cylinder apparatus (HCA) simple shear testing. They compared the peak shear strengths of the hollow cylindrical samples which are subjected to principal stress in different directions, while reconsolidation regime and intermediate principal stress ratio was kept constant. Series of HCA simple shear tests have been made with different intermediate principal stress ratios and their effect on the anisotropic behavior is investigated. The anisotropic behavior observed at different levels are compared with the previous studies on low OCR (OCR=1-4) soils consisting of clay, silt, clayey and silty sands (Whittle et al, 1994; Menkiti, 1995; Zdravkovic, 1996 as cited by Nishimura et al., 2007) as shown in the Figure 2.2.

While the shear strength of low OCR soils and London Clay samples taken at -5.2 m below the ground level, were decreasing as the inclination of the sample becomes more horizontal ($\alpha$=90°), London Clay samples taken at -10.5 m below the ground level, behaved the opposite. Authors concluded that this might be due to the highly fissured, discontinuous macrofabric of the samples taken at -10.5 m depth and heavy overconsolidation (OCR>9) which may have changed the

microstructural anisotropy and may also have caused the mentioned discontinues (Nishimura et al., 2007).

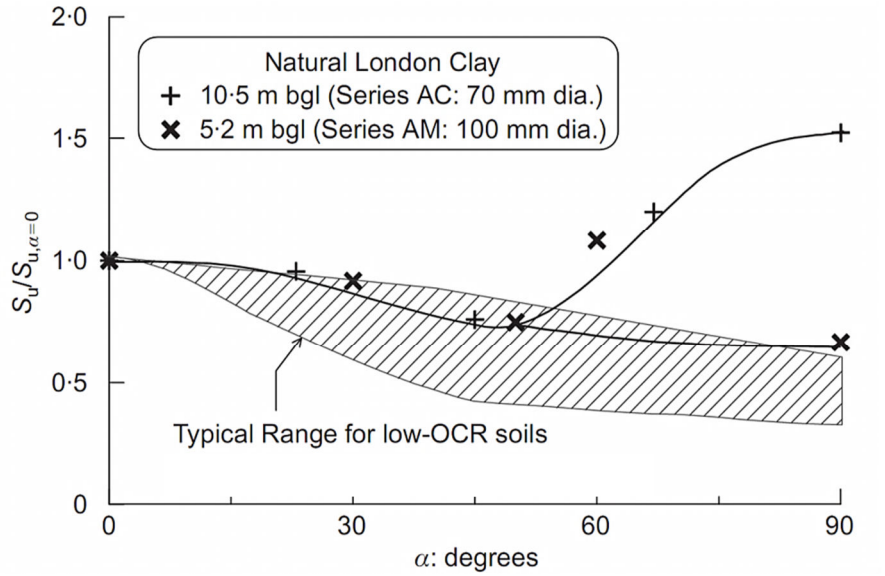


**Figure 2.2.** Comparison of Anisotropy Ratio of low-OCR soils with the values obtained from HCA simple shear tests on London Clay samples taken from 5.2 and 10.5 m below the ground level. (Nishimura et al., 2007)

The same study by Nishimura et al (2007), also involved the triaxial compression, extension and simple shear testing of the rotary core samples taken between 6 to 35 m below the ground level, concluding that shear strength anisotropy of the London Clay increases with the depth. The authors also expressed that, the difference in sample size difference affects the shear strength behavior, and the shear strength of the large sized samples might be very low against the extensional loading, if the samples contain an intense discontinuity network.

Attom and Al-Akhras (2008), studied anisotropic shear strength behavior of overconsolidated clays in Irbid, Jordan and concluded them to be anisotropic considering unconfined compressive strength tests conducted on the 36 mm

diameter samples in vertical direction to be higher than that in the 45° inclined and horizontal directions (See Figure 2.3).

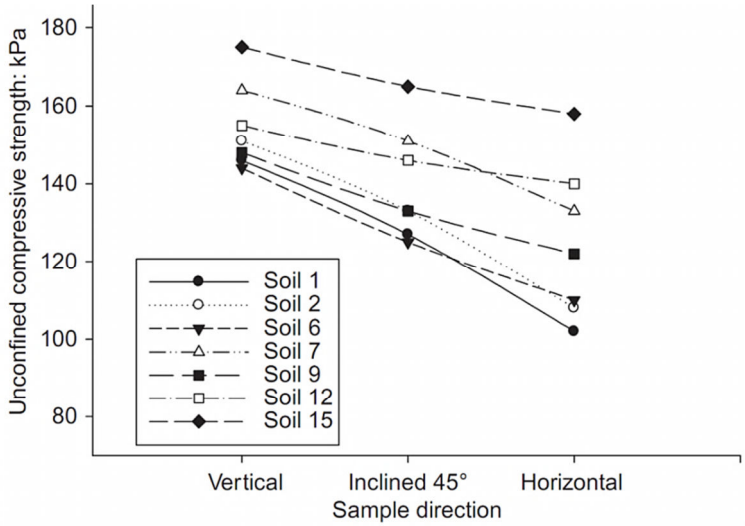


**Figure 2.3.** Variation of Unconfined Compressive Strength of Irbid Clay with the sampling inclination angle. (Attom and Al-Akhras, 2008)

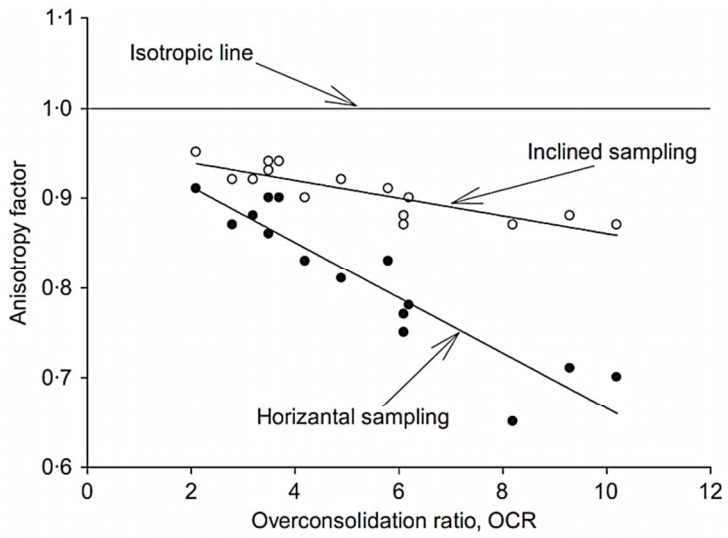


**Figure 2.4.** Variation of Anisotropy Factor of Irbid Clay with OCR. (Attom and Al-Akhras, 2008)

According to study of Attom and Al-Akhras (2008), the anisotropy in undrained shear strength of the Irbid Clay is found to be increasing with the increase in overconsolidation ratio (see Figure 2.4). On the other hand, it is found that anisotropy ratio increases and becomes closer to the unity as the depth increases. At greater depths, anisotropy ratio is expected to reach a value about 1, which means that soil will become somehow isotropic. This result disagrees with the findings of Nishimura et al (2007) on London Clay, which is probably due to the nature of both clays being relatively different, as also noted by the authors.

Rowshanzamir and Askari (2010) investigated the factors affecting the anisotropy in compacted clayey soils which are similar to those used in impermeable cores of the earth dams. Their study revealed that, all of the compacted samples are anisotropic by a ratio of vertical to horizontal strength varying between 1.04 ~ 1.23. It was also observed that the level of anisotropy increased as the level of compaction and saturation are increased.

## 2.3. Ankara Clay and its Geological Properties

The predominant, sedimentary formation which makes the Ankara Basin consists of reddish-brown, brown, stiff, preconsolidated, inorganic, highly plastic and fissured clay which is named as “Ankara Clay” (Ordemir et al, 1965; Birand, 1978).

The two-thirds of the Ankara, the capital city of Turkey with more than four million metropolitan population, sits on the Ankara Clay (Tonoz et. al, 2003) which is predominant especially in the central and Southwestern parts of the city (Ergüler and Ulusay, 2003a).

The formation mainly consists of clay, and there are also sandy and gravelly levels of variable thicknesses within the clay formation. Thin lime levels, nodules, concretions and lenses with no lateral continuity are present within the clay, typically at shallow depths (Ergüler and Ulusay, 2003a).

Network of haircracks and slickensides are usually present in the Ankara Clay and the surfaces of fragments are usually polished and glossy in the nature. The undisturbed sampling is rather difficult and specimens tend to fail along the fissures and irregular surfaces (Ordemir et al, 1965).

The typical range of index properties of Ankara Clay is wide and varying. The Ankara Clay is usually highly plastic and classified as CH or MH with a typical range of the plastic limit and water content varying between 20 and 40%, while typical liquid limit is not less than 50%. Yet lower plasticity can also be observed. (Ordemir et al, 1965; Mirata, 1976; Erguler & Ulusay, 2003a).

## 2.4. Anisotropy in Engineering Properties of Ankara Clay

Ağaoğlu (1973) studied the possible anisotropy in one dimensional compressibility behavior of Ankara Clay (also known as, METU Campus Clay) for the first 4 meters below the ground, using standard consolidation device. While a slight anisotropy was observed for pressures lower than 200 kPa, the compressibility under higher pressures was isotropic for specimens taken in vertical (0°), inclined (45°) and horizontal (90°) directions (see Figure 2.5 and Figure 2.6). The author concluded that consolidation characteristics do not show a marked difference with orientation, therefore Ankara Clay might be considered to behave isotropic in terms of compressibility for the shallow depths.

As cited by Avşar et al. (2009); Üner (1977), Çetinkaya (1978), Ergüler (2001), and Ergüler and Ulusay (2003b) have investigated the anisotropy in swelling behavior of Ankara Clay on a limited number of specimens and observed that swelling amount is higher in the horizontal direction compared to those on vertical, while Sapaz (2004) observed an opposite behavior.

Avşar et al. (2009) studied the anisotropic swelling behavior of the Ankara Clay on an increased number of samples from several different sites. Contrarily to the most of the previous works, they have observed a higher swelling in vertical direction, with anisotropy ratio varying between 0.34 and 0.98.

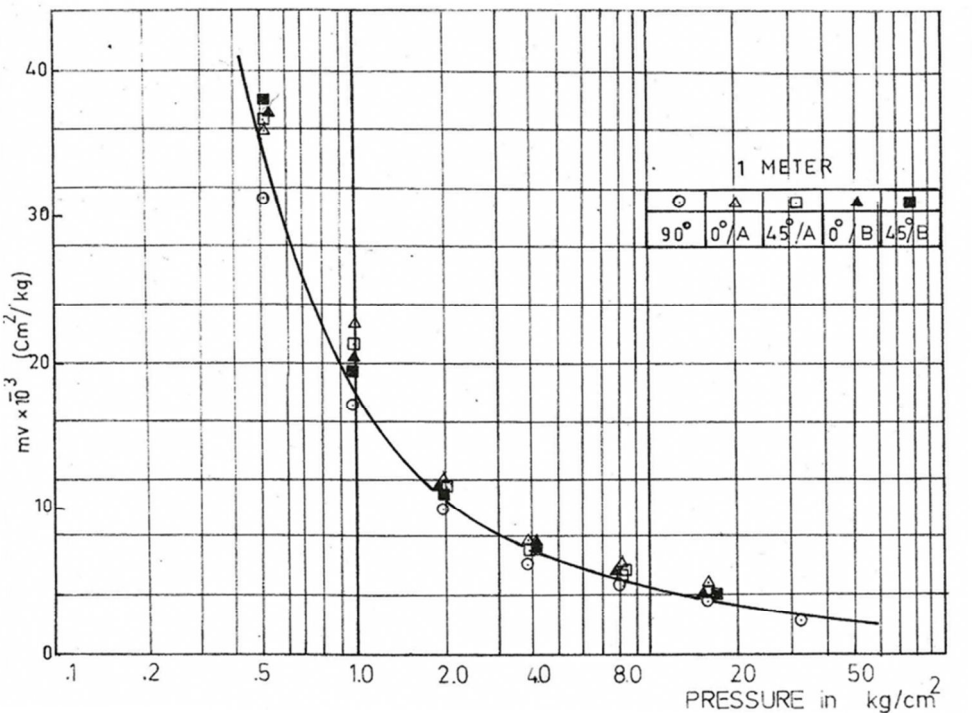


**Figure 2.5.** The Coefficient of Volume Compressibility versus Pressure, for Ankara Clay at 1 m depth (Ağaoğlu, 1973)

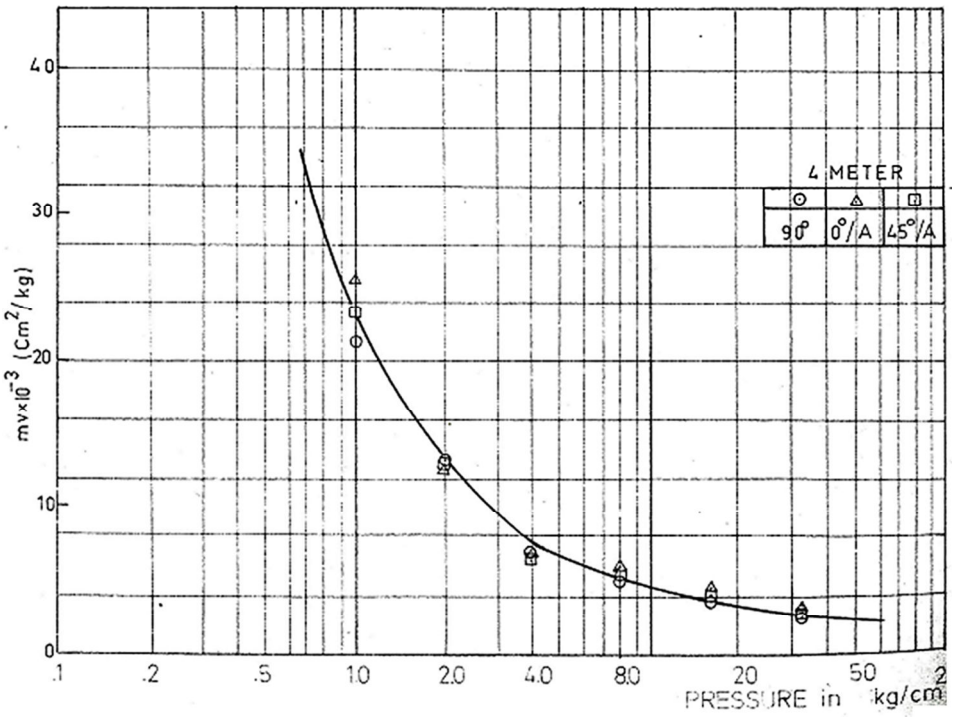


**Figure 2.6.** The The Coefficient of Volume Compressibility versus Pressure, for Ankara Clay at 4 m depth (Ağaoğlu, 1973)

# CHAPTER 3

# SAMPLING AND INDEX PROPERTIES

## 3.1. Sampling Works and Locations

According to available geological information and geotechnical investigations, observations were made on the construction sites involving deep excavations in the areas which are known to be founded on Ankara Clay deposits. The area of sampling was mainly focused on the deep excavations in Balgat/Çukurambar area next to Konya Road (See Figure 3.1).

Among the available sites involving on-going deep excavations, the slopes and excavated soil have been investigated for the suitability for large diameter undisturbed sampling. The areas and depths with sand bands, large number of calcareous concretions, gravels and observable fragments and cracks were tried to be avoided.

At each sampling site, a testing pit/trench which was about 1.5 ~ 2 m deep was opened and the sampling tubes with a diameter of 100 mm and a height ranging between 200 and 300 mm were pushed into the soil in vertical and horizontal directions, by the means of hydraulic jacks or available site equipment which help pushing of the tubes into the stiff soil without disturbing the sample.

All of the sampling work was focused on a certain area of the site, and samples were taken as close as possible trying to minimize the possible differences in index properties and sample characteristics which have potential to affect the results obtained.

Four different sampling locations were selected at three different sites in Çukurambar/Balgat Area along the Konya Road, to be named as Site-A1, Site-A2, Site-B and Site-C. The ranges of index properties were determined for each site in order to understand and interpret their characteristics better.


**Figure 3.1.** Location of the Sampling Sites

**Site-A:**

Two distinct sampling works at different locations and elevations were performed in Site-A which is located on Konya Road (39°53'17.39"N - 32°48'40.60"E). The Site-A consisted of a stiff, red to reddish-brown, fissured Ankara Clay with slickensides, calcareous concretions and gravels.

Site A1 - This preliminary sampling work involved 9 vertical and 9 horizontal 100mm diameter cylindrical samples taken at an approximate depth of 4 m below the original ground level in a freshly excavated testing trench.

This shallow depth was consisting of clay with high concentration of gravels and cobbles, which resulted two thirds of the specimens to get disturbed during the preparation for the test. Regarding such difficulties observed for preparing an undisturbed sample for such heterogeneous clay, it has been decided to increase the number of specimens for the future sampling works which would allow testing an adequate number of control groups.

**Table 3.1.** Preconsolidation Characteristics of Ankara Clay at Site-A1

| **SITE – A1** | |
|---|---|
| Approximate Sampling Depth (m) | - 4 |
| Average Bulk Density (kN/m$^3$) | 18 |
| Specific Gravity | 2.60 |
| Approximate Overburden Pressure (kPa) | 72 |
| Apparent Average Preconsolidation Pressure (kPa) | 130 |
| Over Consolidation Ratio (OCR) | 1.81 |

**Table 3.2.** Index Properties of Ankara Clay at Site-A1

| SITE – A1 | | | | |
|---|---|---|---|---|
| Atterberg Limits | **$W_n$ (%)** | **LL (%)** | **PL (%)** | **$I_P$ (%)** |
| | 33 ~ 39 | 58 ~ 66 | 24 ~ 33 | 29 ~ 35 |
| Particle Size Distribution (USCS) | **Gravel (%)** | **Sand (%)** | **Silt (%)** | **Clay (%)** |
| | 5.3 ~ 9.0 | 23.1 ~ 17.8 | 29.8 ~ 31.2 | 45.4 ~ 45.8 |

Site A2 - The second sampling work involved a comprehensive sampling at an approximate depth of 16 m below the natural ground level (±0.00 = ~ +982.00 MSL). This sampling work involved 30 vertical specimens and 30 horizontal cylindrical specimens with 100 mm diameter.

Notable discontinuities and high concentration of calcareous concretions in several zones were observed in the deeper sampling area, and the presence of fissures and slickensides close to the vertical direction could be easily noticed in the slopes of fresh excavations. Although extreme discontinuities were eliminated in the samples by investigating several areas of the site for relatively more homogenous zones, such discontinuities were always present in specimens at acceptable quantities.

**Table 3.3.** Preconsolidation Characteristics of Ankara Clay at Site-A2

| SITE – A2 | |
|---|---|
| Approximate Sampling Depth (m) | - 16 |
| Average Bulk Density (kN/m$^3$) | 19 |
| Specific Gravity | 2.63 |
| Approximate Overburden Pressure (kPa) | 304 |
| Apparent Average Preconsolidation Pressure (kPa) | 440 |
| Over Consolidation Ratio (OCR) | 1.45 |

**Table 3.4.** Index Properties of Ankara Clay at Site-A2

| SITE – A2 | | | | |
|---|---|---|---|---|
| Atterberg Limits | **$W_n$ (%)** | **LL (%)** | **PL (%)** | **$I_P$ (%)** |
| | 30 ~ 37 | 59 ~ 68 | 27 ~ 30 | 31 ~ 40 |
| Particle Size Distribution (USCS) | **Gravel (%)** | **Sand (%)** | **Silt (%)** | **Clay (%)** |
| | 1.6 ~ 6.1 | 12.4 ~ 15.7 | 18.2 ~ 18.9 | 60.0 ~ 67.1 |

More than 50% of the samples were unsuitable for 100 mm diameter triaxial testing due to several reasons which included;

- Unsuitable height to diameter ratio as some fissures and slickensides going through the whole diameter of the sample disallowed obtaining a complete undisturbed sample.
- Presence of very high non-cohesive discontinuities which would affect the overall behavior of the sample.
- Very hard nature of lime concretions and gravel formations within the clay made it impossible to prepare samples.

**Site-B:**

The Site B which consisted of hard, light brown, highly fissured Ankara Clay with some gravels reaching up cobble sizes was also located in Konya Road (39°54'4.58"N, 32°48'47.87"E) which is about 1,5 kilometers North of the Site-A. There used to be a light structure existing at the site.

A total number of 38 samples (19 vertical and 19 horizontal) were taken from a depth of approximately 15 m below the ground level which was freshly excavated.

Several problems during sampling and sample preparation due to very hard and highly fissured nature of the clay have caused only about 25% of the samples to be properly tested.

**Table 3.5.** Preconsolidation Characteristics of Ankara Clay at Site-B

| **SITE – B** | |
|---|---|
| Approximate Sampling Depth (m) | - 15 |
| Average Bulk Density (kN/m$^3$) | 19 |
| Specific Gravity | 2.71 |
| Approximate Overburden Pressure (kPa) | 285 |
| Apparent Average Preconsolidation Pressure (kPa) | 410 |
| Over Consolidation Ratio (OCR) | 1.44 |

**Table 3.6.** Index Properties of Ankara Clay at Site-B

| **SITE – B** | | | | |
|---|---|---|---|---|
| Atterberg Limits | **$W_n$ (%)** | **LL (%)** | **PL (%)** | **$I_P$ (%)** |
| | 25 ~ 31 | 50 ~ 52 | 21 ~ 23 | 27 ~ 31 |
| Particle Size Distribution (USCS) | **Gravel (%)** | **Sand (%)** | **Silt (%)** | **Clay (%)** |
| | 3 ~ 11.1 | 13.3 ~ 15.6 | 30.0 ~ 31.4 | 45.6 ~ 50.0 |

**Site-C:**

The Site C, which consisted of reddish-brown Ankara Clay with fissures, slickensides and gravelly/sandy formations, was located at 39°53'30.18"N, 32°48'42.48"E between Site A and B.

19 vertical and 19 horizontal samples were gathered from 21 m below the natural ground level (±0.00 = ~ +959.00 MSL). About 50% of the specimens were unsuitable for testing due to high concentration of coarse particles within the sample.

**Table 3.7.** Preconsolidation Characteristics of Ankara Clay at Site-C

| **SITE – C** | |
|---|---|
| Approximate Sampling Depth (m) | - 21 |
| Average Bulk Density (kN/m$^3$) | 20 |
| Specific Gravity | 2.65 |
| Approximate Overburden Pressure (kPa) | 420 |
| Apparent Average Preconsolidation Pressure (kPa) | 420~450 |
| Over Consolidation Ratio (OCR) | 1 ~ 1.1 |

**Table 3.8.** Index Properties of Ankara Clay at Site-C

| **SITE – C** | | | | |
|---|---|---|---|---|
| Atterberg Limits | **$W_n$ (%)** | **LL (%)** | **PL (%)** | **$I_P$ (%)** |
| | 23 ~ 28 | 54 ~ 56 | 22 ~ 23 | 32 ~ 34 |
| Particle Size Distribution (USCS) | **Gravel (%)** | **Sand (%)** | **Silt (%)** | **Clay (%)** |
| | 2.2 ~ 3.1 | 16.0 ~ 26.2 | 22.9 ~ 28.9 | 51.3 ~ 52 |

## 3.2. Comparison of Index Properties at Different Sites

The index properties of samples gathered from all sites were within the typical range of Ankara Clay as shown in Table 3.9, Table 3.10 and Table 3.11.

**Table 3.9.** Comparison of Preconsolidation Characteristics of the Samples

| Site | Approximate Sampling Depth (m) | Average Bulk Density ($kN/m^3$) | Approximate Overburden Pressure (kPa) | Apparent Average Preconsolidation Pressure (kPa) | OCR |
|---|---|---|---|---|---|
| **A1** | - 4 | 18 | 72 | 130 | 1.81 |
| **A2** | - 16 | 19 | 304 | 440 | 1.45 |
| **B** | -15 | 19 | 285 | 410 | 1.44 |
| **C** | -21 | 20 | 420 | 420 | 1 |

**Table 3.10**. Variation in Particle Size Distribution according to USCS

| | Gravel % | Sand % | Silt % | Clay % |
|---|---|---|---|---|
| **Site-A1** | 5.3 ~ 9.0 | 23.1 ~ 17.8 | 29.8 ~ 31.2 | 45.4 ~ 45.8 |
| **Site-A2** | 1.6 ~ 6.1 | 12.4 ~ 15.7 | 18.2 ~ 18.9 | 60.0 ~ 67.1 |
| **Site-B** | 3.0 ~ 11.1 | 13.3 ~ 15.6 | 30.0 ~ 31.4 | 45.6 ~ 50.0 |
| **Site-C** | 2.2 ~ 3.1 | 16.0 ~ 26.2 | 22.9 ~ 28.9 | 51.3 ~ 52.0 |

**Table 3.11.** Variation in Specific Gravity, Natural Moisture Content and Atterberg Limits at Different Sites

| | Specific Gravity, $G_S$ | Moisture Content, $W_n$ (%) | Liquid Limit, LL (%) | Plastic Limit, PL (%) | Plasticity Index, $I_P$ (%) | Classification |
|---|---|---|---|---|---|---|
| **Site-A1** | 2.60 | 33 ~ 39 | 58 ~ 66 | 24 ~ 33 | 29 ~ 35 | MH - CH |
| **Site-A2** | 2.63 | 30 ~ 37 | 59 ~ 68 | 27 ~ 30 | 31 ~ 40 | CH |
| **Site-B** | 2.71 | 25 ~ 31 | 50 ~ 52 | 21 ~ 23 | 27 ~ 31 | CH |
| **Site-C** | 2.65 | 23 ~ 28 | 54 ~ 56 | 22 ~ 23 | 32 ~ 34 | CH |

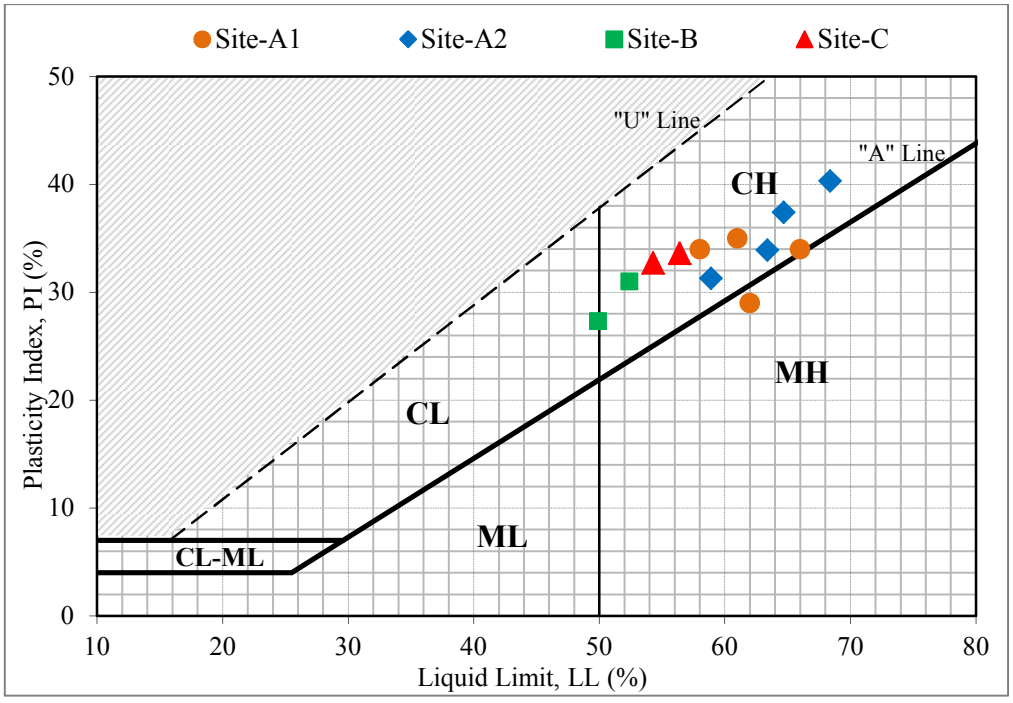


**Figure 3.2.** Distribution of Atterberg Limits of Samples on Plasticity Chart

### 3.3. Sample Preparation

After the sampling, ends of the tubes were trimmed and waxed in order to prevent changes in the original moisture content. All of the samples were transferred to the laboratory with care in order to prevent any disturbance, and were kept in the moisture room until being tested.

In order to minimize any effect of disturbance, sample tubes were kept at the horizontal or vertical position depending on the original orientation and tested as soon as possible after the sampling.

The samples were extruded from the tubes using a hydraulic sample extruder working with electricity, which was able to supply a constant and steady force throughout the process (Figure 3.2).

**Figure 3.3.** The Sample Extruder used for sample preparation.

The extruded samples were weighted and checked for the presence of any cracks or irregularities on the sides. The samples with cracks, very large voids or important irregularities were eliminated from testing. The small voids present at the sides, were filled with the sample particles left from trimming as per BS 1377-7:1990.

As a result of difficulties in obtaining large diameter undisturbed samples with 2:1 height to diameter ratio due to slickensides and fissures, the required ratio for testing triaxial specimens were reduced to 1.5:1 for some samples but horizontal and vertical samples to be compared were tried to be selected from the specimens with the same or similar dimensions.

# CHAPTER 4

# LABORATORY STUDY

## 4.1. Testing Program

Two different sets of laboratory tests have been conducted on Ankara Clay in order to observe its anisotropic behavior in shear strength and compressibility characteristics.

In the first series of experiments, in order to investigate the anisotropy in the undrained shear strength of Ankara Clay, a total number of 56 unconsolidated-undrained triaxial tests were performed on 100 mm diameter undisturbed Ankara Clay specimens which were taken in both vertical and horizontal directions.

In the second series of experiments, in order to investigate the anisotropy in the compressibility properties, oedometer/consolidation tests were performed on a total number of 22 samples taken in vertical and horizontal directions from different sites.

## 4.2. Investigation of Shear Strength Anisotropy

Depending on their particle size and plasticity characteristics, soils may be classified into two main groups such as cohesionless and cohesive. The strength characteristics of the cohesive soils are mainly governed by the attraction (cohesion) between the individual soil particles. On the other hand, the strength properties of cohesionless soils mainly depend on the friction between the

particles and interlocking, as there is no attraction between their individual soil particles.

Clays are classified as cohesive soils as there is a strong cohesion between the clay particles mainly due to their chemical properties, size and shape. The shear strength of a cohesive soil is influenced by the two main characteristic properties of the soil, namely cohesion and friction angle (Lambe, 1967).

There are several methods for testing the shear strength of cohesive soils in the laboratory. *Triaxial Compression Test* is the most controllable and reliable shear strength determination test compared to the other common laboratory tests. In triaxial test, the cylindrical specimen with a height to diameter ratio about 2:1 is subjected to a strain-controlled axial loading under a constant confined pressure. The test is repeated under different confined pressures on similar samples. The specimen may be tested under three main limiting consolidation and drainage conditions such as unconsolidated-undrained (UU), consolidated-undrained (CU), and consolidated-drained (CD). The undrained shear strength behavior of undisturbed specimens of Ankara Clay subject to this study is determined using UU Triaxial compression tests.

### 4.2.1. Unconsolidated-Undrained Triaxial Testing

Unconsolidated-undrained triaxial testing is a method of determining undrained shear strength of soil specimens by not permitting a change in the pore water content of the specimen.

During the execution of undrained-unconsolidated triaxial tests, BS 1377-7:1990 was followed as the regulatory standard.

#### 4.2.1.1. Experimental Apparatus

A typical triaxial apparatus was used for conducting the undrained-unconsolidated triaxial tests, which consists of the following elements;

*a) Loading Frame & Device:*

The loading device was capable of applying axial compression at a uniform rate without notable vibration. The loading frame used for the experiments had a capacity of applying 5000 kg axial compression at a rate between 0.001 mm/min to 6 mm/min which covers the required rates by the related standards.

*b) Loading Piston:*

The axial load was applied to the specimen through an axial load piston which sits on the top cap of the specimen.

c) *Load Measuring Device:*

A load ring which was capable of measuring the axial load to an accuracy of 1% of the axial load at the failure was used as the load-measuring device.

*d) Triaxial Cell:*

A triaxial cell was used which was consisting of a transparent cylindrical cell body covered with base and top plates which include necessary inlet, outlet and accessories required for the testing as per BS 1377:1990 (see Figure 4.1).

The triaxial apparatus used in the study is shown in Figure 4.2.

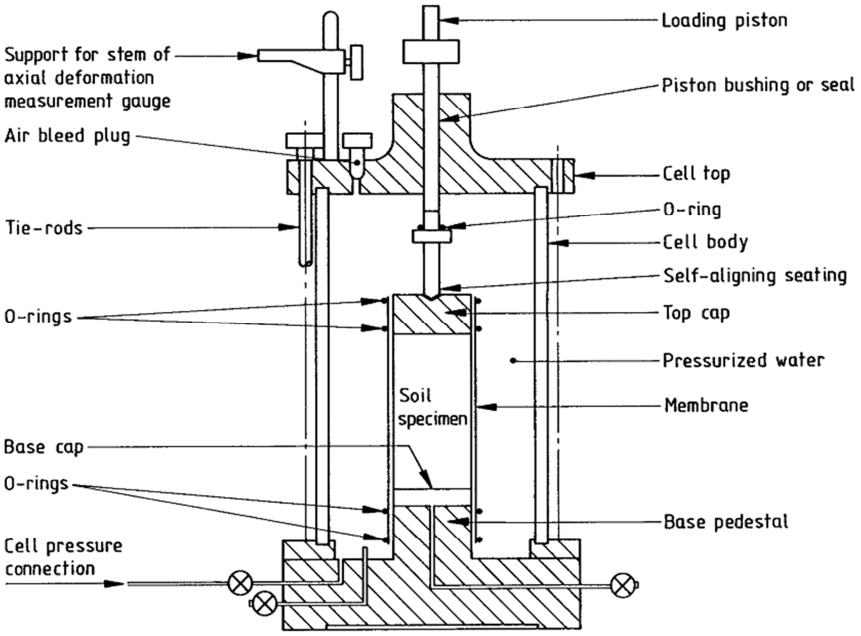


**Figure 4.1.** A Typical Scheme of Triaxial Cell. (BS 1377-7:1990)


**Figure 4.2.** The Triaxial Apparatus used in the Study.

#### 4.2.1.2. Predetermined Test Conditions

Test conditions have direct influence on the results obtained; therefore they were determined before the testing program was commenced. The pre-determined test conditions are listed below;

*a) Sample Type:*

The specimens to be tested in triaxial chamber are either undisturbed or remolded samples. As the purpose of this study was to investigate the existing anisotropic behavior of Ankara Clay, all of the tests were conducted on undisturbed samples.

*b) Sample Size:*

According to BS 1377-7:1990, typical specimen diameters of a standard UU triaxial test vary between 38-110 mm, and height of the specimen is approximately twice the diameter.

Generally, the samples with a diameter size of 38 mm are only suitable to the homogenous clays (BS 1377-7:1990) and it is recommended to use the largest applicable specimen size in order to get more representative results for fissured clays (Ward et. al, 1959).

According to the study by Tezer (1984), effect of specimen size on undrained shear strength of Ankara Clay is relatively small, yet a large gravel present in a small sized sample may affect the results significantly.

Considering the heterogeneous and fissured structure of Ankara Clay, undisturbed specimen diameter of 100 mm was chosen for the triaxial testing. Due to the difficulties of obtaining a height to diameter ratio greater than 2:1, specimens with a height-diameter ratio higher than 1.5:1 were also tested.

*c) Cell Pressure:*

In order to determine the shear strength of the soil, similar specimens are tested under different cell pressures. The magnitude of the applied cell pressure mainly depends on the in-situ conditions of the soil, which is mainly determined by the overburden pressure ($\sigma_v$) existing on the sample in the nature.

In this study, specimens were subjected to cell pressures of 250, 350, 450 and 650 kPa, which were ranging between approximately 0.75 to 1.5 times the overburden pressures.

*a) Rate of Shear:*

Strength behavior of the specimens depends on the rate of shear. Higher rate of shearing usually results a higher strength behavior (Lambe, 1967). Therefore the rate of shear was constant in all comparing groups, and extreme rates of shear were avoided. As a rapid unconsolidated-undrained test was performed, a constant shearing rate of 0.5% strain/min was chosen which allowed breaking the sample in a period of 10 minutes to 15 minutes as recommended by BS 1377-7:1990.

#### 4.2.1.3. Testing Procedure

The suitable undisturbed specimens, which were obtained and prepared in accordance to the Section 3.2, were tested in the triaxial chamber following the procedure described below.

a. After placing the impermeable and non-corrosive base and top caps to the each end of the undisturbed specimen, the sample is enclosed in a thin latex membrane using a membrane stretcher. Along with the rubber o-rings placed at the each caps, the specimen is sealed from any moisture/water interaction.

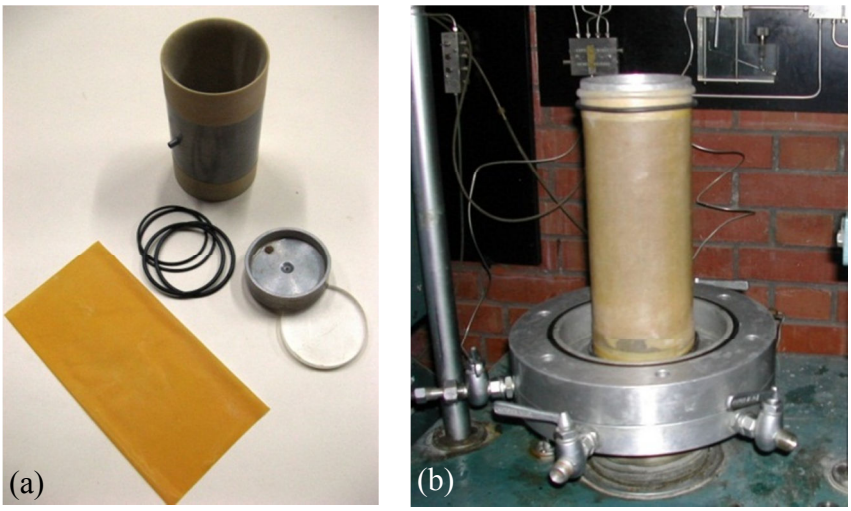


**Figure 4.3.** (a) The Accessories used for 100 mm Diameter Specimen Sealing. (b) Specimen Placed on the Base Pedestal

b. The specimen is placed on the base pedestal of the triaxial cell, and the cell body is fixed. The alignment of piston and loading cap are controlled by moving piston down allowing the piston to touch the seating on the cap. If there is any eccentricity, it is fixed.

c. The triaxial cell is sealed and filled the pressurizing fluid. In this study, water was used as the pressurizing fluid, as the time required for the tests was relatively short.

d. After the cell is filled with the pressurizing fluid, the cell pressure is applied and kept constant throughout the test. For this study, a 1700 kPa capacity *Oil-Water Cylinder* system equipped with a manometer is used as a pressurizer (See Figure 4.2).

e. After the application of the cell pressure, specimen is allowed to stabilize under the applied pressure for about 10 minutes, before starting the test.

Meanwhile, the load ring is assembled and brought to the appropriate position ready for loading and strain measurement.

f. Finally, the loading phase begins with the predetermined loading rate. During the loading, prove ring values are recorded at every %0.125 strain for large diameter specimens. The reading interval may be reduced to %0.25 after %2.5 strain, depending on the loading speed of the specimen.

#### 4.2.1.4. Calculations

In a triaxial test, the applied cell pressure exerts an equal stress all around the specimen which is referred as, minor principal stress ($\sigma_3$). The sum of the all-round pressure and applied axial load makes up the major principal stress ($\sigma_1$). The applied axial load itself is referred as principal stress difference ($\sigma_1$-$\sigma_3$) or deviator stress ($\Delta\sigma$).

$$\sigma_1 = \sigma_3 + \Delta\sigma \tag{4.1}$$

The applied axial load ($P_a$) at each stage is calculated by converting the deflection readings from proving ring to the load, using the proving ring constant. The deviator stress is calculated by dividing the applied load to the corrected cross-sectional area ($A_c$) of the specimen.

$$\Delta\sigma = \frac{P_a}{A_c} \tag{4.2}$$

During the calculation of the deviator stress, the change in the cross-sectional area due to loading is considered. Therefore a corrected cross-sectional area is calculated for each strain level using the equation 4.3.

$$A_c = A_0 \frac{(1-\varepsilon_v)}{(1-\varepsilon_a)} \tag{4.3}$$

Shear Strength Parameters of soil can be calculated by stress path diagrams, which connects a series of points where each point represent a stress state under different confining pressures. Stress path can be constructed by several methods.

In this study, "Modified Failure Envelope ($K_f$-Line) Method" developed by Lambe (1964) as cited in Das (2010) was adopted for calculation of total shear strength parameters which plots the envelope as a function of p and q, where p and q are the coordinates of the top of the Mohr circle (see equations 4.4 and 4.5).

$$p = \frac{(\sigma_1 + \sigma_3)}{2} \tag{4.4}$$

$$q = \frac{(\sigma_1 - \sigma_3)}{2} \tag{4.5}$$

The modified failure envelope is constructed as shown in Figure 4.4 and the shear strength parameters such as cohesion and angle of friction is determined by the Equations (4.6) and (4.7).

$$\phi = \sin^{-1}[\tan(\alpha)] \tag{4.6}$$

$$c = d / \cos(\phi) \tag{4.7}$$

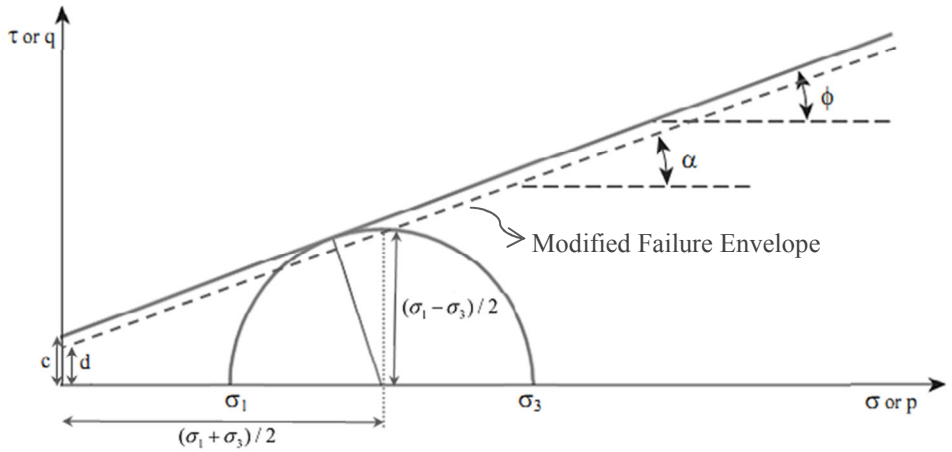


**Figure 4.4.** The Modified Failure Envelope (After Lambe, 1964)

In addition to the modified failure envelope, stress paths were used for representing the results achieved in triaxial tests under different pressures; connecting series of points, each representing the stress state for selected strain levels during the testing progress.

As an approach, approximate theoretical in-situ condition at rest was calculated and plotted using the average of $K_0$ values obtained by the equations (4.8) and (4.9), assuming that effective angle of friction (ϕ') is equal to the angle of friction in terms of total stress (ϕ), for partially saturated Ankara Clay. Therefore a slight difference shall be expected for actual in-situ conditions.

Lateral earth pressure at rest according to Mayne and Kulhawy (1982);

$$K_0 = (1-\sin\phi') \times (OCR)^{\sin\phi'} \tag{4.8}$$

Lateral earth pressure at rest according to Eurocode-7 (BS EN 1997-1:2004);

$$K_0 = (1-\sin\phi') \times \sqrt{OCR} \tag{4.9}$$

## 4.3. Investigation of Anisotropy in Compressibility

Compression of the soils might be described as the volume decrease in soil due to rearrangement of soil particles in a new, closer position as a result of increase in stress. The compressibility of the soil will mainly depend on the structural arrangement of the soil particles and the degree of saturation. In theory, water and soil particles are accepted to be incompressible. Therefore, while dry and partially saturated soils are more compressible due to the presence of air in the voids, some amount of pore water extrusion is needed for the compression of a fully saturated soil (Craig, 2004).

The phenomena of reduction in volume due to slow drainage of the pore water from the voids in a fine-grained, low permeability soil, and the transfer of the stress from dissipating pore water to the soil particles, is called *consolidation*. Therefore the compressibility characteristics of the clays will also be related to the consolidation properties of the soil. The one-dimensional consolidation and compressibility characteristics of a soil might be determined by an oedometer (consolidation) test.

### 4.3.1. The Oedometer Test

The oedometer test involves the determination of consolidation characteristics of a saturated or near-saturated, laterally confined, disc shaped soil specimen with free drainage in vertical direction, under different pressure levels.

This test is mainly applied on undisturbed samples of fine grained soils naturally sedimented in water, although the same procedure is applicable with additional evaluation to the compacted specimens or soils formed by other natural processes (ASTM D2435-04).

During the execution of oedometer / one-dimensional consolidation tests, BS 1377-5:1990 was followed as the regulatory standard.

#### 4.3.1.1. Experimental Apparatus

A typical oedometer test device was used in this study, which consisted of three main components;

*a) Consolidation Cell:*

Consolidation Cell or consolidometer is the seat of the specimen with the sub-components as shown in the Figure 4.5.

The specimen, which was laterally confined by the fixed consolidation ring, was placed between two porous stones in order to allow drainage in both vertical directions. The porous stones had a negligible compressibility, and they were thick enough to prevent breaking under the applied loads. A rigid, centrally mounted, loading cap was placed on the top porous stone for transmitting the load from the load device to the specimen. The consolidation cell was capable of holding water with a level higher than the upper porous stone and all components used in the cell were non-corrosive.

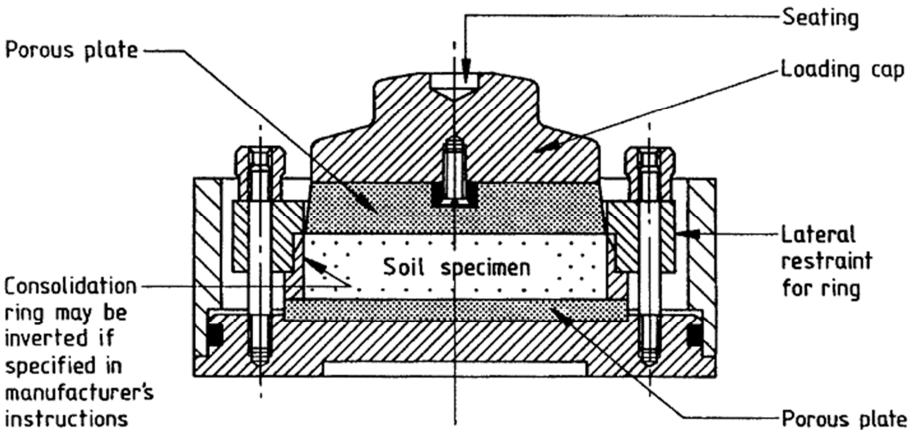


**Figure 4.5.** A Typical Consolidation Cell (BS 1377-5:1990)

*b) Loading Device:*

The loading device, with a counterbalanced lever system, allowed the application of an axial pressure on the specimen through a lever arm, by increasing the calibrated weights on the loading device.

The device was capable of maintaining the applied loads for a long time and was capable of the applying the load immediately without significant impact.

*c) Read-out Unit:*

A displacement transducer (LVDT - Linear Variable Differential Transformer) with 0.001 mm sensitivity was used for measuring the deformation of the sample. Data gathered from the transducers through readout unit were recorded to the computer simultaneously.

**Figure 4.6.** The Consolidation Units used in the Study

#### 4.3.1.2. Testing Procedure:

The oedometer specimens were prepared from undisturbed samples taken from the sampling tubes, in accordance to BS 1377-1:1990. The sample size used for the consolidation test was 20×50 mm. During the preparation of the specimen, irregularities, gravels and moisture loss were tried to be avoided.

a. After the specimen is ready for the placement into the Consolidation Cell, the bottom porous stone is soaked and placed into the central socket, with a filter paper on top in order to prevent clogging due to fine particles.

b. Upper filter paper, upper wet porous stone and loading cap are placed on top of the specimen inside the cutter ring, which is seated on top the consolidation ring. Then the specimen and the accessories placed on top are firmly pushed into the consolidation ring.

c. Following the fixing of the consolidation ring into the consolidation cell, the cell is placed into the loading device and transducers are connected.

d. A small seating pressure about 2 kPa is applied to the specimen while filling the cell with water, checking that no swelling occurs. If swelling occurs, the load is increased until the swelling stops. This load is recorded as swelling pressure.

e. After filling the cell, the initial load shall be applied and strain recording shall be initiated. The initial load must be higher than the swelling pressure. If any swelling is observed, the next phase of loading starts immediately.

f. The applied load shall be held constant for 24 hours and shall be doubled afterwards. For this study, the typical loading sequence was; 50, 100, 200, 400, 800, 1600 kPa.

g. After the loading phase is completed, the unloading phase starts. The selected unloading sequence for this study was; 1600, 400, 100, 50 kPa.

h. At the end of the test, the water in the cell is emptied and the final weight of the specimen is measured. Then specimen is put into oven with a temperature maintained at 105°C. After 24 hours, the dry weight of the specimen is recorded for the determination of initial and final water contents.

#### 4.3.1.3. The Calculations

The compressibility of the clay can be represented by the coefficient of volume compressibility ($m_v$) for a specific load range.

The *coefficient of volume compressibility,* $m_v$ is the volume change per unit volume per unit increase in effective stress (Craig, 2004). The coefficient of volume compressibility, $m_v$ is not a constant but varying value depending on the stress range over which is calculated.

$$m_v = \frac{1}{H_0}\left(\frac{H_0 - H_1}{\sigma_1' - \sigma_0'}\right) \tag{4.10}$$

where;

$m_v$ : Coefficient of Volume Compressibility ($cm^2/kg$)

$H_0$ : Initial Height of the specimen at the beginning of the loading phase (cm)

$H_1$ : Final Height of the specimen at the end of the loading phase (cm)

$\sigma'_0$ : Initial effective stress at the beginning of the loading phase ($kg/cm^2$)

$\sigma'_1$ : Final effective stress at the end of the loading phase ($kg/cm^2$)

# CHAPTER 5

# RESULTS

## 5.1. Anisotropy in Undrained Shear Strength

A total number of 56 specimens from four different locations were subjected to unconsolidated-undrained triaxial compression test. The results obtained from each site were compared for different directions.

**Table 5.1.** The Number of Triaxial Tests Performed for Each Site

| Site | Number of UU Triaxial Tests |
|---|---|
| **A1** | 6 |
| **A2** | 22 |
| **B** | 10 |
| **C** | 18 |

### 5.1.1. Results Obtained from Site A1

A total number of 6 specimens were tested for the preliminary testing site, A1.

**Table 5.2.** The Number of UU triaxial tests performed on Site-A1

| Sampling Orientation | Type of Triaxial Test | Number of Specimens Tested | | | |
|---|---|---|---|---|---|
| | | **Cell Pressure (kPa)** | | | |
| | | *250* | *350* | *450* | *Total* |
| **Vertical Direction** | UU | 1 | 1 | 1 | 3 |
| **Horizontal Direction** | UU | 1 | 1 | 1 | 3 |

**Table 5.3.** Results Obtained under 250 kPa Confining Pressure for Site-A1

| *Confining Pressure: 250 kPa* | Sample Size (mm×mm) | Moisture Content (%) | Bulk Density ($kg/cm^3$) | Deviator Stress (kPa) | Strain at Failure (%) |
|---|---|---|---|---|---|
| **Vertical – A1-VA** | 200×100 | 34.49 | 1.77 | 121.72 | 9.9 |
| **Horizontal – A1-HA** | 185×100 | 36.54 | 1.85 | 144.35 | 14 |

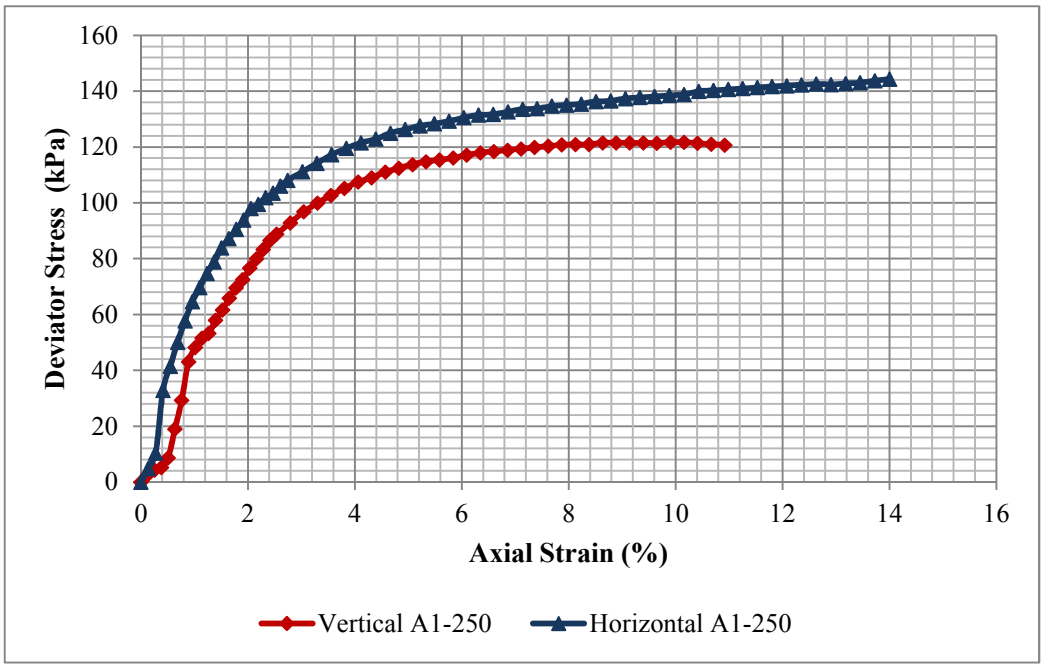


**Figure 5.1.** Comparison of Deviator Stresses under 250 kPa Cell Pressure

**Table 5.4.** Anisotropy Ratio of Undrained Shear Strength at Failure Stress under 250 kPa Confining Pressure for Site-A1

| | Vertical | Horizontal | (K=H/V) |
|---|---|---|---|
| Mean Deviator Stress ($\sigma_1$-$\sigma_3$) | 121.72 | 144.35 | **1.19** |
| Mean Principal Stress Ratio ($\sigma_1/\sigma_3$) | 1.487 | 1.577 | **1.06** |

**Table 5.5.** Anisotropy Ratio of Undrained Shear Strength in terms of Mean Deviator Stresses at Different Strain Levels under 250 kPa C. Pressure for Site-A1

| Strain - ε (%) | Deviator Stress - $\sigma_1$-$\sigma_3$ (kPa) | | Anisotropy Ratio |
|---|---|---|---|
| | **Vertical** | **Horizontal** | **(K=H/V)** |
| **1 %** | 48.20 | 69.66 | **1.45** |
| **2 %** | 76.67 | 97.93 | **1.28** |
| **3 %** | 96.82 | 111.15 | **1.15** |
| **4 %** | 107.47 | 121.14 | **1.13** |
| **5 %** | 113.75 | 126.91 | **1.12** |
| **6 %** | 117.09 | 130.51 | **1.11** |
| **7 %** | 119.16 | 133.50 | **1.12** |
| **8 %** | 120.86 | 135.42 | **1.12** |
| **9 %** | 121.49 | 137.36 | **1.13** |
| **10 %** | 121.68 | 138.81 | **1.14** |

**Table 5.6.** Anisotropy Ratio of Undrained Shear Strength in terms of Mean Principal Stress Ratio at Diff. Strain Levels under 250 kPa C. Pressure for Site-A1

| Strain - ε (%) | Principal Stress Ratio - $\sigma_1/\sigma_3$ | | Anisotropy Ratio |
|---|---|---|---|
| | **Vertical** | **Horizontal** | **(K=H/V)** |
| **1 %** | 1.193 | 1.279 | **1.07** |
| **2 %** | 1.307 | 1.392 | **1.07** |
| **3 %** | 1.387 | 1.445 | **1.04** |
| **4 %** | 1.430 | 1.485 | **1.04** |
| **5 %** | 1.455 | 1.508 | **1.04** |
| **6 %** | 1.468 | 1.522 | **1.04** |
| **7 %** | 1.477 | 1.534 | **1.04** |
| **8 %** | 1.483 | 1.542 | **1.04** |
| **9 %** | 1.486 | 1.549 | **1.04** |
| **10 %** | 1.487 | 1.555 | **1.05** |

**Table 5.7.** Results Obtained under 350 kPa Confining Pressure for Site-A1

| *Confining Pressure: 350 kPa* | Sample Size (mm×mm) | Moisture Content (%) | Bulk Density (kg/cm$^3$) | Deviator Stress (kPa) | Strain at Failure (%) |
|---|---|---|---|---|---|
| **Vertical – A1-VA** | 200x100 | 36.44 | 1.79 | 143.64 | 10.67 |
| **Horizontal – A1-HA** | 200x100 | 34.87 | 1.81 | 168.24 | 15.24 |

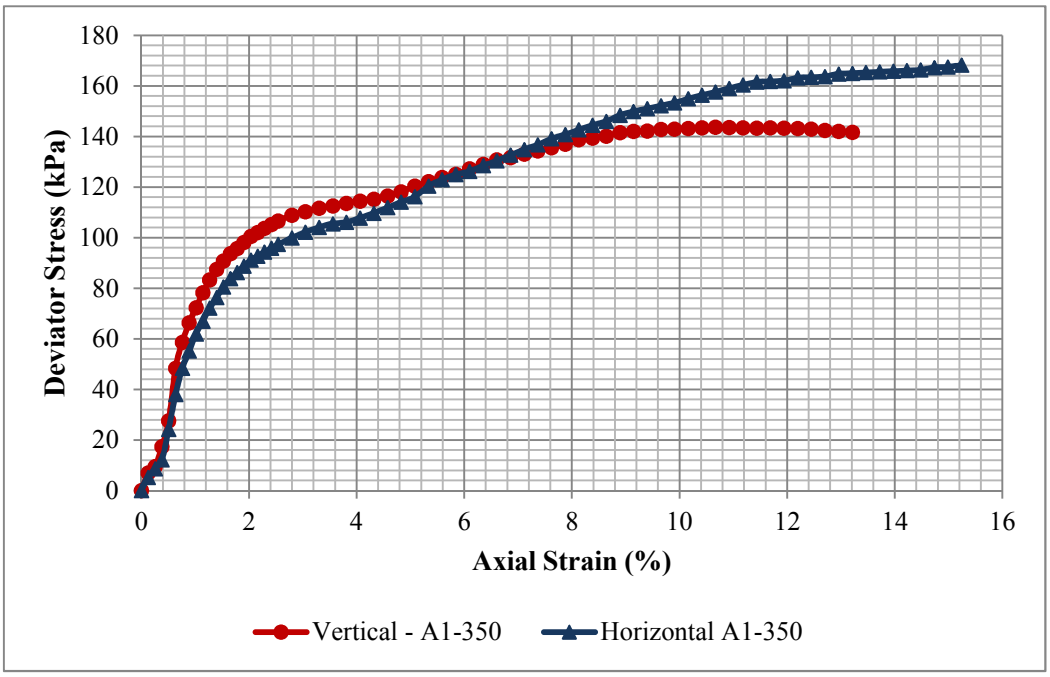


**Figure 5.2.** Comparison of Deviator Stresses under 350 kPa Cell Pressure

**Table 5.8.** Anisotropy Ratio of Undrained Shear Strength at Failure Stress under 350 kPa Confining Pressure for Site-A1

| | Vertical | Horizontal | (K=H/V) |
|---|---|---|---|
| Mean Deviator Stress ($\sigma_1$-$\sigma_3$) | 143.64 | 168.24 | **1.17** |
| Mean Principal Stress Ratio ($\sigma_1/\sigma_3$) | 1.41 | 1.481 | **1.05** |

**Table 5.9.** Anisotropy Ratio of Undrained Shear Strength in terms of Mean Deviator Stresses at Different Strain Levels under 350 kPa C. Pressure for Site-A1

| Strain - ε (%) | Deviator Stress - $\sigma_1$-$\sigma_3$ (kPa) | | Anisotropy Ratio |
|---|---|---|---|
| | **Vertical** | **Horizontal** | **(H/V)** |
| **1 %** | 72.30 | 61.97 | **0.86** |
| **2 %** | 100.52 | 91.15 | **0.91** |
| **3 %** | 110.30 | 102.21 | **0.93** |
| **4 %** | 114.47 | 107.80 | **0.94** |
| **5 %** | 120.34 | 116.22 | **0.97** |
| **6 %** | 127.20 | 126.23 | **0.99** |
| **7 %** | 133.08 | 134.86 | **1.01** |
| **8 %** | 138.80 | 142.63 | **1.03** |
| **9 %** | 142.00 | 149.89 | **1.06** |
| **10 %** | 143.21 | 154.91 | **1.08** |
| **11 %** | 143.44 | 160.41 | **1.12** |
| **12 %** | 143.17 | 163.14 | **1.14** |
| **13 %** | 141.66 | 165.01 | **1.16** |

**Table 5.10.** Anisotropy Ratio of Undrained Shear Strength in terms of Mean Principal Stress Ratio at Diff. Strain Levels under 350 kPa C. Pressure for Site-A1

| Strain - ε (%) | Principal Stress Ratio - $\sigma_1/\sigma_3$ | | Anisotropy Ratio |
|---|---|---|---|
| | **Vertical** | **Horizontal** | **(H/V)** |
| **1 %** | 1.207 | 1.177 | **0.98** |
| **2 %** | 1.287 | 1.26 | **0.98** |
| **3 %** | 1.315 | 1.292 | **0.98** |
| **4 %** | 1.327 | 1.308 | **0.99** |
| **5 %** | 1.344 | 1.332 | **0.99** |
| **6 %** | 1.363 | 1.361 | **1.00** |
| **7 %** | 1.38 | 1.385 | **1.00** |
| **8 %** | 1.397 | 1.408 | **1.01** |
| **9 %** | 1.406 | 1.428 | **1.02** |
| **10 %** | 1.409 | 1.443 | **1.02** |
| **11 %** | 1.41 | 1.458 | **1.03** |
| **12 %** | 1.409 | 1.466 | **1.04** |
| **13 %** | 1.405 | 1.471 | **1.05** |

**Table 5.11.** Results Obtained under 450 kPa Confining Pressure for Site-A1

| *Confining Pressure: 350 kPa* | Sample Size (mm×mm) | Moisture Content (%) | Bulk Density (kg/cm$^3$) | Deviator Stress (kPa) | Strain at Failure (%) |
|---|---|---|---|---|---|
| **Vertical – A1-VC** | 200x100 | 36.32 | 1.82 | 96.79 | 7.12 |
| **Horizontal – A1-HC** | 200x100 | 37.96 | 1.73 | 149.52 | 14.98 |

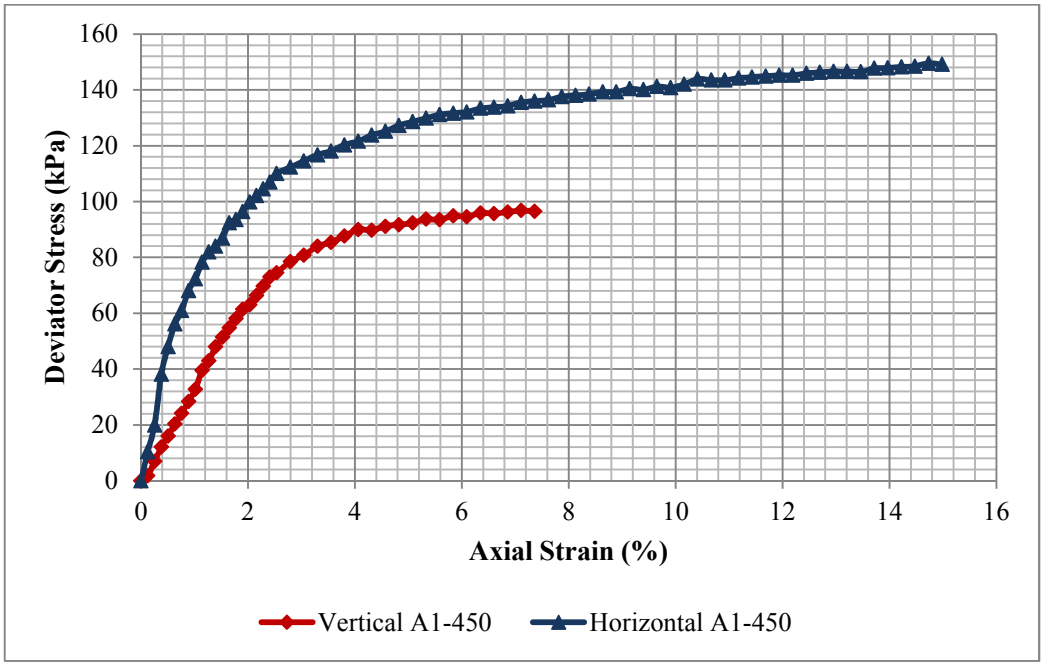


**Figure 5.3.** Comparison of Deviator Stresses under 450 kPa Cell Pressure

**Table 5.12.** Anisotropy Ratio of Undrained Shear Strength at Failure Stress under 450 kPa Confining Pressure for Site-A1

| **Cell Pressure: 450 kPa** | Vertical | Horizontal | (K=H/V) |
|---|---|---|---|
| Mean Deviator Stress ($\sigma_1$-$\sigma_3$) | 96.79 | 149.52 | **1.55** |
| Mean Principal Stress Ratio ($\sigma_1/\sigma_3$) | 1.215 | 1.322 | **1.09** |

The results of obtained under 450 kPa cell pressure were omitted due to irrelevant results in the vertical specimen, which is probably caused by a discontinuity.

**Table 5.13.** The mean Anisotropy Ratio of Undrained Shear Strength in terms of Deviator Stress for Site-A1

| Confining Pressure (kPa) | Mean Deviator Stress ($\sigma_1$-$\sigma_3$) at Failure (kPa) | | Anisotropy Ratio |
|---|---|---|---|
| | **Vertical** | **Horizontal** | **(H/V)** |
| *250* | 121.72 | 144.35 | **1.19** |
| *350* | 143.64 | 168.24 | **1.17** |

**Table 5.14.** The mean Anisotropy Ratio of Undrained Shear Strength in terms of Principal Stress Ratio for Site-A1

| Confining Pressure (kPa) | Mean Principal Stress Ratio ($\sigma_1/\sigma_3$) at Failure (kPa) | | Anisotropy Ratio |
|---|---|---|---|
| | **Vertical** | **Horizontal** | **(H/V)** |
| *250* | 1.487 | 1.577 | **1.06** |
| *350* | 1.410 | 1.481 | **1.05** |

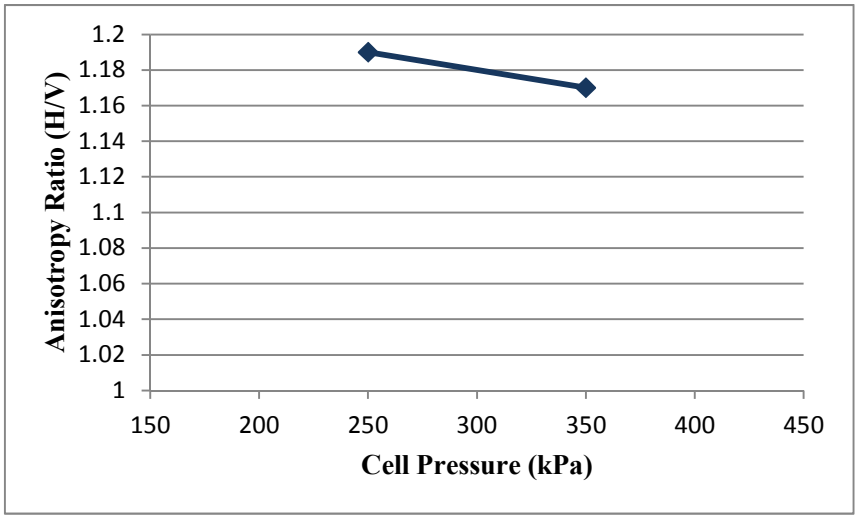


**Figure 5.4.** Variation of Anisotropy Ratio of Undrained Shear Strength in terms of Deviator Stress at Different Confining Pressure Levels for Site-A1

The total shear strength parameters of the samples were calculated using "Modified Failure Envelope" method from the failure stresses obtained under 250 and 350 kPa pressures. Approximate in-situ condition according to $K_0$ calculated by equations (4.8) and (4.9) was plotted and stress paths were drawn by plotting the changes in mean stress at different strain levels for each pressure level.

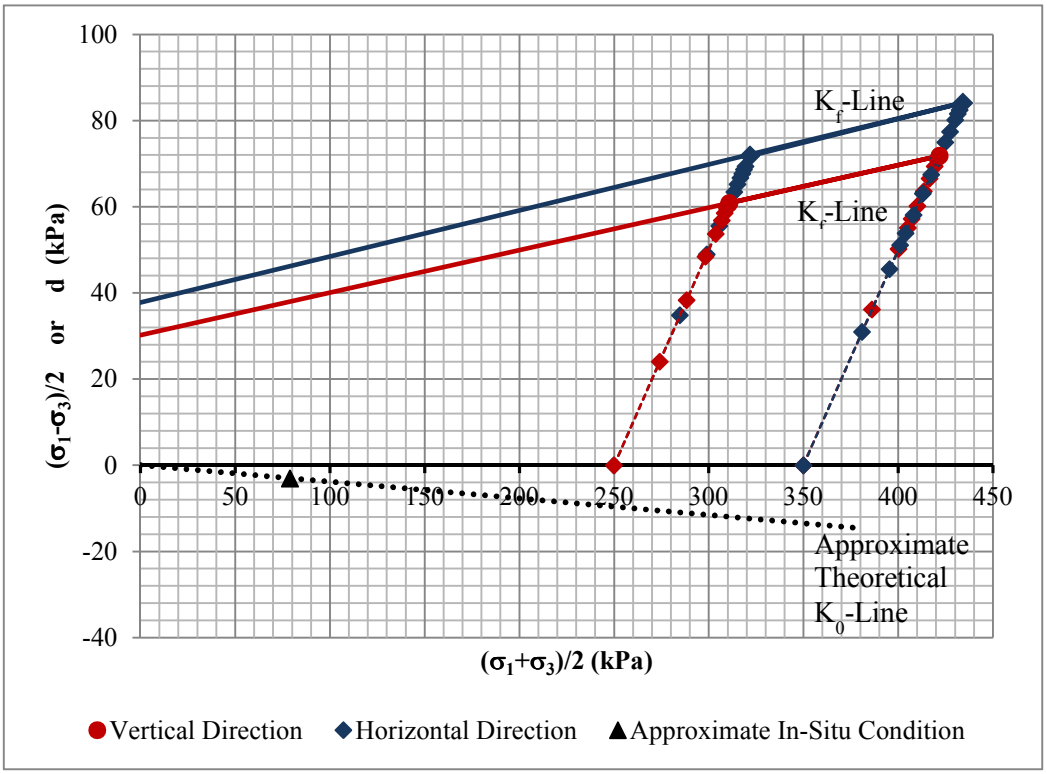


**Figure 5.5.** Failure Envelopes Developed for Site-A1

**Table 5.15.** Total shear strength parameters for each direction at Site-A1

| Total Shear Strength Parameters (kPa) | | | |
|---|---|---|---|
| Vertical | | Horizontal | |
| d | α | d | α |
| 30.2 | 6° | 37.8 | 6° |
| c | ϕ | c | ϕ |
| 30.37 | 6° | 38 | 6° |

### 5.1.2. Results Obtained from Site-A2

Among the samples gathered from Site-A2; a total number of 22 triaxial tests were performed. For each pressure level, at least two control groups were assigned. The specimens from Site-A2 failed at strain rates ranging between app. 2 ~ 6 %. It was also observed that, although the majority of the failures did not occur directly through polished fragment/slickenside surfaces, most of the failure planes were guided by such formations.

**Table 5.16.** The Number of UU Triaxial Tests Performed for Site-A2

| Sampling Orientation | Type of Triaxial Test | Number of Specimens Tested | | | |
|---|---|---|---|---|---|
| | | **Cell Pressure (kPa)** | | | |
| | | *250* | *350* | *450* | *Total* |
| **Vertical Direction** | UU | 2 | 2 | 7 | 11 |
| **Horizontal Direction** | UU | 2 | 2 | 7 | 11 |

Due to the scattered distribution of the deviator stresses under 450 kPa pressure, the number of control groups were raised to seven for this pressure level. In order to present the level of scatter in the results, the ratio of the highest and lowest failure stresses obtained for different pressure levels are presented in Table 5.17.

**Table 5.17.** The Ratio of Highest and Lowest Failure Stresses for each Pressure Level for Site-A2

| Confining Pressure | Vertical Specimen Deviator Stress (kPa) | | | Horizontal Specimen Deviator Stress (kPa) | | |
|---|---|---|---|---|---|---|
| | **Lowest** | **Highest** | **H/L** | **Lowest** | **Highest** | **H/L** |
| *250 kPa* | 277.31 | 279.63 | 1.01 | 303.28 | 311.57 | 1.03 |
| *350 kPa* | 360.62 | 379.06 | 1.05 | 363.38 | 381.19 | 1.05 |
| *450 kPa* | 321.43 | 415.65 | 1.29 | 288.9 | 420.44 | 1.46 |

**Table 5.18.** Results Obtained under 250 kPa Confining Pressure for Site-A2

| *Confining Pressure: 250 kPa* | Sample Size (mm×mm) | Moisture Content (%) | Bulk Density (kg/cm$^3$) | Deviator Stress (kPa) | Strain at Failure (%) |
|---|---|---|---|---|---|
| **Vertical – A2-VA** | 200x100 | 35.69 | 1.93 | 273.74 | 5.33 |
| **Vertical – A2-VB** | 185x100 | 37.55 | 1.91 | 266.93 | 5.84 |
| Vertical Mean | | | | **270.34** | |
| **Horizontal – A2-HA** | 200x100 | 35.51 | 1.87 | 311.57 | 5.08 |
| **Horizontal – A2-HB** | 190x100 | 33.68 | 1.96 | 300.04 | 4.01 |
| Horizontal Mean | | | | **305.81** | |

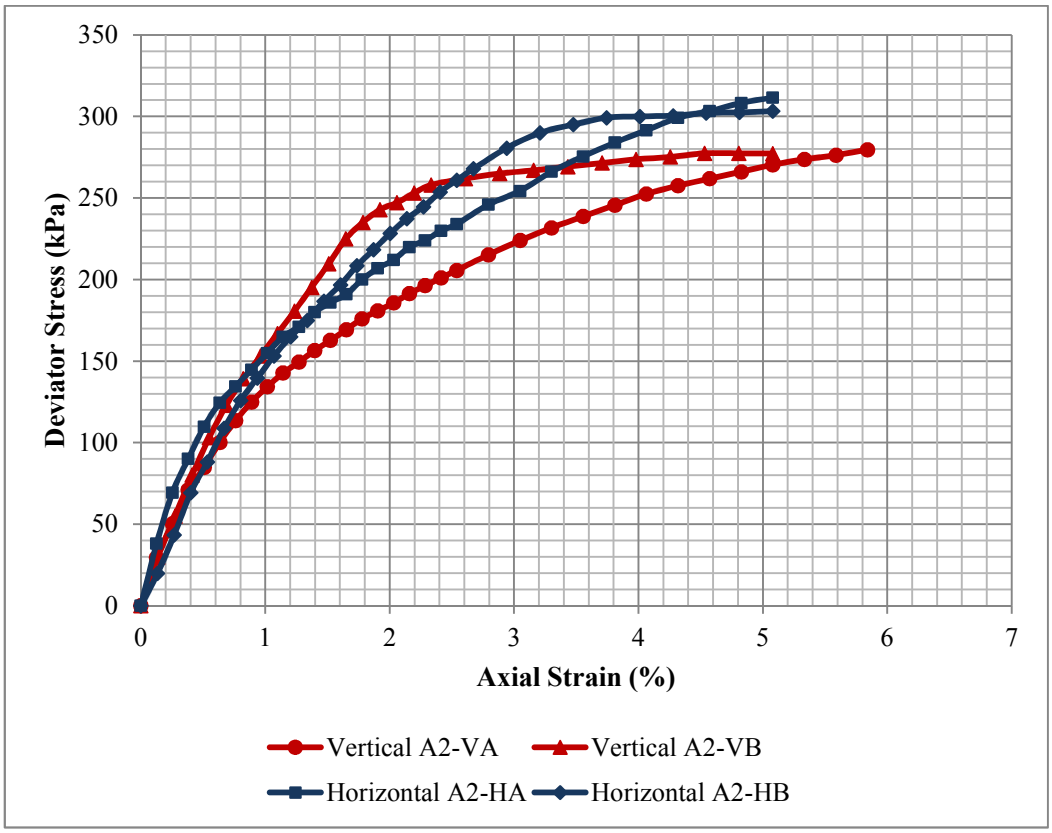


**Figure 5.6.** Comparison of Deviator Stresses under 250 kPa Cell Pressure

**Table 5.19.** Anisotropy Ratio of Undrained Shear Strength at Failure Stress under 250 kPa Confining Pressure

| **Cell Pressure: 250 kPa** | Vertical | Horizontal | (K=H/V) |
|---|---|---|---|
| Mean Deviator Stress - $\sigma_1$-$\sigma_3$ (kPa) | 270.34 | 305.81 | **1.13** |
| Mean Principal Stress Ratio - $\sigma_1/\sigma_3$ | 2.081 | 2.223 | **1.07** |

**Table 5.20.** Anisotropy Ratio of Undrained Shear Strength in terms of Mean Deviator Stresses at Different Strain Levels under 250 kPa C. Pressure for Site-A2

| Strain - ε | Deviator Stress - $\sigma_1$-$\sigma_3$ (kPa) | | Anisotropy Ratio |
|---|---|---|---|
| | **Vertical** | **Horizontal** | **(H/V)** |
| **1%** | 93.97 | 99.05 | **1.05** |
| **2%** | 150.6 | 154.03 | **1.02** |
| **3%** | 193.82 | 191.39 | **0.99** |
| **4%** | 219.36 | 224.71 | **1.02** |
| **5%** | 234.33 | 250.95 | **1.07** |
| **6%** | 245.8 | 272.11 | **1.11** |

**Table 5.21.** Anisotropy Ratio of Undrained Shear Strength in terms of Mean Principal Stress Ratio at Diff. Strain Levels under 250 kPa C. Pressure for Site-A2

| Strain - ε | Principal Stress Ratio - $\sigma_1/\sigma_3$ | | Anisotropy Ratio |
|---|---|---|---|
| | **Vertical** | **Horizontal** | **(H/V)** |
| **1%** | 1.376 | 1.396 | **1.01** |
| **2%** | 1.602 | 1.616 | **1.01** |
| **3%** | 1.775 | 1.766 | **0.99** |
| **4%** | 1.877 | 1.899 | **1.01** |
| **5%** | 1.937 | 2.004 | **1.03** |
| **6%** | 1.983 | 2.088 | **1.05** |

**Table 5.22.** Results Obtained under 350 kPa Confining Pressure for Site-A2

| *Confining Pressure: 350 kPa* | Sample Size (mm×mm) | Moisture Content (%) | Bulk Density (kg/cm$^3$) | Deviator Stress (kPa) | Strain at Failure (%) |
|---|---|---|---|---|---|
| **Vertical – A2-VC** | 200×100 | 36.99 | 1.83 | 379.06 | 4.06 |
| **Vertical – A2-VD** | 205×108 | 32.53 | 1.9 | 360.62 | 5.95 |
| Vertical Mean | | | | **369.84** | |
| **Horizontal – A2-HC** | 200×100 | 32.07 | 1.91 | 381.19 | 4.57 |
| **Horizontal – A2-HD** | 175×105 | 31.19 | 1.89 | 363.38 | 5.81 |
| Horizontal Mean | | | | **372.29** | |

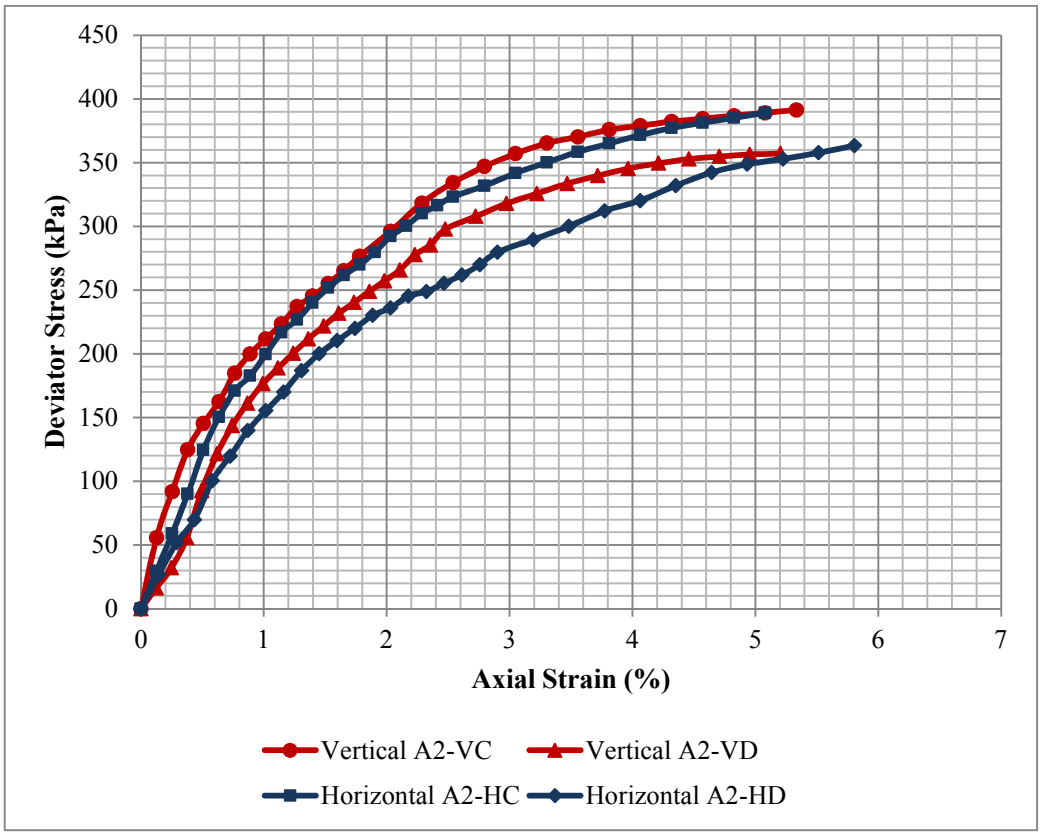


**Figure 5.7.** Comparison of Deviator Stresses under 350 kPa Cell Pressure

**Table 5.23.** Anisotropy Ratio of Undrained Shear Strength at Failure Stress under 350 kPa Confining Pressure for Site-A2

| **Cell Pressure: 350 kPa** | Vertical | Horizontal | (K=H/V) |
|---|---|---|---|
| Mean Deviator Stress - $\sigma_1$-$\sigma_3$ (kPa) | 369.84 | 372.29 | **1.01** |
| Mean Principal Stress Ratio - $\sigma_1/\sigma_3$ | 2.057 | 2.064 | **1** |

**Table 5.24.** Anisotropy Ratio of Undrained Shear Strength in terms of Mean Deviator Stresses at Different Strain Levels under 350 kPa C. Pressure for Site-A2

| Strain - ε (%) | Deviator Stress - $\sigma_1$-$\sigma_3$ (kPa) | | Anisotropy Ratio |
|---|---|---|---|
| | **Vertical** | **Horizontal** | **(H/V)** |
| **1 %** | 194.08 | 177.52 | **0.91** |
| **2 %** | 276.66 | 264.11 | **0.95** |
| **3 %** | 337.43 | 312.47 | **0.93** |
| **4 %** | 362.21 | 345.92 | **0.96** |
| **5 %** | 372.71 | 369.39 | **0.99** |
| **6 %** | 379.27 | 387.79 | **1.02** |

**Table 5.25.** Anisotropy Ratio of Undrained Shear Strength in terms of Mean Principal Stress Ratio at Diff. Strain Levels under 350 kPa C. Pressure for Site-A2

| Strain - ε (%) | Deviator Stress - $\sigma_1$-$\sigma_3$ (kPa) | | Anisotropy Ratio |
|---|---|---|---|
| | **Vertical** | **Horizontal** | **(H/V)** |
| **1 %** | 194.08 | 177.52 | **0.91** |
| **2 %** | 276.66 | 264.11 | **0.95** |
| **3 %** | 337.43 | 312.47 | **0.93** |
| **4 %** | 362.21 | 345.92 | **0.96** |
| **5 %** | 372.71 | 369.39 | **0.99** |
| **6 %** | 379.27 | 387.79 | **1.02** |

**Table 5.26.** Results Obtained under 450 kPa Confining Pressure for Site-A2

| *Confining Pressure: 450 kPa* | Sample Size (mm×mm) | Moisture Content (%) | Bulk Density (kg/cm$^3$) | Deviator Stress (kPa) | Strain at Failure (%) |
|---|---|---|---|---|---|
| **Vertical – A2-VE** | 210×100 | 35.03 | 1.86 | 386.36 | 2.66 |
| **Vertical – A2-VF** | 205×100 | 36.42 | 1.87 | 415.65 | 2.73 |
| **Vertical – A2-VG** | 190×100 | 33.78 | 1.93 | 328.03 | 2.27 |
| **Vertical – A2-VH *** | 210×100 | 32.17 | 1.84 | 153.88 | 1.69 |
| **Vertical – A2-VI *** | 210×100 | 35.16 | 1.84 | 155.59 | 1.69 |
| **Vertical – A2-VJ** | 185×110 | 33.21 | 1.90 | 321.43 | 2.33 |
| **Vertical – A2-VK** | 150×110 | 36.73 | 1.96 | 396.26 | 3.90 |
| Vertical Mean (* Omitting A2-VH & A2-VI) | | | | **369.55** | |
| **Horizontal – A2-HE** | 200×100 | 34.74 | 1.93 | 417.60 | 3.05 |
| **Horizontal – A2-HF** | 200×100 | 33.55 | 1.90 | 288.90 | 2.29 |
| **Horizontal – A2-HG** | 200×100 | 30.95 | 1.92 | 299.87 | 2.03 |
| **Horizontal – A2-HH** | 185×100 | 33.91 | 1.93 | 299.33 | 2.20 |
| **Horizontal – A2-HI** | 190×100 | 35.09 | 1.91 | 303.37 | 4.01 |
| **Horizontal – A2-HJ** | 160×100 | 31.31 | 1.90 | 420.44 | 3.49 |
| **Horizontal – A2-HK** | 160×100 | 32.96 | 1.87 | 313.87 | 3.81 |
| Horizontal Mean | | | | **334.77** | |

It should be noted that, the failure of Vertical A2-VH and A2-VI is probably due to discontinuities present in the samples; both samples broke at an early stage with a failure plane closer to the upper part of the specimen through polished slickenside surface. Therefore those results were omitted in the mean axial stress calculations.

The Deviator Stress vs. Axial Strain graph for 450 kPa cell pressure is presented in the Figure 5.8.

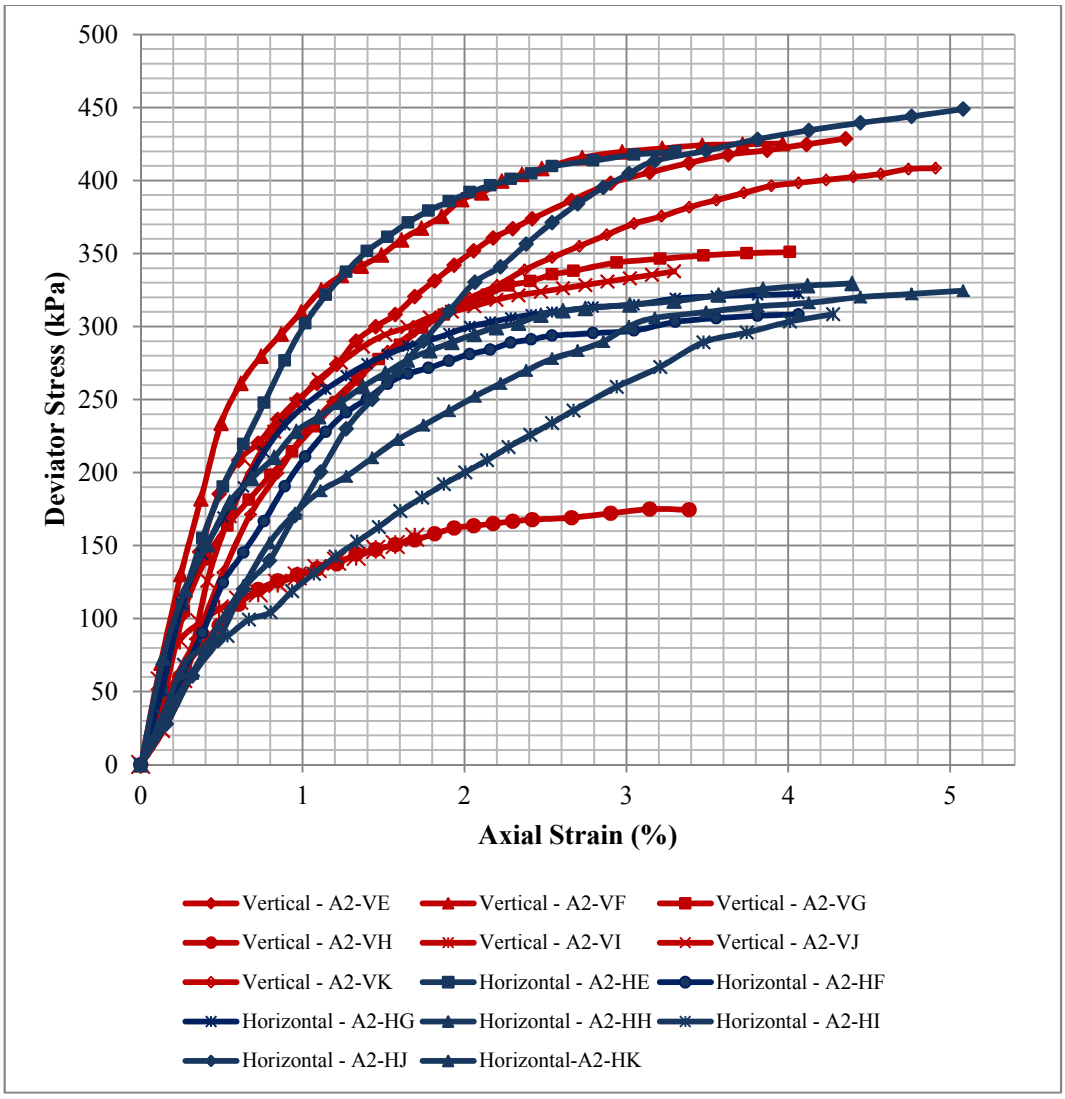


**Figure 5.8.** Comparison of Deviator Stresses under 450 kPa Cell Pressure

**Table 5.27.** Anisotropy Ratio of Undrained Shear Strength at Failure Stress under 450 kPa Confining Pressure for Site-A2

| **Cell Pressure: 450 kPa** | Vertical | Horizontal | (K=H/V) |
|---|---|---|---|
| Mean Deviator Stress - $\sigma_1$-$\sigma_3$ (kPa) | 369.55 | 334.77 | **0.91** |
| Mean Principal Stress Ratio - $\sigma_1/\sigma_3$ | 1.821 | 1.744 | **0.96** |

**Table 5.28.** Anisotropy Ratio of Undrained Shear Strength in terms of Mean Deviator Stresses at Different Strain Levels under 450 kPa C. Pressure for Site-A2

| Strain - ε (%) | Deviator Stress - $\sigma_1$-$\sigma_3$ (kPa) | | Anisotropy Ratio |
|---|---|---|---|
| | **Vertical** | **Horizontal** | **(H/V)** |
| **1 %** | 258.725 | 210.118 | **0.81** |
| **2 %** | 337.479 | 292.868 | **0.87** |
| **3 %** | 374.512 | 329.734 | **0.88** |
| **4 %** | 389.677 | 348.433 | **0.89** |

**Table 5.29.** Anisotropy Ratio of Undrained Shear Strength in terms of Mean Principal Stress Ratio at Diff. Strain Levels under 450 kPa C. Pressure for Site-A2

| Strain - ε (%) | Deviator Stress - $\sigma_1$-$\sigma_3$ (kPa) | | Anisotropy Ratio |
|---|---|---|---|
| | **Vertical** | **Horizontal** | **(H/V)** |
| **1 %** | 1.575 | 1.467 | **0.93** |
| **2 %** | 1.750 | 1.651 | **0.94** |
| **3 %** | 1.832 | 1.733 | **0.95** |
| **4 %** | 1.866 | 1.774 | **0.95** |

**Table 5.30.** The mean Anisotropy Ratio of Undrained shear strength in terms of Deviator Stress for Site-A2

| Confining Pressure (kPa) | Mean Deviator Stress at Failure (kPa) | | Anisotropy Ratio |
|---|---|---|---|
| | **Vertical** | **Horizontal** | **(K=H/V)** |
| *250* | 270.34 | 305.81 | **1.13** |
| *350* | 369.84 | 372.29 | **1.01** |
| *450* | 369.55 | 334.77 | **0.91** |

**Table 5.31.** The mean Anisotropy Ratio of Undrained shear strength in terms of Principal Stress Ratio for Site-A2

| Confining Pressure (kPa) | Mean Principal Stress Ratio ($\sigma_1/\sigma_3$) at Failure (kPa) | | Anisotropy Ratio |
|---|---|---|---|
| | **Vertical** | **Horizontal** | **(K=H/V)** |
| *250* | 2.081 | 2.223 | **1.07** |
| *350* | 2.057 | 2.064 | **1** |
| *450* | 1.821 | 1.744 | **0.96** |

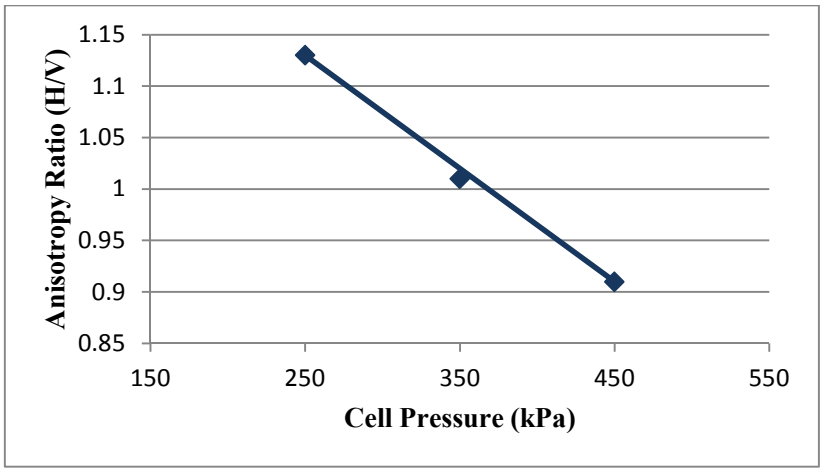


**Figure 5.9.** Variation of Anisotropy Ratio of Undrained Shear Strength in terms of Deviator Stress at Different Confining Pressure Levels for Site-A2

The total shear strength parameters of the samples were calculated using "Modified Failure Envelope" method from the failure stresses obtained under 250 and 450 kPa pressures. Approximate in-situ condition according to $K_0$ calculated by equations (4.8) and (4.9) was plotted and stress paths were drawn by plotting the changes in mean stress at different strain levels for each pressure level.

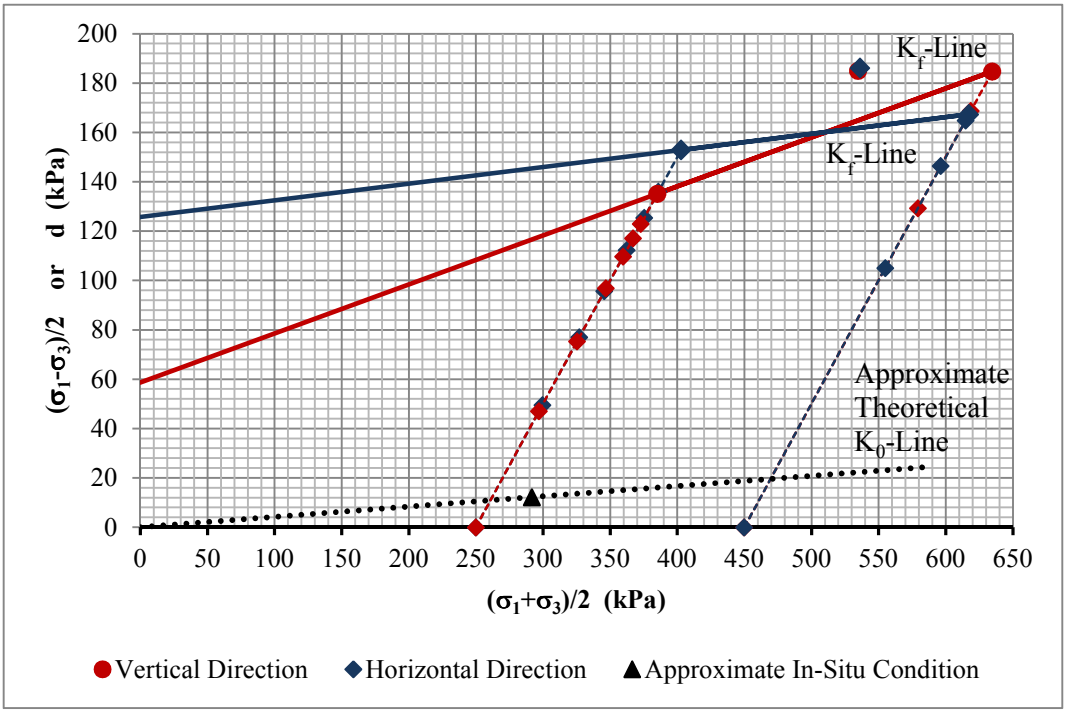


**Figure 5.10.** Failure Envelopes and Stress Paths Developed for Site-A2

**Table 5.32.** Total Shear Strength Parameters for each Direction at Site-A2

| Total Shear Strength Parameters (kPa) | | | |
|---|---|---|---|
| Vertical | | Horizontal | |
| d | α | d | α |
| 58.62 | 11° | 125.76 | 4° |
| c | ϕ | c | ϕ |
| 59.76 | 11.2° | 126.01 | 4° |

### 5.1.3. Results Obtained from Site-B

Among the samples gathered from Site-B; a total number of 10 triaxial tests were performed. The specimens failed at strain rates ranging between 3.10 ~ 5.43 % which were tested under the pressures of 250 kPa and 450 kPa.

**Table 5.33.** The Number of UU Triaxial Tests Performed for Site-B

| Sampling Orientation | Type of Test | Number of Specimens Tested | | | |
|---|---|---|---|---|---|
| | | **Confining Pressure (kPa)** | | | **Total** |
| | | *250* | *350* | *450* | - |
| **Vertical Direction** | UU | 2 | - | 3 | 5 |
| **Horizontal Direction** | UU | 2 | - | 3 | 5 |

Only for this site, a limited number of smaller size (50×100 mm) specimens were also tested and put into comparison as their results were compatible with large diameter specimens.

The lowest and highest deviator stresses obtained under specified confining pressures for different control group specimens are presented in Table 5.34.

**Table 5.34.** The Ratio of Highest and Lowest Failure Stresses for each Pressure Level for Site-B

| Confining Pressure | Vertical Specimen – Deviator Stress (kPa) | | | Horizontal Specimen – Deviator Stress (kPa) | | |
|---|---|---|---|---|---|---|
| | **Lowest** | **Highest** | **H/L** | **Lowest** | **Highest** | **H/L** |
| *250 kPa* | 703.1 | 741.17 | 1.05 | 610.62 | 650.37 | 1.07 |
| *450 kPa* | 865.39 | 908.56 | 1.05 | 805.97 | 943.54 | 1.17 |

**Table 5.35.** Results Obtained under 250 kPa Confining Pressure for Site-B

| *Confining Pressure: 250 kPa* | Sample Size (mm×mm) | Moisture Content (%) | Bulk Density (kg/cm$^3$) | Deviator Stress (kPa) | Strain at Failure (%) |
|---|---|---|---|---|---|
| **Vertical – B-VA** | 150x100 | 26.71 | 1.92 | 741.17 | 5.08 |
| **Vertical – B-VB** | 100x50 | 25.90 | 1.94 | 703.1 | 5.08 |
| Vertical Mean | | | | **722.09** | |
| **Horizontal – B-HA** | 195x100 | 30.36 | 1.86 | 610.62 | 4.17 |
| **Horizontal – B-HB** | 100x50 | 31.51 | 1.88 | 650.37 | 3.48 |
| Horizontal Mean | | | | **630.50** | |

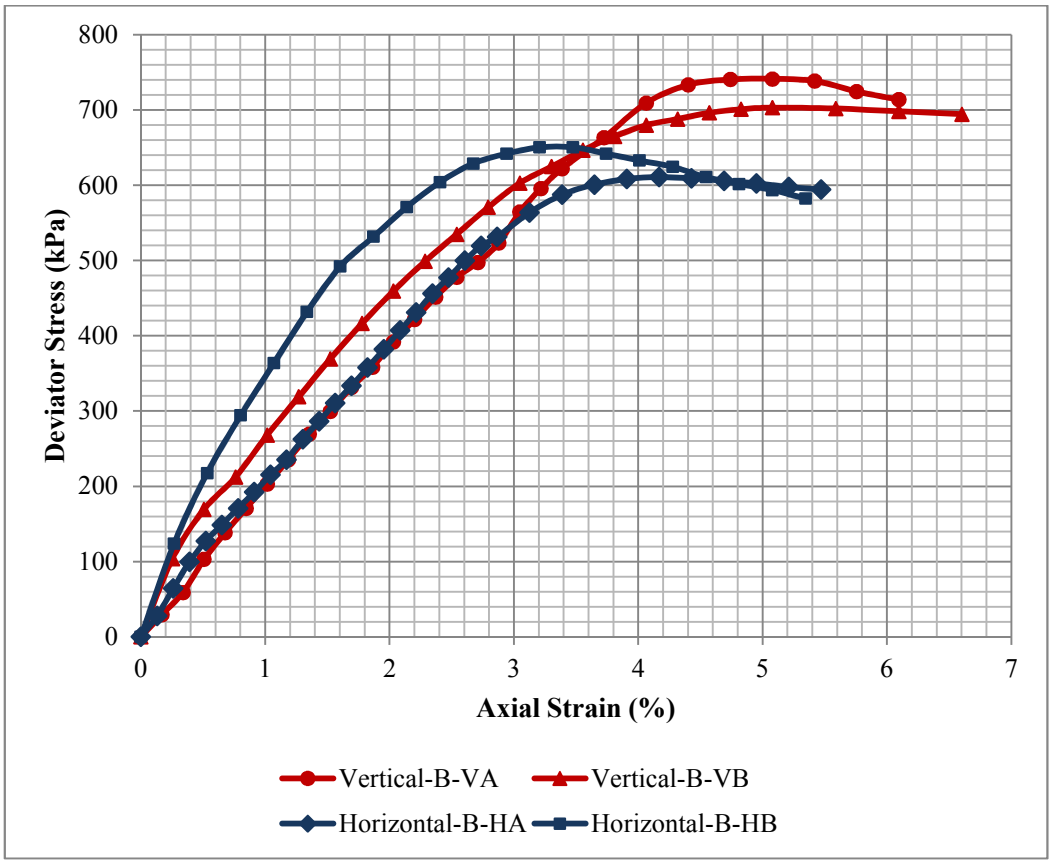


**Figure 5.11.** Comparison of Deviator Stresses under 250 kPa Cell Pressure

**Table 5.36.** Anisotropy Ratio of Undrained Shear Strength at Failure Stress under 250 kPa Confining Pressure for Site-B

| **Cell Pressure: 250 kPa** | Vertical | Horizontal | (K=H/V) |
|---|---|---|---|
| Mean Deviator Stress - $\sigma_1$-$\sigma_3$ (kPa) | 722.09 | 630.50 | **0.87** |
| Mean Principal Stress Ratio - $\sigma_1/\sigma_3$ | 880.47 | 860.27 | **0.98** |

**Table 5.37.** Anisotropy Ratio of Undrained Shear Strength in terms of Mean Deviator Stresses at Different Strain Levels under 250 kPa C. Pressure for Site-B

| Strain - ε | Deviator Stress - $\sigma_1$-$\sigma_3$ (kPa) | | Anisotropy Ratio |
|---|---|---|---|
| | **Vertical** | **Horizontal** | **(H/V)** |
| **1 %** | 235.63 | 289.339 | **1.23** |
| **2 %** | 425.568 | 489.005 | **1.15** |
| **3 %** | 583.718 | 602.732 | **1.03** |
| **4 %** | 694.495 | 620.521 | **0.89** |
| **5 %** | 722.091 | 597.938 | **0.83** |

**Table 5.38.** Anisotropy Ratio of Undrained Shear Strength in terms of Mean Principal Stress Ratio at Diff. Strain Levels under 250 kPa C. Pressure for Site-B

| Strain - ε | Principal Stress Ratio - $\sigma_1/\sigma_3$ | | Anisotropy Ratio |
|---|---|---|---|
| | **Vertical** | **Horizontal** | **(H/V)** |
| **1 %** | 1.943 | 2.157 | **1.11** |
| **2 %** | 2.702 | 2.956 | **1.09** |
| **3 %** | 3.335 | 3.411 | **1.02** |
| **4 %** | 3.778 | 3.482 | **0.92** |
| **5 %** | 3.888 | 3.392 | **0.87** |

**Table 5.39.** Results Obtained under 450 kPa Confining Pressure for Site-B

| *Confining Pressure: 450 kPa* | Sample Size (mm×mm) | Moisture Content (%) | Bulk Density (kg/cm$^3$) | Deviator Stress (kPa) | Strain at Failure (%) |
|---|---|---|---|---|---|
| **Vertical – B-VC** | 200x105 | 22.17 | 1.97 | 908.56 | 4.95 |
| **Vertical – B-VD** | 150x100 | 25.83 | 1.91 | 867.45 | 4.40 |
| **Vertical – B-VE** | 100x50 | 24.47 | 1.94 | 865.39 | 3.81 |
| Vertical Mean | | | | **880.47** | |
| **Horizontal – B-HC** | 200x100 | 29.60 | 1.97 | 805.97 | 4.45 |
| **Horizontal – B-HD** | 195x100 | 25.50 | 1.87 | 831.30 | 5.34 |
| **Horizontal – B-HE** | 180x100 | 30.01 | 1.83 | 943.54 | 3.10 |
| Horizontal Mean | | | | **860.27** | |

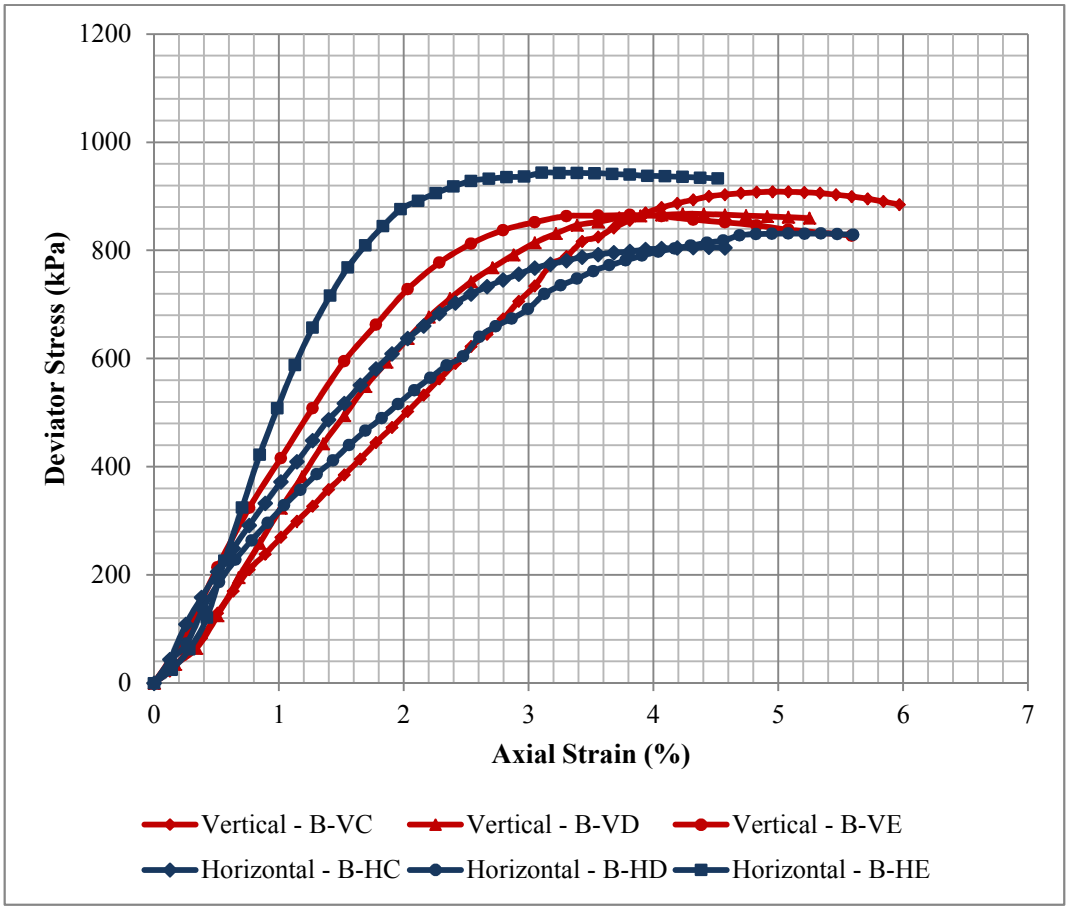


**Figure 5.12**. Comparison of Deviator Stresses under 450 kPa Cell Pressure

**Table 5.40.** Anisotropy Ratio of Undrained Shear Strength at Failure Stress under 450 kPa Confining Pressure for Site-B

| **Cell Pressure: 250 kPa** | Vertical | Horizontal | (K=H/V) |
|---|---|---|---|
| Mean Deviator Stress - $\sigma_1$-$\sigma_3$ (kPa) | 880.47 | 860.27 | **0.98** |
| Mean Principal Stress Ratio - $\sigma_1/\sigma_3$ | 2.957 | 2.912 | **0.99** |

**Table 5.41.** Anisotropy Ratio of Undrained Shear Strength in terms of Mean Deviator Stresses at Different Strain Levels under 450 kPa C. Pressure for Site-B

| Strain - ε | Deviator Stress - $\sigma_1$-$\sigma_3$ (kPa) | | Anisotropy Ratio |
|---|---|---|---|
| | **Vertical** | **Horizontal** | **(H/V)** |
| **1 %** | 336.307 | 402.822 | **1.20** |
| **2 %** | 622.495 | 684.953 | **1.10** |
| **3 %** | 800.06 | 798.437 | **1.00** |
| **4 %** | 869.284 | 846.092 | **0.97** |
| **5 %** | 869.289 | 853.913 | **0.98** |

**Table 5.42.** Anisotropy Ratio of Undrained Shear Strength in terms of Mean Principal Stress Ratio at Diff. Strain Levels under 450 kPa C. Pressure for Site-B

| Strain - ε | Principal Stress Ratio - $\sigma_1/\sigma_3$ | | Anisotropy Ratio |
|---|---|---|---|
| | **Vertical** | **Horizontal** | **(H/V)** |
| **1 %** | 1.747 | 1.895 | **1.08** |
| **2 %** | 2.383 | 2.522 | **1.06** |
| **3 %** | 2.778 | 2.774 | **1.00** |
| **4 %** | 2.932 | 2.88 | **0.98** |
| **5 %** | 2.932 | 2.898 | **0.99** |

**Table 5.43.** The mean Anisotropy Ratio of Undrained Shear Strength in terms of Deviator Stress for Site-B

| Confining Pressure (kPa) | Mean Deviator Stress at Failure (kPa) | | Anisotropy Ratio |
|---|---|---|---|
| | **Vertical** | **Horizontal** | **(H/V)** |
| *250* | 722.09 | 630.50 | **0.87** |
| *450* | 880.47 | 860.27 | **0.98** |

**Table 5.44.** The mean Anisotropy Ratio of Undrained Shear Strength in terms of Principal Stress for Site-B

| Confining Pressure (kPa) | Mean Principal Stress Ratio ($\sigma_1/\sigma_3$) at Failure (kPa) | | Anisotropy Ratio |
|---|---|---|---|
| | **Vertical** | **Horizontal** | **(H/V)** |
| *250* | 3.888 | 3.522 | **0.91** |
| *450* | 2.957 | 2.912 | **0.99** |

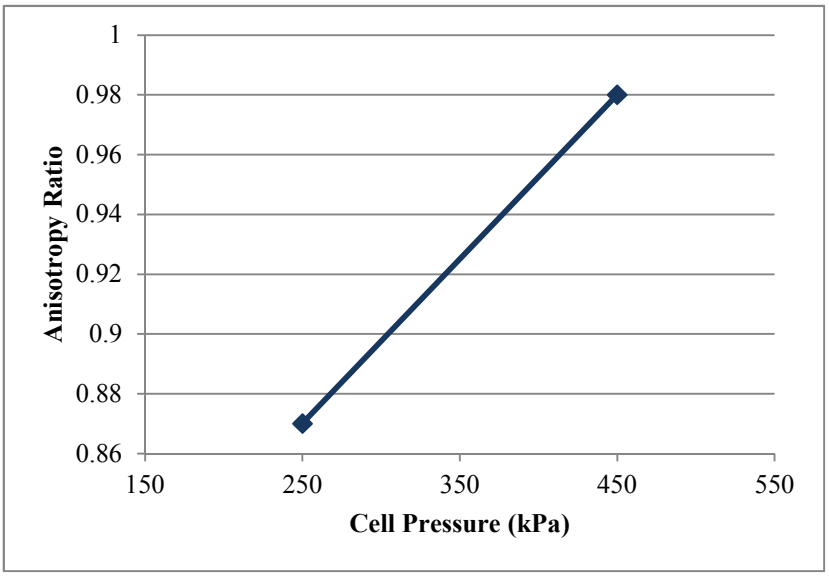


**Figure 5.13.** Variation of Anisotropy Ratio of Undrained Shear Strength in terms of Deviator Stress at Different Confining Pressure Levels for Site-B

The total shear strength parameters of the samples were calculated using "Modified Failure Envelope" method from the failure stresses obtained under 250 and 450 kPa pressures. Approximate in-situ condition according to $K_0$ calculated by equations (4.8) and (4.9) was plotted and stress paths were drawn by plotting the changes in mean stress at different strain levels for each pressure level.

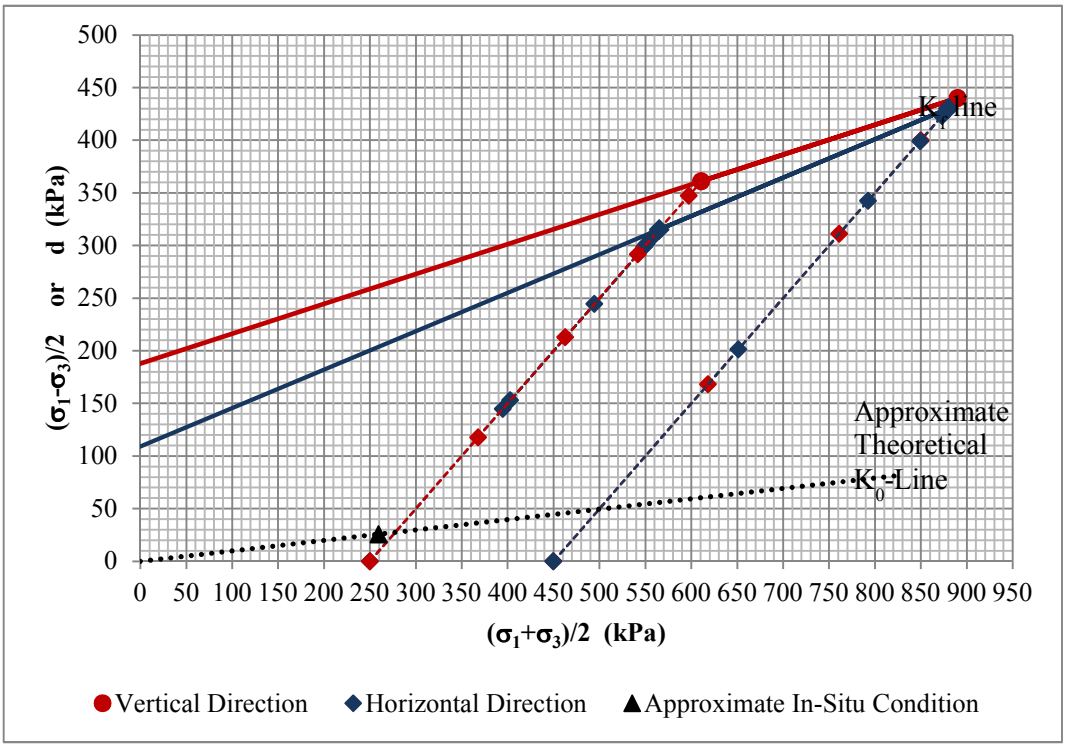


**Figure 5.14.** Failure Envelopes and Stress Paths Developed for Site-B

**Table 5.45.** Total Shear Strength Parameters for each Direction at Site-B

| Total Shear Strength Parameters (kPa) | | | |
|---|---|---|---|
| Vertical | | Horizontal | |
| d | α | d | α |
| 187.73 | 16° | 109.02 | 21° |
| c | ϕ | c | ϕ |
| 196 | 16.7° | 117 | 21.3° |

### 5.1.4. Results Obtained from Site-C

Among the samples gathered from Site-C; a total number of 18 triaxial tests were performed. As most of the specimens failed through the polished slickenside surfaces under 250 kPa confining pressure, the results obtained under this pressure is omitted. Most of the samples failed at strain rates ranging between 3.30 ~ 4.30 % under 450 kPa confining pressure and strain rates ranging between 2.54 ~ 5.08 % under 650 kPa confining pressure.

**Table 5.46.** The Number of UU Triaxial Tests Performed for Site-C

| Sampling Orientation | Type of Test | Number of Specimens Tested | | | |
|---|---|---|---|---|---|
| | | **Confining Pressure (kPa)** | | | **Total** |
| | | *250* | *450* | *650* | - |
| **Vertical Direction** | UU | 2 | 3 | 3 | 8 |
| **Horizontal Direction** | UU | 2 | 4 | 4 | 10 |

The lowest and highest deviator stresses obtained under specified confining pressures for different control group specimens are presented in Table 5.47.

**Table 5.47.** The Ratio of Highest and Lowest Failure Stresses for each Pressure Level for Site-C

| Confining Pressure | Vertical Specimen Deviator Stress (kPa) | | | Horizontal Specimen Deviator Stress (kPa) | | |
|---|---|---|---|---|---|---|
| | **Lowest** | **Highest** | **H/L** | **Lowest** | **Highest** | **H/L** |
| *250 kPa* | 147.67 | 405.13 | 2.74 | 183.02 | 306.95 | 1.68 |
| *450 kPa* | 323.29 | 500.19 | 1.55 | 403.59 | 560.80 | 1.39 |
| *650 kPa* | 400.03 | 565.87 | 1.42 | 356.24 | 534.60 | 1.50 |

**Table 5.48.** Results Obtained under 250 kPa Confining Pressure for Site-C

| *Confining Pressure: 250 kPa* | Sample Size (mm×mm) | Moisture Content (%) | Bulk Density ($kg/cm^3$) | Deviator Stress (kPa) | Strain at Failure (%) |
|---|---|---|---|---|---|
| **Vertical – C-VA** | 200x100 | 22.97 | 2.01 | 405.13 | 3.81 |
| **Vertical – C-VB *** | 200x100 | 23.99 | 2.09 | 147.67 | 5.08 |
| | | | | | |
| **Horizontal – C-HA *** | 200x100 | 24.83 | 2.01 | 183.02 | 1.65 |
| **Horizontal – C-HB *** | 195x100 | 23.51 | 2.05 | 306.95 | 2.21 |

*** Failed along the slickenside**

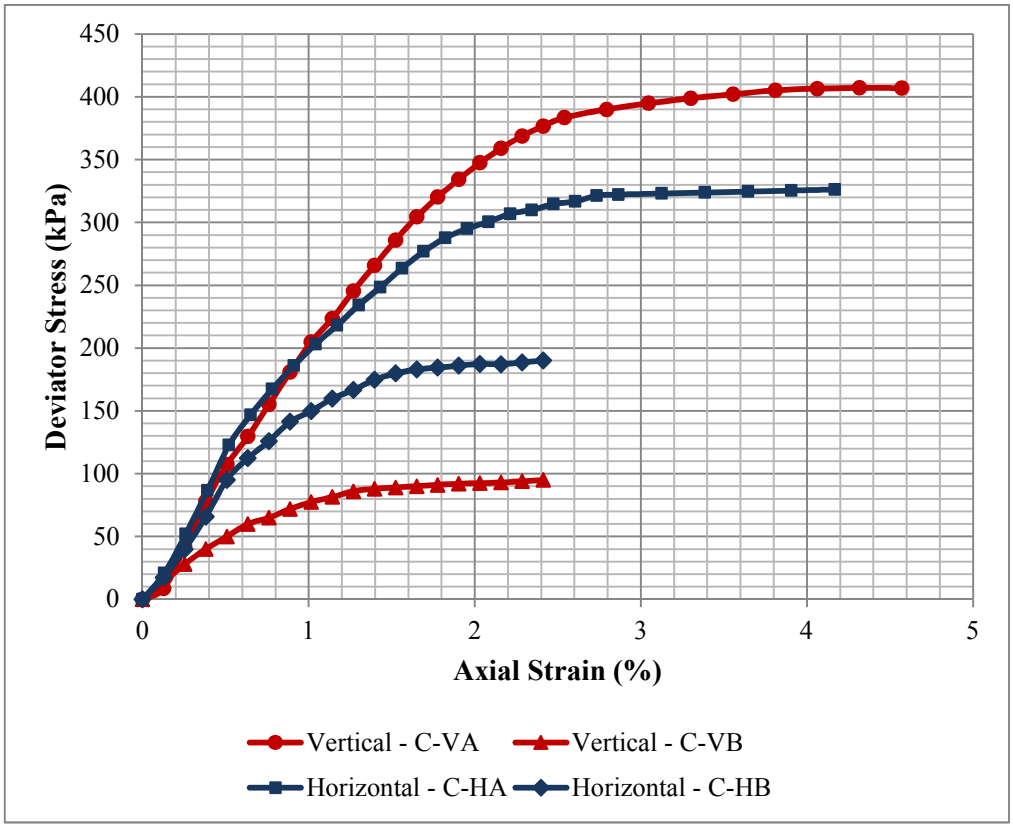


**Figure 5.15.** Comparison of Deviator Stresses under 250 kPa Cell Pressure

The results obtained under 250 kPa confining pressure is omitted due to the failures along the slickenside surfaces and fissures.

**Table 5.49.** Results Obtained under 450 kPa Confining Pressure for Site-C

| *Confining Pressure: 450 kPa* | Sample Size (mm×mm) | Moisture Content (%) | Bulk Density (kg/cm$^3$) | Deviator Stress (kPa) | Strain at Failure (%) |
|---|---|---|---|---|---|
| **Vertical – B-VC** | 195x105 | 25.10 | 2.04 | 500.19 | 3.91 |
| **Vertical – B-VD** | 190x100 | 24.18 | 1.97 | 446.49 | 3.48 |
| **Vertical – B-VE** | 160x100 | 26.10 | 2.02 | 323.29 | 3.49 |
| Vertical Mean | | | | **423.32** | |
| **Horizontal – B-HC** | 195x105 | 26.11 | 2.06 | 560.80 | 4.30 |
| **Horizontal – B-HD** | 185x100 | 23.70 | 1.98 | 403.59 | 3.30 |
| **Horizontal – B-HE** | 160x100 | 24.69 | 2.06 | 461.55 | 3.81 |
| **Horizontal – B-HF *** | 180x100 | 22.71 | 2.03 | 238.77 | 1.91 |
| Horizontal Mean (* Omitting B-HE) | | | | **475.31** | |

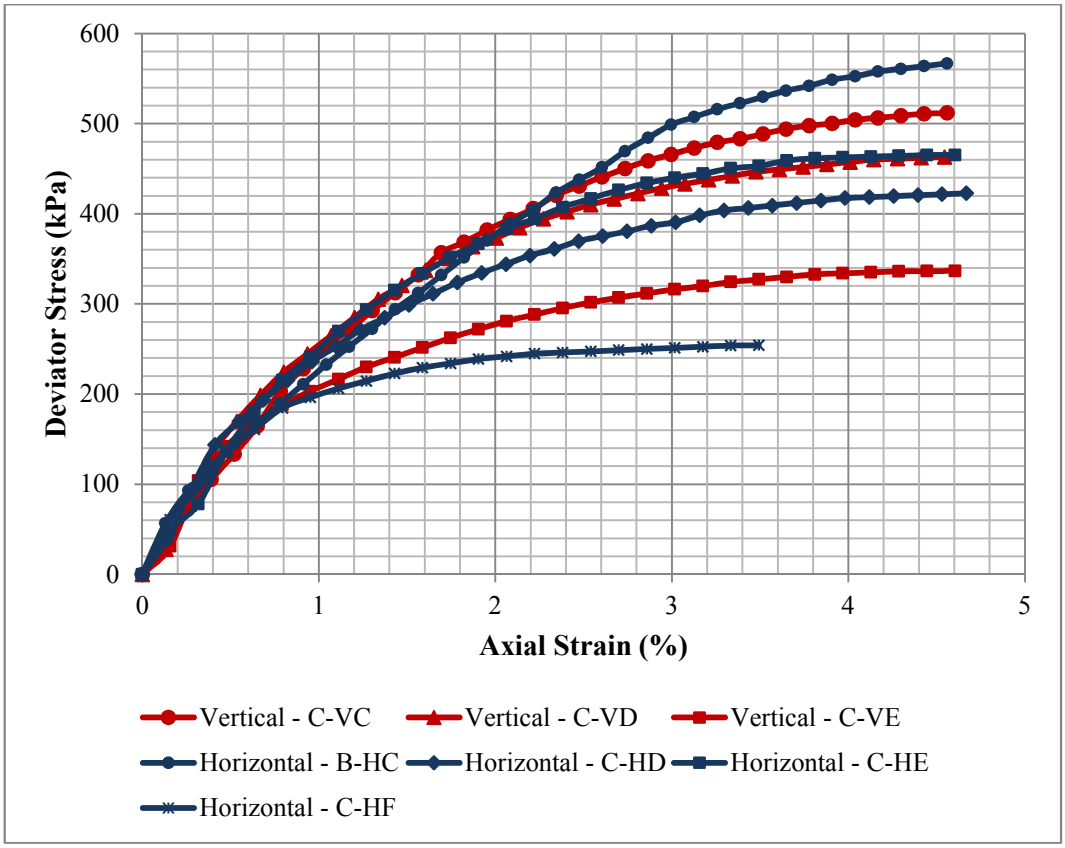


**Figure 5.16.** Comparison of Deviator Stresses under 450 kPa Cell Pressure

**Table 5.50.** Anisotropy Ratio of Undrained Shear Strength at Failure Stress under 450 kPa Confining Pressure

| **Cell Pressure: 450 kPa** | Vertical | Horizontal | (K=H/V) |
|---|---|---|---|
| Mean Deviator Stress - $\sigma_1$-$\sigma_3$ (kPa) | 423.32 | 475.31 | **1.12** |
| Mean Principal Stress Ratio - $\sigma_1/\sigma_3$ | 1.941 | 2.056 | **1.06** |

**Table 5.51.** Anisotropy Ratio of Undrained Shear Strength in terms of Mean Deviator Stresses at Different Strain Levels under 450 kPa C. Pressure for Site-C

| Strain - ε | Deviator Stress - $\sigma_1$-$\sigma_3$ (kPa) | | Anisotropy Ratio |
|---|---|---|---|
| | **Vertical** | **Horizontal** | **(H/V)** |
| **1 %** | 242.166 | 240.344 | **0.99** |
| **2 %** | 372.121 | 349.336 | **0.94** |
| **3 %** | 443.1 | 405.083 | **0.91** |
| **4 %** | 477.455 | 431.775 | **0.90** |
| **5 %** | 488.207 | 441.871 | **0.91** |

**Table 5.52** Anisotropy Ratio of Undrained Shear Strength in terms of Mean Principal Stress Ratio at Diff. Strain Levels under 450 kPa C. Pressure for Site-C

| Strain - ε | Principal Stress Ratio - $\sigma_1/\sigma_3$ | | Anisotropy Ratio |
|---|---|---|---|
| | **Vertical** | **Horizontal** | **(H/V)** |
| **1 %** | 1.538 | 1.534 | **1.00** |
| **2 %** | 1.827 | 1.776 | **0.97** |
| **3 %** | 1.985 | 1.900 | **0.96** |
| **4 %** | 2.061 | 1.960 | **0.95** |
| **5 %** | 2.085 | 1.982 | **0.95** |

**Table 5.53.** Results Obtained under 650 kPa Confining Pressure for Site-C

| *Confining Pressure: 650 kPa* | Sample Size (mm×mm) | Moisture Content (%) | Bulk Density (kg/cm$^3$) | Deviator Stress (kPa) | Strain at Failure (%) |
|---|---|---|---|---|---|
| **Vertical – B-VF** | 185x100 | 23.56 | 2.03 | 521.11 | 4.26 |
| **Vertical – B-VG** | 170x100 | 23.26 | 2.08 | 400.03 | 3.74 |
| **Vertical – B-VH** | 150x100 | 25.22 | 2.01 | 565.87 | 2.54 |
| Vertical Mean | | | | **495.67** | |
| **Horizontal – B-HF** | 200x100 | 28.05 | 2.03 | 356.24 | 2.92 |
| **Horizontal – B-HG** | 150x100 | 25.54 | 2.02 | 452.78 | 4.06 |
| **Horizontal – B-HH** | 150x100 | 22.89 | 2.08 | 534.60 | 5.08 |
| **Horizontal – B-HI *** | 185x100 | 25.11 | 1.99 | 136.25 | 0.83 |
| Horizontal Mean (* Omitting B-HI) | | | | **447.87** | |

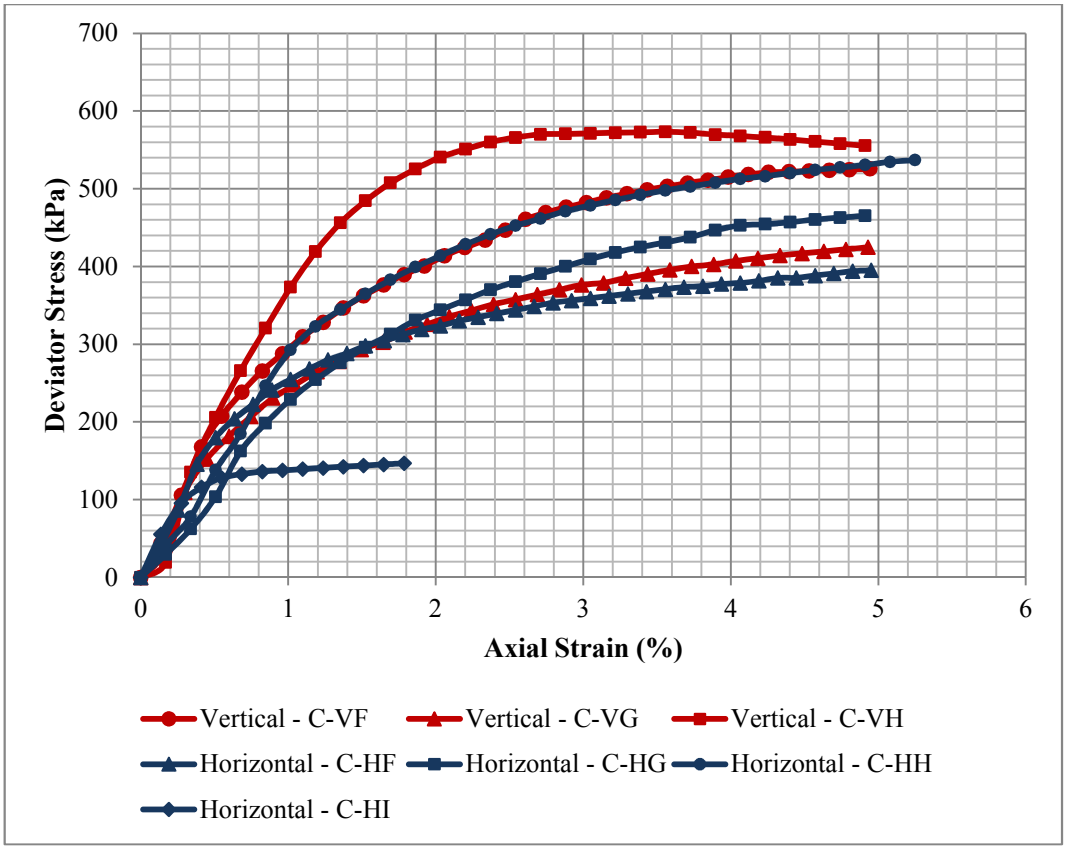


**Figure 5.17.** Comparison of Deviator Stresses under 650 kPa Cell Pressure

**Table 5.54.** Anisotropy Ratio of Undrained Shear Strength at Failure Stress under 650 kPa Confining Pressure

| **Cell Pressure: 650 kPa** | Vertical | Horizontal | (K=H/V) |
|---|---|---|---|
| Mean Deviator Stress - $\sigma_1$-$\sigma_3$ (kPa) | 495.67 | 447.87 | **0.90** |
| Mean Principal Stress Ratio - $\sigma_1/\sigma_3$ | 1.763 | 1.689 | **0.96** |

**Table 5.55.** Anisotropy Ratio of Undrained Shear Strength in terms of Mean Deviator Stresses at Different Strain Levels under 650 kPa C. Pressure for Site-C

| Strain - ε | Deviator Stress - $\sigma_1$-$\sigma_3$ (kPa) | | Anisotropy Ratio |
|---|---|---|---|
| | **Vertical** | **Horizontal** | **(H/V)** |
| **1 %** | 310.249 | 258.724 | **0.83** |
| **2 %** | 429.986 | 360.529 | **0.84** |
| **3 %** | 476.601 | 415.778 | **0.87** |
| **4 %** | 496.689 | 448.106 | **0.90** |
| **5 %** | 501.939 | 466.181 | **0.93** |

**Table 5.56.** Anisotropy Ratio of Undrained Shear Strength in terms of Mean Principal Stress Ratio at Diff. Strain Levels under 650 kPa C. Pressure for Site-C

| Strain - ε | Principal Stress Ratio - $\sigma_1/\sigma_3$ | | Anisotropy Ratio |
|---|---|---|---|
| | **Vertical** | **Horizontal** | **(H/V)** |
| **1 %** | 1.477 | 1.398 | **0.95** |
| **2 %** | 1.662 | 1.555 | **0.94** |
| **3 %** | 1.733 | 1.64 | **0.95** |
| **4 %** | 1.764 | 1.689 | **0.96** |
| **5 %** | 1.772 | 1.717 | **0.97** |

**Table 5.57.** The mean Anisotropy Ratio of Undrained Shear Strength in terms of Deviator Stress for Site-C

| Confining Pressure ($\sigma_3$) (kPa) | Mean Deviator Stress ($\sigma_1$-$\sigma_3$) at Failure (kPa) | | Anisotropy Ratio (K) |
|---|---|---|---|
| | **Vertical** | **Horizontal** | **(H/V)** |
| *450* | 423.32 | 475.31 | **1.12** |
| *650* | 495.67 | 447.87 | **0.90** |

**Table 5.58.** The mean Anisotropy Ratio of Undrained Shear Strength in terms of Principal Stress for Site-C

| Confining Pressure ($\sigma_3$) (kPa) | Mean Principal Stress Ratio ($\sigma_1/\sigma_3$) at Failure (kPa) | | Anisotropy Ratio (K) |
|---|---|---|---|
| | **Vertical** | **Horizontal** | **(H/V)** |
| *450* | 1.941 | 2.056 | **1.06** |
| *650* | 1.763 | 1.689 | **0.96** |

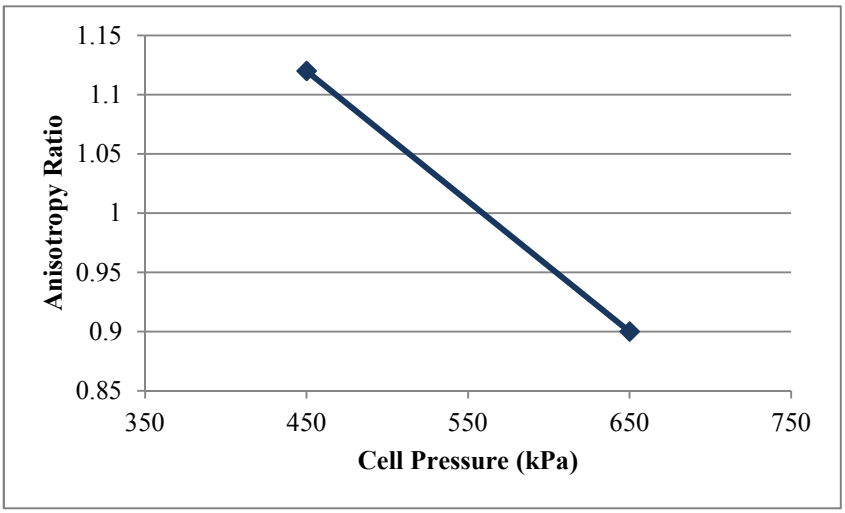


**Figure 5.18.** Variation of Anisotropy Ratio of Undrained Shear Strength in terms of Deviator Stress at Different Confining Pressure Levels for Site-C

The total shear strength parameters of the samples were calculated using "Modified Failure Envelope" method from the failure stresses obtained under 450 and 650 kPa pressures. Approximate in-situ condition according to $K_0$ calculated by equations (4.8) and (4.9) was plotted and stress paths were drawn by plotting the changes in mean stress at different strain levels for each pressure level.

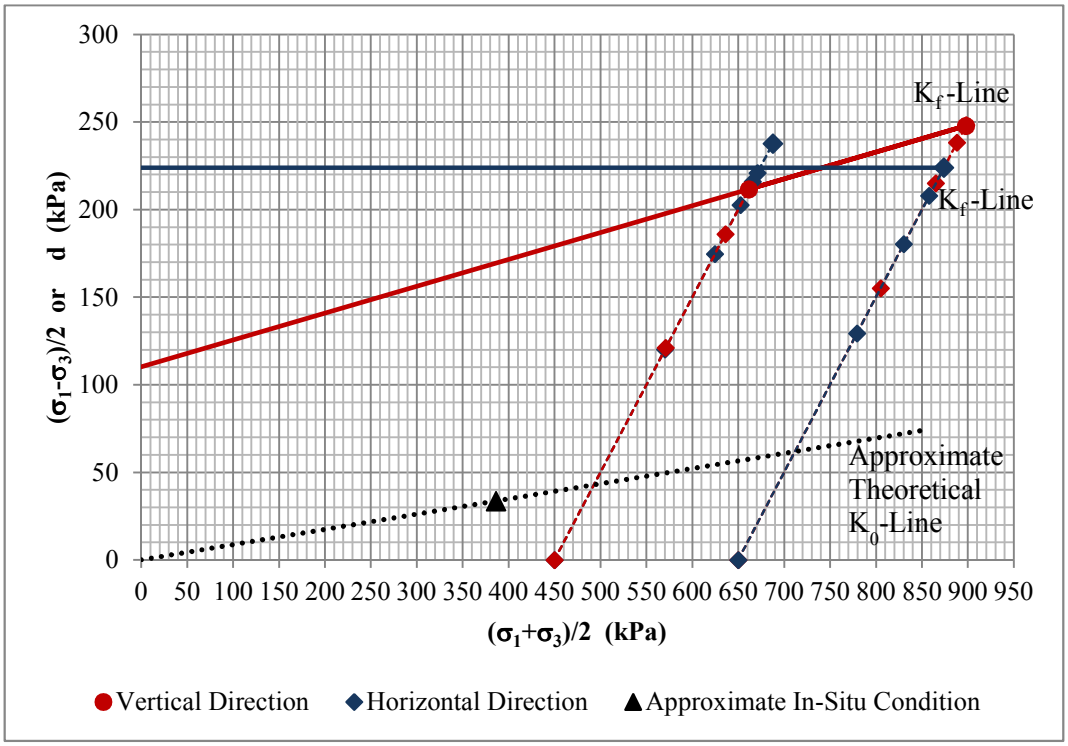


**Figure 5.19.** Failure Envelopes and Stress Paths Developed for Site-C

**Table 5.59.** Total Shear Strength Parameters for each Direction at Site-C

| Total Shear Strength Parameters (kPa) | | | |
|---|---|---|---|
| Vertical | | Horizontal | |
| d | α | d | α |
| 110.31 | 9° | 223.93 | 0° |
| c | ϕ | c | ϕ |
| 111.72 | 9.1° | 223.93 | 0° |

## 5.2. Anisotropy in Compressibility

In order to interpret the compressibility anisotropy present in Ankara Clay, coefficient of volume compressibility per loading sequence was calculated for tested specimens and compared with the similar samples in the other direction.

At least three control groups for each direction were tested at different sites and mean values of coefficient of volume compressibility were compared for each pressure range.

**Table 5.60.** The Number of Oedometer Tests Performed for Each Site

| Site | Number of Oedometer Tests |
|---|---|
| **A1** | - |
| **A2** | 8 |
| **B** | 8 |
| **C** | 6 |

The results achieved from oedometer tests of different control groups were also varying like in the results of triaxial tests, especially under lower pressures. From the results obtained, mean $m_v$ values were calculated and accepted as the basis of the comparison.

The distribution and comparison of coefficient of volume compressibility values at different pressure ranges for each site are presented below.

### 5.2.1. Results Obtained from Site-A2

A Total number of 8 consolidation tests were performed on specimens taken in vertical and horizontal positions.

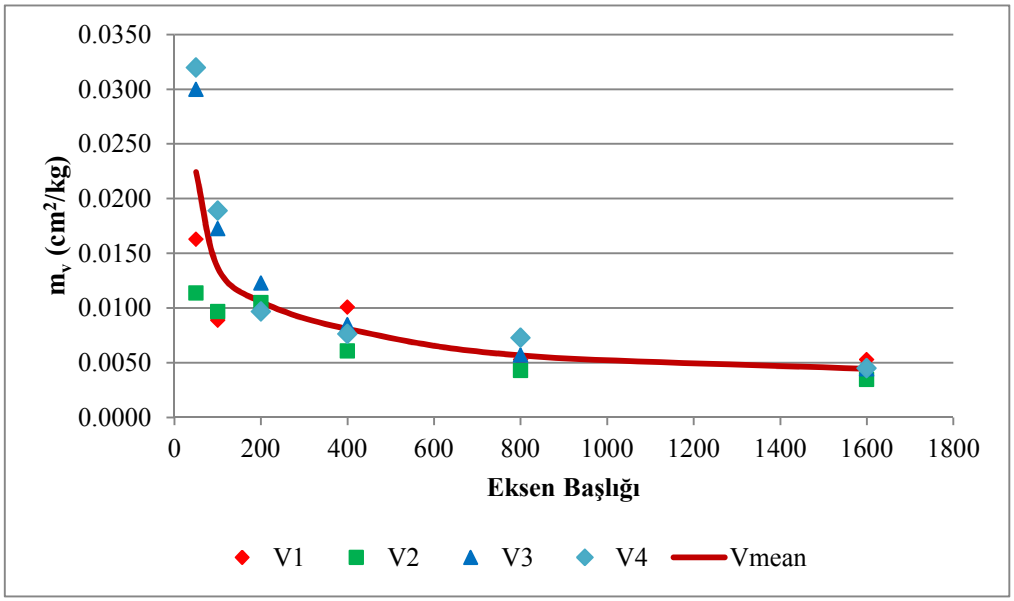


**Figure 5.20.** Mean Coefficient of Volume Compressibility vs. Pressure Graph of Vertical Specimens at Site-A2

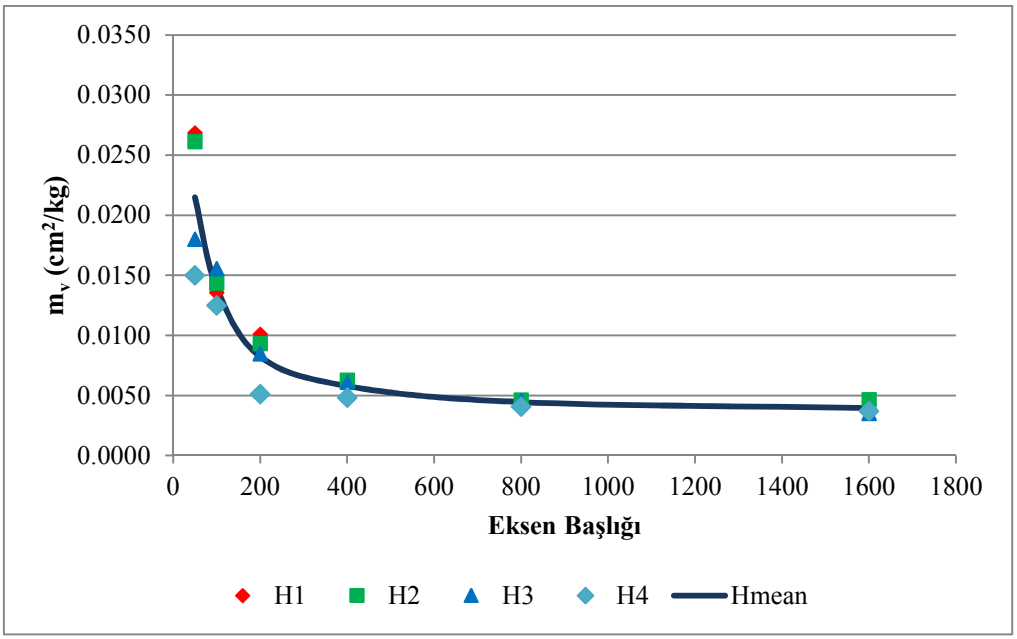


**Figure 5.21.** Mean Coefficient of Volume Compressibility vs. Pressure Graph of Horizontal Specimens at Site-A2

**Table 5.61.** Anisotropy Ratio in Compressibility in terms for Coefficient of Volume Compressibility for Different Pressure Ranges for Site-A2

| Pressure (kPa) | Vertical Specimen | Horizontal Specimen | Anisotropy Ratio |
|---|---|---|---|
| | **$m_v$ ($cm^2/kg$)** | **$m_v$ ($cm^2/kg$)** | **$mv_{hor.}/mv_{ver.}$** |
| **0-50** | 0.0224 | 0.0215 | 0.96 |
| **50-100** | 0.0137 | 0.0140 | 1.02 |
| **100-200** | 0.0106 | 0.0082 | 0.77 |
| **200-400** | 0.0081 | 0.0058 | 0.72 |
| **400-800** | 0.0057 | 0.0044 | 0.77 |
| **800-1600** | 0.0044 | 0.0039 | 0.89 |

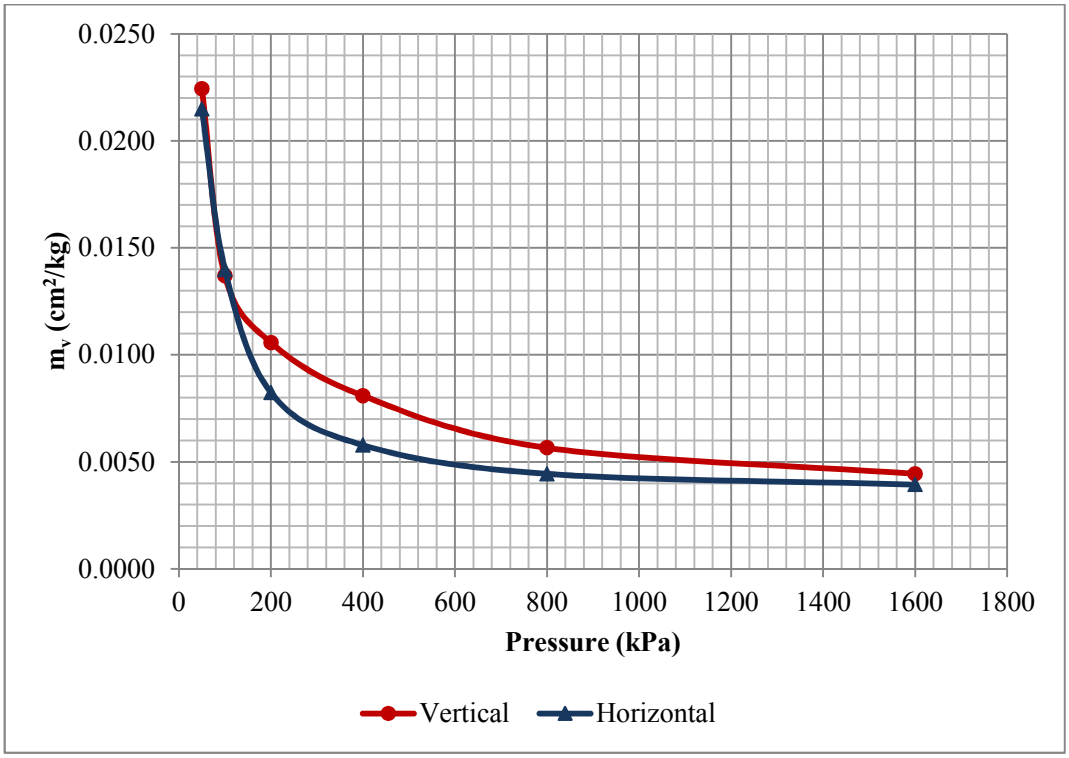


**Figure 5.22.** Comparison of $m_v$ values for Site-A2

### 5.2.2. Results Obtained from Site-B

A Total number of 8 consolidation tests were performed on specimens taken in vertical and horizontal positions from Site-B.

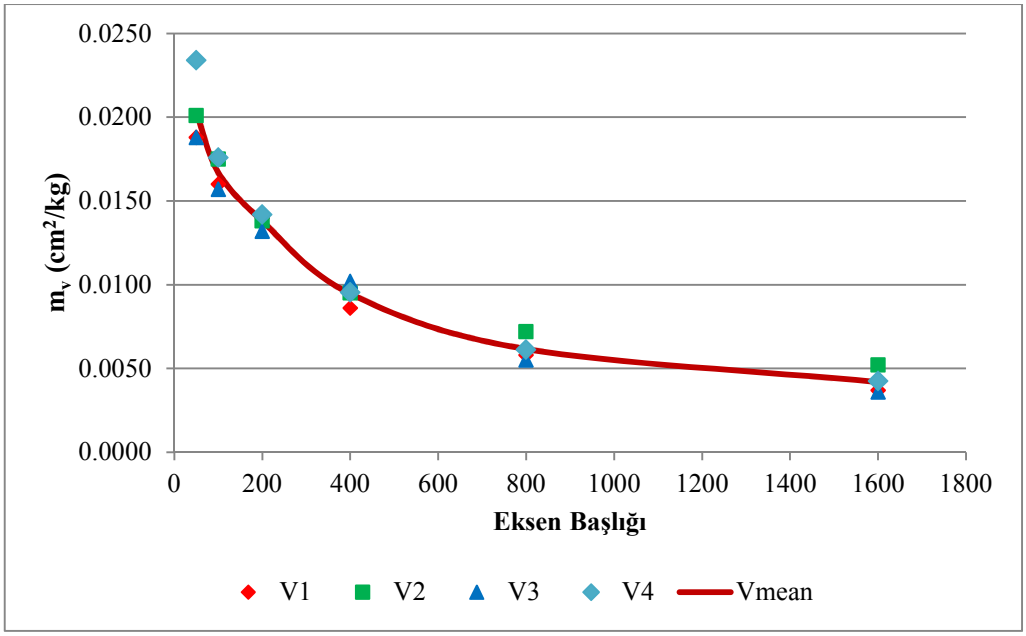


**Figure 5.23.** Mean Coefficient of Volume Compressibility vs. Pressure Graph of Vertical Specimens at Site-B

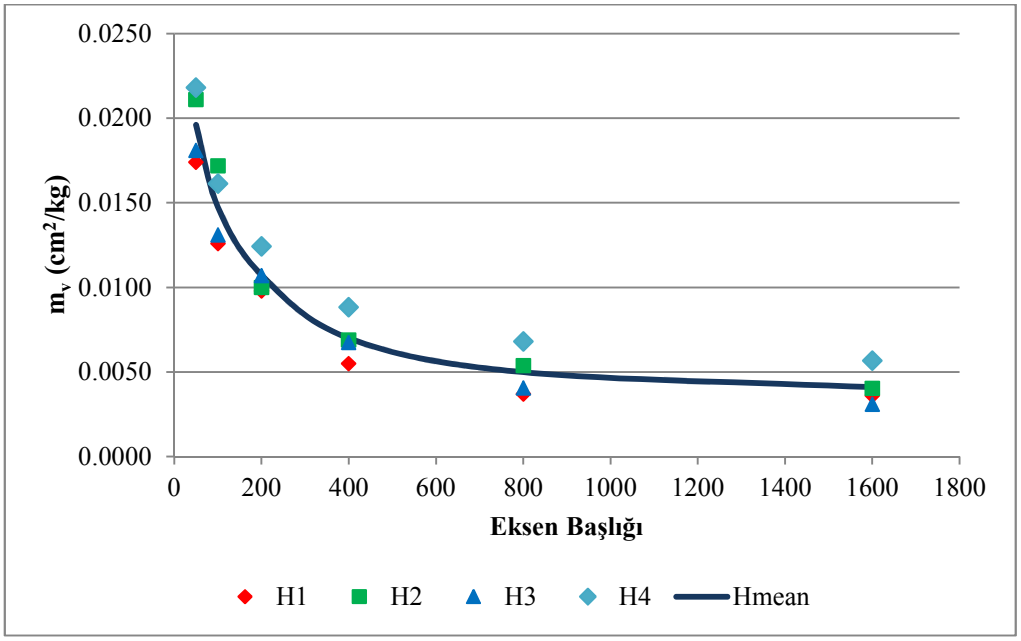


**Figure 5.24.** Mean Coefficient of Volume Compressibility vs. Pressure Graph of Horizontal Specimens at Site-B

**Table 5.62.** Anisotropy Ratio in Compressibility in terms for Coefficient of Volume Compressibility for Different Pressure Ranges for Site-B

| Pressure (kPa) | Vertical Specimen | Horizontal Specimen | Anisotropy Ratio |
|---|---|---|---|
| | **$m_v$ ($cm^2/kg$)** | **mv ($cm^2/kg$)** | **$mv_{hor.}/mv_{ver.}$** |
| **0-50** | 0.0198 | 0.0196 | 0.99 |
| **50-100** | 0.0167 | 0.0148 | 0.88 |
| **100-200** | 0.0135 | 0.0107 | 0.79 |
| **200-400** | 0.0095 | 0.0070 | 0.74 |
| **400-800** | 0.0062 | 0.0050 | 0.81 |
| **800-1600** | 0.0042 | 0.0041 | 0.98 |

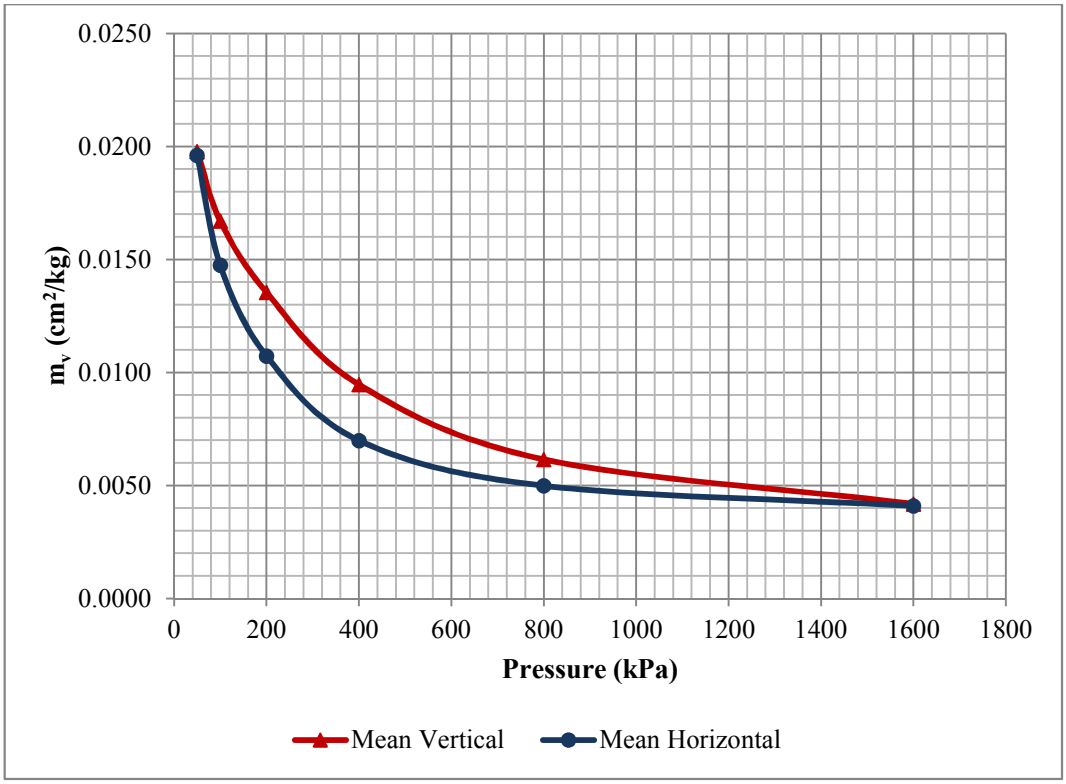


**Figure 5.25.** Comparison of $m_v$ values for Site-B

### 5.2.3. Results Obtained from Site- C

A Total number of 6 consolidation tests were performed on specimens taken in vertical and horizontal positions from Site-C.

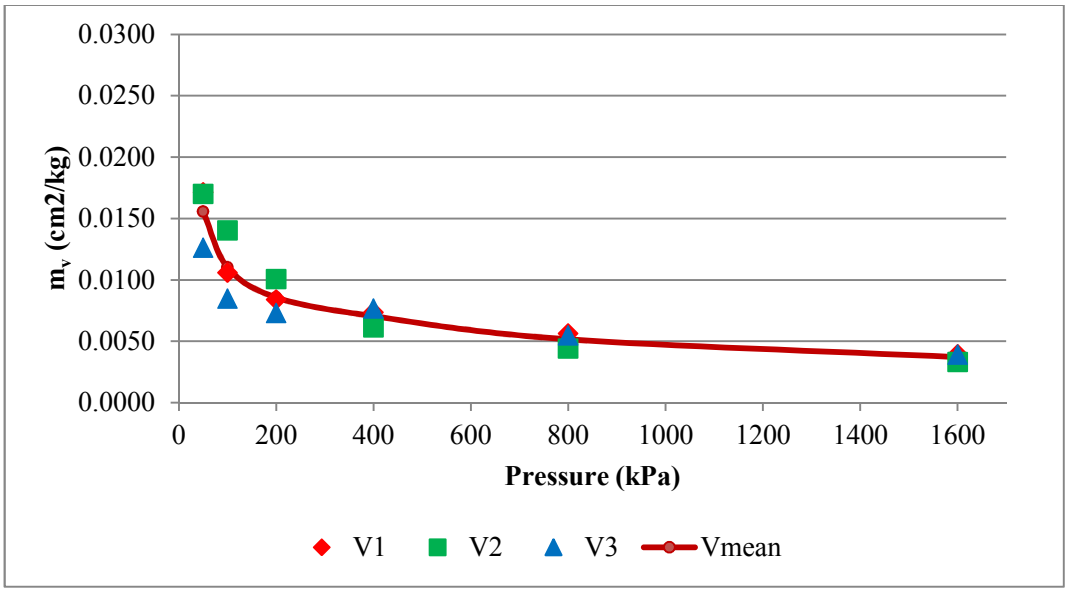


**Figure 5.26.** Mean Coefficient of Volume Compressibility vs. Pressure Graph of Vertical Specimens at Site-C

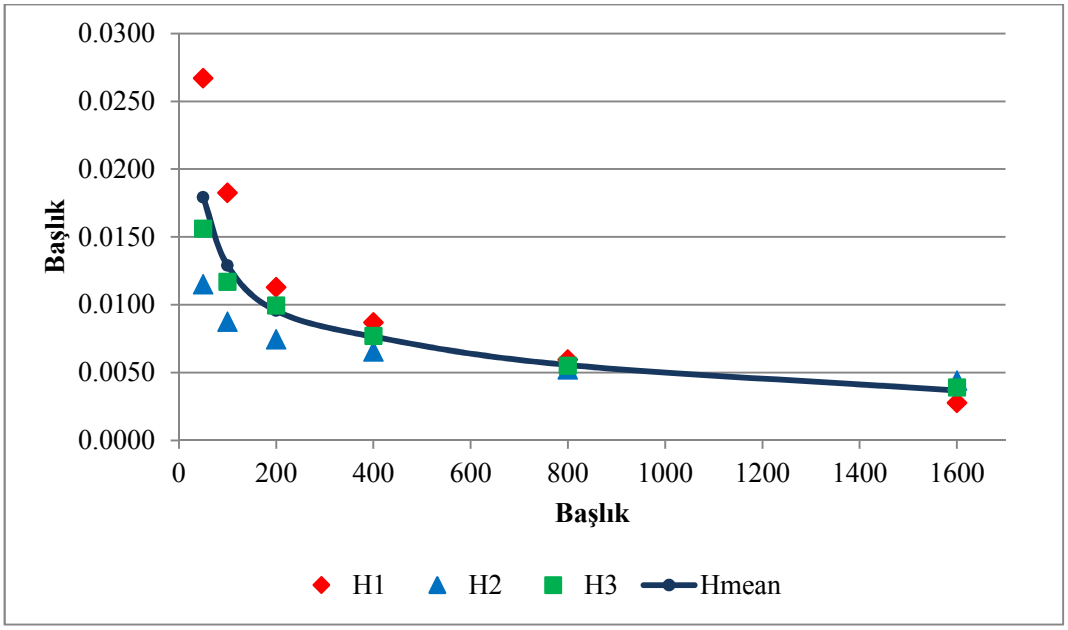


**Figure 5.27.** Mean Coefficient of Volume Compressibility vs. Pressure Graph of Horizontal Specimens at Site-C

**Table 5.63.** Anisotropy Ratio in Compressibility in terms for Coefficient of Volume Compressibility for Different Pressure Ranges for Site-C

| Pressure (kPa) | Vertical Specimen | Horizontal Specimen | Anisotropy Ratio |
|---|---|---|---|
| | **$m_v$ ($cm^2/kg$)** | **$m_v$ ($cm^2/kg$)** | **$mv_{hor.}/mv_{ver.}$** |
| **0-50** | 0.0156 | 0.0179 | 1.15 |
| **50-100** | 0.0110 | 0.0129 | 1.17 |
| **100-200** | 0.0086 | 0.0096 | 1.11 |
| **200-400** | 0.0070 | 0.0076 | 1.09 |
| **400-800** | 0.0052 | 0.0056 | 1.08 |
| **800-1600** | 0.0037 | 0.0037 | 1.00 |

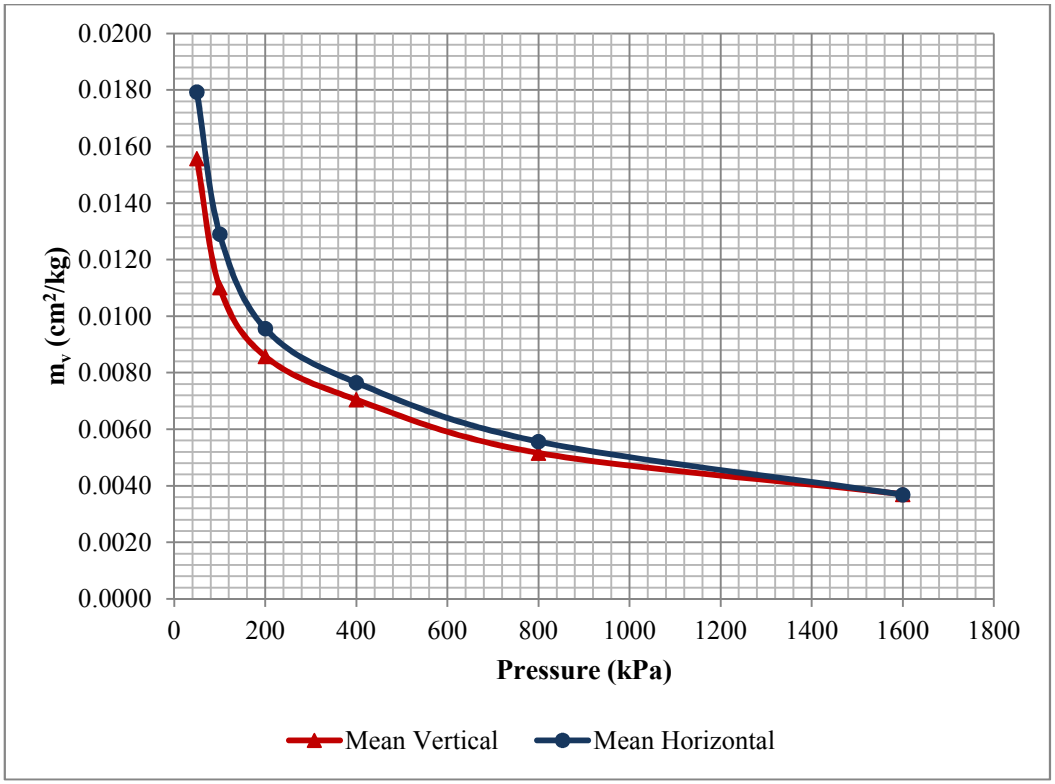


**Figure 5.28.** Comparison of $m_v$ values for Site-C

# CHAPTER 6

# EVALUATION OF TEST RESULTS

## 6.1. Evaluation of Triaxial Test Results

The unconsolidated-undrained triaxial test results have shown that there is a slight anisotropy in the total shear strength of tested Ankara Clay specimens which is ranging between 0.87 and 1.19 in terms of deviator stress.

According to the results obtained in Site-A2 and Site-C; Ankara Clay had higher shear strength in horizontal direction for lower pressures, while it was vice versa for Site-B as shown in Table 6.1 and Table 6.2.

It was observed that, as the confining pressure increased, the behavior of the samples became closer to the isotropy. On the other hand, especially at pressures higher than the preconsolidation pressure, the anisotropy slightly increased in the opposite direction to the previous state observed in lower pressures. This may be due to effect of higher pressures on predominant fissure orientation during shear.

**Table 6.1.** Anisotropy ratio in total shear strength at failure in terms of ($\sigma_1$-$\sigma_3$)

| Confining Pressure (kPa) | Anisotropy Ratio (H/V) in Total Shear Strength at Failure | | | |
|---|---|---|---|---|
| | **Site-A1** | **Site-A2** | **Site-B** | **Site-C** |
| *250* | 1.19 | 1.13 | 0.87 | - |
| *350* | 1.17 | 1.01 | - | - |
| *450* | - | 0.91 | 0.98 | 1.12 |
| *650* | - | - | - | 0.90 |

**Table 6.2.** Anisotropy ratio in total shear strength at failure in terms of $\sigma_1/\sigma_3$

| Confining Pressure (kPa) | Anisotropy Ratio in Total Shear Strength at Failure | | | |
|---|---|---|---|---|
| | **Site-A1** | **Site-A2** | **Site-B** | **Site-C** |
| *250* | 1.06 | 1.07 | 0.91 | - |
| *350* | 1.05 | 1.00 | - | - |
| *450* | - | 0.96 | 0.99 | 1.06 |
| *650* | - | - | - | 0.96 |

For most of the sites, the anisotropy in total shear strength in terms of deviator stress tended to decrease by the increase in strain level up to 3% yet a valid pattern couldn't be observed up to the failure strain. On the other hand, anisotropy ratio increased with further shearing after the failure of specimens in both directions as shown in Table 6.3 and Table 6.4.

**Table 6.3.** Anisotropy Ratio of Undrained Shear Strength at Different Strain Levels in terms of Deviator Stress under 250 kPa Confining Pressure

| Strain - ε (%) | Anisotropy Ratio (H/V) | | |
|---|---|---|---|
| | **Site-A1** | **Site-A2** | **Site-B** |
| **1 %** | 1.45 | 1.05 | 1.23 |
| **2 %** | 1.28 | 1.02 | 1.15 |
| **3 %** | 1.15 | 0.99 | 1.03 |
| **4 %** | 1.13 | 1.02 | 0.89 |
| **5 %** | 1.12 | 1.07 | 0.83 |
| **6 %** | 1.11 | 1.11 | - |
| **7 %** | 1.12 | - | - |
| **8 %** | 1.12 | - | - |
| **9 %** | 1.13 | - | - |
| **10 %** | 1.14 | - | - |
| **Range of Failure Strain (Vertical)** | 9 ~ 10 % | 5 ~ 6 % | ~ 5 % |
| **Range of Failure Strain (Horizontal)** | 14 ~ 15 % | 4 ~ 5 % | 3 ~ 5 % |

**Table 6.4 -** Anisotropy Ratio of Undrained Shear Strength at Different Strain Levels in terms of Deviator Stress under 450 kPa Confining Pressure

| Strain - ε (%) | Anisotropy Ratio (H/V) | | |
|---|---|---|---|
| | **Site-A2** | **Site-B** | **Site-C** |
| **1 %** | 0.81 | 1.20 | 0.99 |
| **2 %** | 0.87 | 1.10 | 0.94 |
| **3 %** | 0.88 | 1.00 | 0.91 |
| **4 %** | 0.89 | 0.97 | 0.90 |
| **5 %** | - | 0.98 | 0.91 |
| **Range of Failure Strain (Vertical)** | 2 ~ 4 % | 3 ~ 5 % | 3 ~ 4 % |
| **Range of Failure Strain (Horizontal)** | 2 ~ 4 % | 3 ~ 5 % | 3 ~ 4 % |

For all sites, the results showed a great variation under same pressure even between the samples with same orientation, especially at higher pressures.

At high pressures, while the results obtained from different samples were scattered, the range of undrained shear strength of samples in both orientations was mostly overlapped. Therefore, both horizontal and vertical samples may be considered to behave similarly, almost isotropic under high pressures with a wide range of shear strength due to heterogeneous nature of the clay.

In this regard, the anisotropy observed in lower pressures may be considered as the result of fissures relaxing at pressures lower than the in-situ stresses. Therefore the results of the tests might have been affected by the soil fabric and orientation of weak planes and fissures present in the samples.

This behavior can also be observed when the coordinates of the top of the Mohr circles developed from different control groups are plotted on the same graph, as shown in Figure 6.2, Figure 6.3 and Figure 6.4.

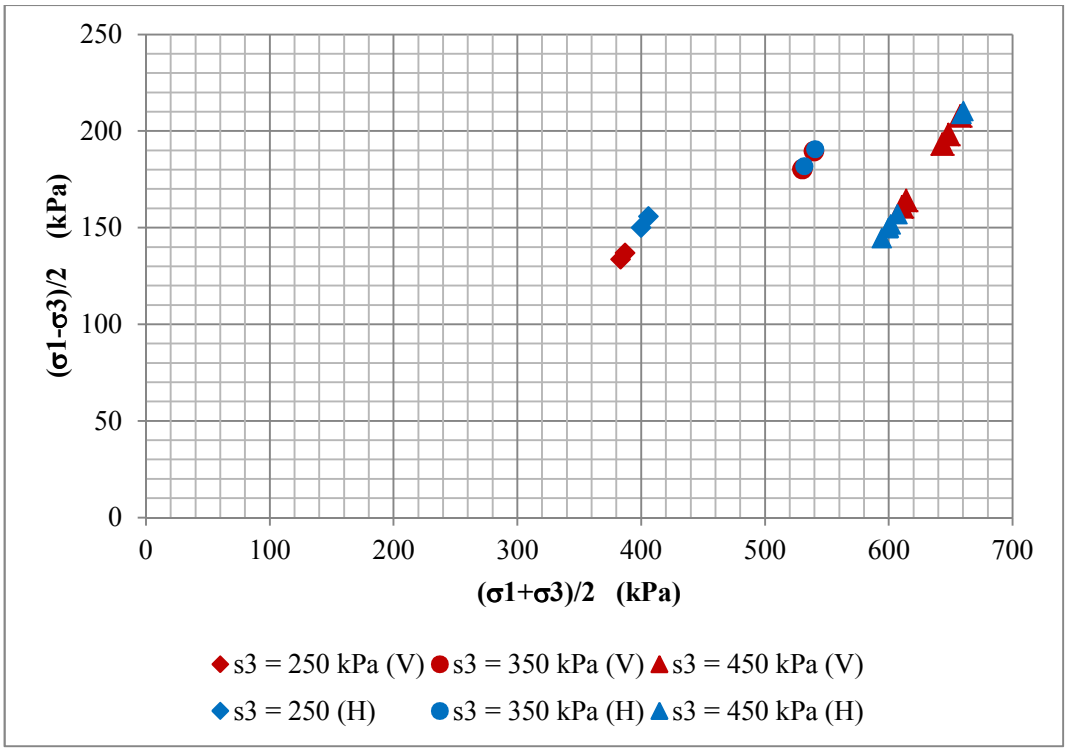


**Figure 6.1.** The Results obtained in Site-A2 from each control group

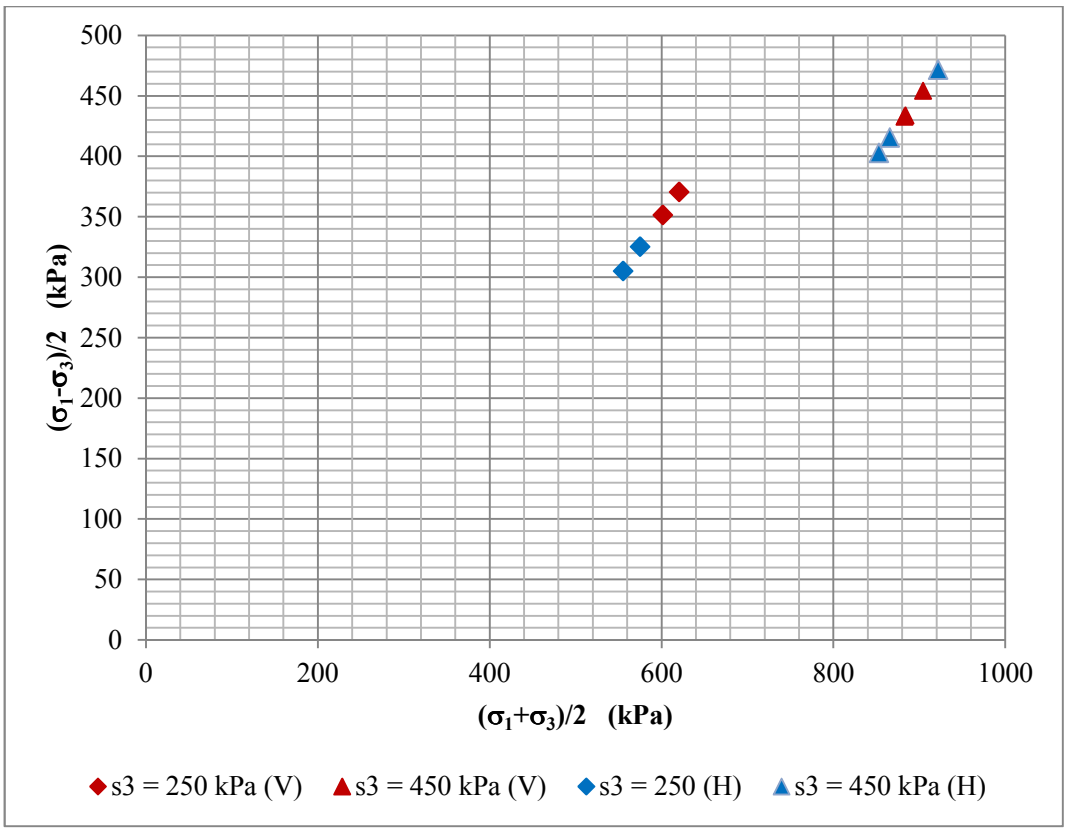


**Figure 6.2.** The Results obtained in Site-B from each control group

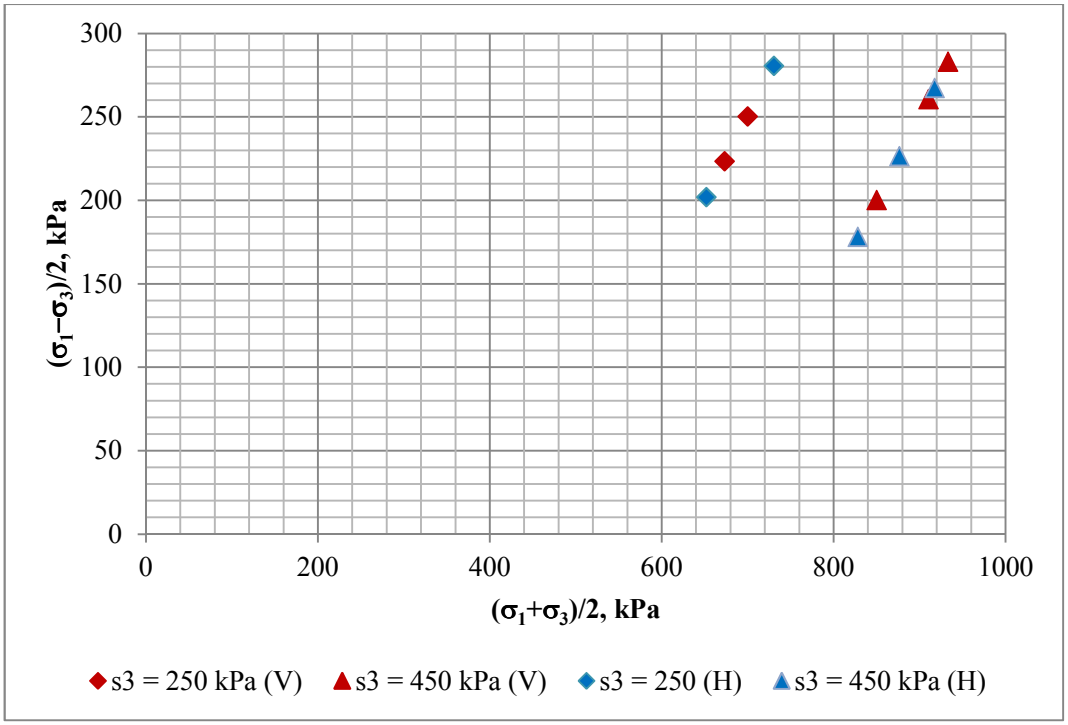


**Figure 6.3.** The Results obtained in Site-C from each control group

The influence of different index properties at different sites such as plasticity index, water content or particle size distribution could not be observed, as the index properties were pretty close to each other for a comparable effect on anisotropy characteristics. A direct influence of different specimen heights on the test results was not also observed.

## 6.2. Evaluation of Oedometer Test Results

The oedometer test results have shown that there is some anisotropy, ranging between 0.72 and 1.17, in the compressibility of tested Ankara Clay specimens for different pressure ranges.

The compressibility in the horizontal direction proved to be lower than the compressibility in the vertical direction for most of the pressure ranges, according to the results obtained from Site-A2 and Site-B in terms of mean coefficient of

volume compressibility. On the other hand, an opposite yet closer to isotropic behavior is observed in Site-C as shown in Table 6.5.

**Table 6.5.** The Anisotropy Ratio in Compressibility in terms of mean Coefficient of Volume Compressibility at different pressures.

| Pressure Range (kPa) | Anisotropy Ratio ($K = mv_{hor.}/mv_{ver.}$) | | |
|---|---|---|---|
| | **Site-A2** | **Site-B** | **Site-C** |
| **0-50** | 0.96 | 0.99 | 1.15 |
| **50-100** | 1.02 | 0.88 | 1.17 |
| **100-200** | 0.77 | 0.79 | 1.11 |
| **200-400** | 0.72 | 0.74 | 1.09 |
| **400-800** | 0.77 | 0.81 | 1.08 |
| **800-1600** | 0.89 | 0.98 | 1.00 |

No pattern could be observed regarding the relationship of anisotropy ratio with the pressure range. The results obtained from consolidation tests were also varying like in the triaxial tests, although the effect of fissures and planes of weaknesses may be expected less in consolidation tests since the samples are much smaller.

A direct relation between anisotropy in compressibility and anisotropy in undrained shear strength could not be observed. While the undrained shear strength in horizontal direction was higher than the vertical direction in Site-A2 and Site-C; their compressibility behaviors were different.

For instance, while the mean compressibility in horizontal direction at Site-A2 was lower than the vertical direction, it was slightly higher yet almost isotropic at Site-C for most of the pressure ranges. Considering that the samples taken from Site-C was normally consolidated (OCR≈1) while the samples taken from Site-A2 was slightly overconsolidated (OCR≈1.45), it may be said that overconsolidation

is somewhat more effective on the anisotropic behavior in compressibility properties of Ankara Clay.

Ankara Clay at Site-B (OCR≈1.44) which had a similar overconsolidation ratio to Site-A2 (OCR≈1.45) showed similar behavior compared to the Site-A2. On the other hand, while Ankara Clay at Site-B was less compressible in horizontal direction despite the fact that the shear strength was lower in horizontal direction for this site. This unlikely behavior of Site-B may be explained by the possible effects of fissures and weak planes being more effective in large specimens used in triaxial testing.

# CHAPTER 7

# CONCLUSIONS

In this study, the anisotropy in undrained shear strength and drained compressibility of natural, stiff, lightly overconsolidated, fissured Ankara Clay has been investigated. As a part of the experimental work, series of unconsolidated-undrained triaxial tests and standard oedometer tests were executed on the sample groups obtained from different sites along the Konya Road in Çukurambar/Balgat Area. The following conclusions can be drawn from the results of the experimental work.

1) Ankara Clay is slightly anisotropic in total shear strength, especially at low pressures. The anisotropy ratio in terms of deviator stress ranges between 0.87-1.19.

2) The failure stresses in Ankara Clay is mainly governed by the weak planes formed by fissures and slickensides. Therefore the results achieved from the tests are highly variable and anisotropy ratio depends on the confining pressure.

3) Ankara Clay becomes less anisotropic in terms of total shear strength as the confining pressure increases.

4) The compressibility of Ankara Clay is slightly anisotropic by ratios varying between 0.96~1.15 at 0-50 kPa, 0.88~1.17 at 50-100 kPa,

0.77~1.11 at 100-200 kPa, 0.72~1.09 at 200-400 kPa, 0.77~1.08 at 400-800 kPa and 0.89~1.00 at 800-1600 kPa pressure ranges, in terms of mean coefficient of volume compressibility.

5) Ankara Clay becomes more anisotropic in terms of compressibility as the overconsolidation ratio increases. The compressibility in horizontal direction is lower than the vertical direction for the overconsolidated samples studied in this experimental work.

6) The results of this study have shown that the undrained shear strength in horizontal direction is close to the behavior in vertical direction and higher in some cases. Similarly, drained compressibility in horizontal direction is close to the behavior in vertical direction or lower. These results contradict with the typical behavior of lightly overconsolidated clays, most probably due to the stiff fissured nature of the Ankara Clay.

7) It may be said that the stiff fissured clay studied at sites A, B and C behaves quite isotropic in terms of shear strength for practical purposes, while it behaves slightly anisotropic in terms of compressibility depending on the overconsolidation and pressure applied.

# REFERENCES


1. Aas G., 1967. “Vane Tests for Investigation of Anisotropy of Undrained Shear Strength of Clays” *Proc. Geotechnical Conf.*, Oslo, Vol. 1 pp. 3-8

2. Ağaoğlu S., 1973. “Anisotropy in Compressibility of METU Campus Clay” MSc. Thesis, Middle East Technical University, Ankara.

3. ASTM, 2011. “Annual Book of ASTM Standards Volume 04.08 Soil and Rock (I) : D420 - D5876” ASTM International, West Conshohocken/PA.

4. ASTM, 2011. “Annual Book of ASTM Standards Volume 04.09 Soil and Rock (II): D5877 – latest**”** ASTM International, West Conshohocken/PA.

5. Avşar E., Ulusay R., Sönmez H., 2009. “Assessments of swelling anisotropy of Ankara clay” *Engineering Geology* Vol. 105 No.1-2, pp. 24–31

6. Atom M. F. and Al-Akhras N. M., 2008 “Investigating Anisotropy in Shear Strength of Clayey Soils”, *Proceedings of the ICE - Geotechnical Engineering*, Vol. 161, No. 5, pp. 269 –273

7. Berre, T. and Bjerrum L., 1973. “Shear Strength of Normally Consolidated Clays” *Proc. 8$^{th}$ ICSMFE*, Vol. 1, pp. 39-49

8. Birand A., 1978. "A Review of Soils and Geotechnical Problems in Ankara Region" *3$^{rd}$ Symposium on the Problems of Ankara*, Turkish Geological Society, pp 55-60 (In Turkish)

9. Bishop A.W., 1966. “The Strength of Soils as Engineering Materials”, *Géotechnique* Vol. 16 No. 2, pp. 91-130

10. Bjerrum L., 1973. “ Problems of Soil and Construction on Soft Clays and Structurally Unstable Soils (Collapsible, Expansive and others)”, *Proc. 8th ICSMFE*, pp. 111-159

11. BS 1377-1:1990, “Methods of Test for Soils for Civil Engineering Purposes: General Requirements and Sample Preparation”, British Standards Institute Group, 38 pages.

12. BS 1377-2:1990, “Methods of Test for Soils for Civil Engineering Purposes: Classification Tests”, British Standards Institute Group, 68 pages.

13. BS 1377-5:1990, “Methods of Test for Soils for Civil Engineering Purposes: Compressibility”, British Standards Institute Group, 42 pages.

14. BS 1377-7:1990, “Methods of Test for Soils for Civil Engineering Purposes: Shear Strength Tests (Total Stress)”, British Standards Institute Group, 62 pages.

15. BS EN 1997-1:2004, “ Eurocode 7: Geotechnical Design - General Rules”, British Standards Institute Group, 174 pages.

16. Casagrande A. and Carillo N., 1944. “Shear Failure of Anisotropic Materials”, *Proc. Boston Soc. Civ. Engineers*, V.31, pp. 74-87

17. Clough G.W. and Hansen L.A., 1981. “Clay Anisotropy and Braced Wall Behavior” *ASCE, Journal of the Geotechnical Engineering Division*, Vol. 107, No. 7, pp.893-913

18. Craig R.F, 2004. “Craig’s Soil Mechanics”, 7th Edition, Taylor & Francis Group, New York City/NY, 447 pages.

19. Çetinkaya A.S., 1978. “Preconsolidation pressure and its effects on some properties of METU Campus clay” MSc. Thesis, Middle East Technical University, Ankara.

20. Das B.M., 2010. “Principles of Geotechnical Engineering”, 7th Edition, Cengage Learning, Stamford/CT, 666 pages.

21. Duncan J.M. and Seed H.B., 1966a. “Anisotropy and Stress Reorientation in Clay”, *ASCE, Journal of the Geotechnical Engineering Division*, Vol. 92, No. 5, 21-50

22. Duncan J.M. and Seed H.B., 1966b. “Strength Variation Along Failure Surfaces in Clay”, *ASCE, Journal of the Geotechnical Engineering Division*, Vol. 92, No. 6, 81-104

23. Ergüler Z.A., Ulusay R., 2001. “An Investigation on the Swelling Behavior of Ankara Clay and Effect of Disturbance on Swelling, Determination of Swelling Potential by Empirical Equations.” MSc. Thesis, Hacettepe University, Ankara. (In Turkish)

24. Ergüler Z.A., Ulusay R., 2003a. "Engineering Characteristics and Environmental Impact of The Expansive Ankara Clay, and Swelling Maps for SW and Central Parts of Ankara (Turkey) Metropolitan Area". *Environmental Geology* Vol.44 No.8, pp.979 –992.

25. Ergüler Z.A., Ulusay R., 2003b. “A simple test and predictive models for assessing swell potential of Ankara (Turkey) Clay.” *Engineering Geology* Vol. 67, No. 3-4 pp.331 –352.

26. Hansen J.B. and Gibson R.E., 1949. "Undrained Shear Strength of Anisotropically Consolidated Clays", *Géotechnique* Vol. 1, No. 3, pp.189-200

27. Jacobson B., 1955. "Isotropy of Clays", *Géotechnique*, Vol. 5, No. 1, pp.23-28

28. Kamei T. and Nakase A., 1989. "Undrained Shear Strength Anisotropy of Ko-Overconsolidated Cohesive Soils", *Soils and Foundations*, Vol. 29, No. 3, pp.145-151

29. Kurukulasuriya L, Oda M. and Kazama H., 1999 "Anisotropy of Undrained Shear Strength of An Over-Consolidated Soil by Triaxial and Plane Strain Tests", *Soils and Foundations*, Vol. 39 No.1, pp.21-29

30. Ladd C.C., Foott R., Ishihara K., Schlosser F., and Poulos H.G., 1977. "Stress-Deformation and Strength Characteristics: SOA Report." *Proc., 9th ICSMFE Tokyo*, Vol. 2, pp. 421-494. 1977.

31. Lambe T.W., 1964. "Methods of Estimating Settlement," *Journal of the Soil Mechanics and Foundations Division, ASCE,* Vol. 90, No. 5, pp. 47–74.

32. Lambe T.W., 1967. "Soil Testing for Engineers" 12th Edition, John Wiley and Sons Inc. New York City/NY, 165 pages.

33. Lo K.Y., 1965. "Stability of Soils in Anisotropic Soils" *ASCE*, *Journal of the Soil Mechanics and Foundations Division*, Vol. 91, No. 4, pp. 85-106

34. Lo K.Y., Leonards G.A., Yuen C., 1977. "Interpretation And Significance Of Anisotropic Deformation Behavior Of Soft Clays", *Norwegian Geotechnical Institute*, No:117

35. Martin T.R., 1962. “Research on the Physical Properties of Marine Soils, August 1961-July 1962” *Research Report R62-42, Soil Eng. Div. Publication*, No.127 M.I.T Cambridge Mass.

36. Menkiti C.O., 1995. “Behavior of Clayey-Sand with Particular Reference to Principal Stress Rotation” PhD Thesis, Imperial College, University of London.

37. Mirata T., 1976. **“**Short Term Stability of Slopes in Ankara Clay” Joint PhD Thesis, University of London and Middle East Technical University, Ankara.

38. Mitachi T. and Fujiwara Y., 1987. “Undrained Shear Behavior of Clays undergoing long-term anisotropic consolidation”, *Soils and Foundations*, Vol. 27:4, 45-61

39. Mitchell J.K, 1956. “The Fabric of Natural Clays and its Relation to Engineering Properties” *Proc. Highway Research Bd. Washington D.C.*, Vol. 35 pp. 693-713

40. Nakase A. and Kamei T., 1983. “Undrained Shear Strength of Normally Consolidated Cohesive Soils”, *Soils and Foundations*, Vol.23 No.1

41. Nishimura S, Minh N. A. and Jardine R. J., 2007. “Shear strength anisotropy of London Clay”, *Géotechnique* Vol. 57, No. 1, pp. 49-62

42. Ohta H and Nishihara A, 1985. “Anisotropy of Undrained Shear Strength of Clays under Axi-Symmetric Loading Conditions”, *Soils and Foundations* Vol. 25, No.2, pp. 73-86

43. Ordemir, İ., Alyanak, I. and Birand, A.A., 1965, "Report on Ankara Clay", METU Publication No.12, Ankara, 30 pages.

44. Rowshanzamir M.A. and Askaria A.M., 2010. “An investigation on the strength anisotropy of compacted clays” *Applied Clay Science* Vol. 50, No. 4, pp. 520-524

45. Sapaz, B., 2004. “Lateral versus vertical swell pressures in expansive soils” MSc. Thesis, Middle East Technical University, Ankara.

46. Tezer A.B, 1984. “Effect of Specimen Size on Undrained Shear Strength of Stiff Fissured Ankara Clay” MSc. Thesis, Middle East Technical University, Ankara.

47. Tonoz M.C., Gökçeoğlu T., Ulusay R., 2003 “A laboratory-scale experimental investigation on the performance of lime columns in expansive Ankara (Turkey) Clay”, *Bulletin of Engineering Geology and the Environment*, Vol.62, No.2, pp.91-106

48. Üner A.K., 1977. “A comparison of engineering properties of two soil types in the Ankara region.” MSc. Thesis, Middle East Technical University, Ankara.

49. Vaid Y.P. and Campanella R.G., 1974. “Triaxial and Plane Strain Behavior of Natural Clay” *ASCE, Journal of the Geotechnical Engineering Division*, Vol. 100, No. 3, pp. 207-224

50. Ward, W.H., Samuels, S.G. and Butler, M.E., 1959. “Further studies of the properties of London Clay.” *Géotechnique*, Vol.9, No.2, 33-58.

51. Wesley L.D., 1975. “Influence of Stress Path and Anisotropy on the Behaviour of a Soft Alluvial Clay” PhD Thesis, Imperial College, University of London.

52. Wesley L.D., 2010, “Fundamentals of Soil Mechanics for Sedimentary and Residual Soils” John Wiley and Sons Inc., Haboken-NJ, 431 pages

53. Whittle A.J, DeGroot D.J., Ladd C.C., Seah T.H., 1994. “Model Prediction of anisotropic behavior of Boston Blue Clay” *Journal of the Geotechnical Engineering Division*, *ASCE* Vol.120 No.1, pp.199-224.

54. Zdravkovic, L., 1996. “The Stress-Strain-Strength Anisotropy of a Granular Medium under General Stress Conditions” PhD Thesis, Imperial College, University of London